



## OBSERVER DESIGN FOR WEIGHTED TIMED EVENT GRAPHS IN A DIOID FRAMEWORK

Pâmela Grazielle Lopes Siekmann

Dissertação de Mestrado apresentada ao Programa de Pós-graduação em Engenharia Elétrica, COPPE, da Universidade Federal do Rio de Janeiro, como parte dos requisitos necessários à obtenção do título de Mestre em Engenharia Elétrica.

Orientadores: Lilian Kawakami Carvalho  
Jörg Raisch

Rio de Janeiro  
Agosto de 2019

OBSERVER DESIGN FOR WEIGHTED TIMED EVENT GRAPHS IN A DIOID  
FRAMEWORK

Pâmela Grazielle Lopes Siekmann

DISSERTAÇÃO SUBMETIDA AO CORPO DOCENTE DO INSTITUTO  
ALBERTO LUIZ COIMBRA DE PÓS-GRADUAÇÃO E PESQUISA DE  
ENGENHARIA (COPPE) DA UNIVERSIDADE FEDERAL DO RIO DE  
JANEIRO COMO PARTE DOS REQUISITOS NECESSÁRIOS PARA A  
OBTENÇÃO DO GRAU DE MESTRE EM CIÊNCIAS EM ENGENHARIA  
ELÉTRICA.

Examinada por:

---

Prof. Lilian Kawakami Carvalho, D.Sc.

---

Prof. João Carlos dos Santos Basilio, Ph.D.

---

Prof. Carlos Andrey Maia, D.Sc.

RIO DE JANEIRO, RJ – BRASIL  
AGOSTO DE 2019

Siekmann, Pâmela Grazielle Lopes

Observer Design for Weighted Timed Event Graphs in a Dioid Framework/Pâmela Grazielle Lopes Siekmann. – Rio de Janeiro: UFRJ/COPPE, 2019.

XIII, 81 p.: il.; 29, 7cm.

Orientadores: Lilian Kawakami Carvalho

Jörg Raisch

Dissertação (mestrado) – UFRJ/COPPE/Programa de Engenharia Elétrica, 2019.

Referências Bibliográficas: p. 75 – 77.

1. Discrete event systems. 2. Petri nets. 3. Timed Petri nets. 4. Dioids. I. Carvalho, Lilian Kawakami *et al.* II. Universidade Federal do Rio de Janeiro, COPPE, Programa de Engenharia Elétrica. III. Título.

*À minha querida Svea Marie...  
sentir você chegar aos meus  
braços abriu no meu coração um  
espaço que será apenas e para  
sempre seu.*

# Acknowledgements

First and foremost I would like to thank GOD, for from Him and through Him and for Him are all things.

While I am solely responsible for this thesis, my overall achievements is the product of fruitful interaction with diverse and very special people, who helped me reach this milestone.

I would like to show my appreciation for my supervisor Prof. D.Sc. Lilian Kawakami Carvalho for her unlimited and continued support on various fronts throughout my masters degree. Thank you for being a mentor, for your constructive feedback and for the time invested attending those meetings, reading my thesis.

I am also indebted to my second supervisor Prof. Dr.-Ing. Jörg Raisch for making it possible to write my thesis in partnership with the Control Systems Group at the TU Berlin.

It was also my privilege to work with Johannes Trunk und Germano Schafaschek, who gave me the guidance and technical support as well as creating a friendly work atmosphere during the entire work.

Gratitude is also due to Prof. Ph.D. João Carlos dos Santos Basilio and for Prof. D.Sc. Carlos Andrey Maia for kindly agreeing to join the examiner panel of my thesis defense.

A big thanks goes to my family. Words cannot express my gratitude for their support. I would like to thank my husband Oliver, my mother Patricia, my father Hugo and my sister Priscila, who believe in me. I can never be thankful enough for all what they have done for me.

Resumo da Dissertação apresentada à COPPE/UFRJ como parte dos requisitos necessários para a obtenção do grau de Mestre em Ciências (M.Sc.)

PROJETO DE OBSERVADOR PARA GRAFOS DE EVENTOS  
TEMPORIZADOS PONDERADOS NA ESTRUTURA DE DIÓIDES

Pâmela Grazielle Lopes Siekmann

Agosto/2019

Orientadores: Lilian Kawakami Carvalho

Jörg Raisch

Programa: Engenharia Elétrica

Um observador é utilizado em um sistema de controle por realimentação, para compensar o fato de que nem todos os estados podem ser medidos. Esse trabalho aborda sistemas que podem ser modelados por redes de Petri temporizadas, mais precisamente, por Grafos de Eventos Temporizados Ponderados (WTEGs). A estrutura do WTEG permite a modelagem de problemas sem conflitos de recursos. No contexto de sistemas de manufatura, os WTEGs são apropriados para reproduzir linhas de montagem complexas, em que o comportamento dinâmico é descrito pelos efeitos de sincronização e saturação. Neste trabalho é proposto o projeto de um observador para WTEGs que consiste na construção: (i) do Observador Ótimo que se baseia na conversão do WTEG para o Grafo de Evento Temporizado (TEG), o qual possui uma representação linear na estrutura matemática dos dióides; (ii) do Simulador, que é uma cópia do sistema sem os distúrbios; (iii) e da Interface que é utilizada para conectar o WTEG ao Observador Ótimo e ao Simulador.

Abstract of Dissertation presented to COPPE/UFRJ as a partial fulfillment of the requirements for the degree of Master of Science (M.Sc.)

## OBSERVER DESIGN FOR WEIGHTED TIMED EVENT GRAPHS IN A DIOID FRAMEWORK

Pâmela Grazielle Lopes Siekmann

August/2019

Advisors: Lilian Kawakami Carvalho  
Jörg Raisch

Department: Electrical Engineering

An observer is used in a feedback control system to compensate for the fact that not all states can be measured. This work refers to systems that can be modeled by timed Petri nets, more precisely, Weighted Timed Event Graphs (WTEGs). The WTEG allows modeling of problems without conflicts of resources. In the context of manufacturing systems, WTEGs are appropriate to design complex assembly lines, where dynamic behavior is described by the synchronization and saturation effects. We propose the design of an observer for WTEGs that, which consists of: (i) an Optimal Observer that is based on the conversion of the WTEG to the Timed Event Graph(TEG), which has a linear representation in the mathematical structure of the dioids; (ii) a Simulator, which is a copy of the system without disturbances; (iii) and an Interface that is used to connect the WTEG to the Optimal Observer and to the Simulator.

# Contents

<b>List of Figures</b>	<b>x</b>
<b>List of Tables</b>	<b>xii</b>
<b>Lista de Abreviaturas</b>	<b>xiii</b>
<b>1 Introduction</b>	<b>1</b>
<b>2 Modeling preliminaries</b>	<b>4</b>
2.1 Petri nets . . . . .	4
2.1.1 Petri net graphs . . . . .	4
2.1.2 Petri net dynamics . . . . .	5
2.1.3 Properties . . . . .	7
2.1.4 Incidence matrix and state equation . . . . .	8
2.2 Timed Petri nets . . . . .	10
2.2.1 Timed Petri net . . . . .	11
2.2.2 Weighted Timed Event Graphs . . . . .	11
2.2.3 Timed Event Graphs . . . . .	13
2.3 Transformation Algorithm . . . . .	14
2.3.1 Algorithm to Convert WTEGs into TEGs . . . . .	14
<b>3 Algebraic background</b>	<b>26</b>
3.1 Dioids . . . . .	26
3.2 Matrix dioids . . . . .	30
3.3 Mappings . . . . .	31
3.4 Residuation Theory . . . . .	31
3.4.1 Residual of right and left product . . . . .	32
3.5 Dioid models of TEGs . . . . .	33
<b>4 Observer Design for Timed Petri nets</b>	<b>38</b>
4.1 Observer for TEGs . . . . .	38
4.2 Observer for WTEGs . . . . .	45



4.2.1	Interface . . . . .	46
4.2.2	Input/Output behavior . . . . .	49
4.3	Implementation of Observer for WTEGs . . . . .	53
<b>5</b>	<b>Conclusion and Future Works</b>	<b>74</b>
	<b>Bibliography</b>	<b>75</b>
<b>A</b>	<b>Dioid <math>\mathcal{M}_{in}^{ax}[\gamma, \delta]</math></b>	<b>78</b>
A.0.1	Dioid $\mathcal{M}_{in}^{ax}[\gamma, \delta]$ . . . . .	78
A.0.2	Causal Series in $\mathcal{M}_{in}^{ax}[\gamma, \delta]$ . . . . .	81

# List of Figures

2.1	Petri net graph of Example 1. . . . .	5
2.2	Petri net of Example 2 with initial marking $\mathcal{M}^0 = [0\ 2\ 0]^T$ . . . . .	6
2.3	Petri net of Example 2 with initial marking $\mathcal{M}^1 = [0\ 1\ 1]^T$ . . . . .	6
2.4	Petri net of Example 3 with $t_1$ enabled and $t_2$ disabled for $\mathcal{M}^0 = [2\ 0]^T$ . . . . .	7
2.5	(a) a 2-bounded Petri net and (b) an unbounded Petri net. . . . .	7
2.6	A live Petri net. . . . .	8
2.7	(a) a not strongly connected Petri net and (b) a strongly connected Petri net. . . . .	8
2.8	Petri net of Example 4. . . . .	9
2.9	Petri net of Example 5. . . . .	10
2.10	Timed Petri net of Example 6. . . . .	11
2.11	WTEG with initial marking $\mathcal{M}^0 = [4\ 1\ 0]^T$ . . . . .	12
2.12	WTEG after the firing of $t_2$ , with marking $\mathcal{M}^1 = [1\ 1\ 5]^T$ . . . . .	12
2.13	Part of a general TEG with holding times [1]. . . . .	13
2.14	TEG with holding times. . . . .	13
2.15	Consistent WTEG. . . . .	16
2.16	TEG corresponding to the consistent WTEG of Figure 2.15. . . . .	20
2.17	Consistent WTEG. . . . .	21
2.18	TEG corresponding to the consistent WTEG of Figure 2.17. . . . .	24
3.1	Properties of residuated mapping $f : \mathcal{D} \rightarrow \mathcal{C}$ and the corresponding residual mapping $f^\# : \mathcal{C} \rightarrow \mathcal{D}$ [2]. . . . .	32
3.2	TEG with one controllable input transition ( $u_1$ ), two uncontrollable input transitions ( $w_1, w_2$ ) and one measurable output transition ( $y_1$ ). . . . .	34
3.3	Model of a TEG in $\mathcal{M}_{in}^{ax}[[\gamma, \delta]]$ . . . . .	35
4.1	The observer structure of Max-plus linear systems [3]. . . . .	39
4.2	TEG model [3]. . . . .	41
4.3	The realization of $L_{opt+}$ . . . . .	43
4.4	The observer for TEG of Figure 4.2. . . . .	44
4.5	Interface insertion in Observer for WTEGs realization. . . . .	46

4.6	Input Interface for $n = 2$ .	47
4.7	Output Interface for $n = 3$ .	48
4.8	Consistent WTEG.	50
4.9	“Equivalent” TEG corresponding to the WTEG of Figure 4.8.	50
4.10	Interfaces that will be connected to the input and to the output of the TEG.	51
4.11	TEG with Input and Output Interface.	51
4.12	Consistent WTEG.	55
4.13	“Equivalent” TEG corresponding to the WTEG of Figure 4.12.	63
4.14	“Equivalent” TEG corresponding to the WTEG of Figure 4.12 with Artificial Transitions.	65
4.15	The $L_{opt+}$ realization corresponding to the TEG of Figure 4.12.	68
4.16	$\mathcal{I}_1$ to connect $WTEG \rightarrow L_{opt+}$ .	69
4.17	(a) $\mathcal{O}_1$ with size $n = 6$ and (b) $\mathcal{O}_2$ with size $n = 2$ .	70
4.18	Simulator $\mathcal{S}$ to WTEG of Figure 4.12	70
4.19	$Obs(WTEG)$ .	73
A.1	$s$ and its south-east cone (gray) [4].	79

# List of Tables

2.1	Firing Table for the consistent WTEG of Figure 2.15. . . . .	20
2.2	Firing Table for the TEG of Figure 2.16. . . . .	20
2.3	Firing Table for the WTEG of Figure 2.17. . . . .	24
2.4	Firing Table for the TEG of Figure 2.18. . . . .	24
4.1	Firing Table WTEG of Figure 4.8. . . . .	52
4.2	Firing Table for TEG with Interface of Figure 4.11. . . . .	53

# Lista de Abreviaturas

DESs	Discrete Event Systems, p. 1, 38
TEGs	Timed Event Graphs, p. 1, 4, 13, 14, 33, 38, 78
WTEGs	Weighted Timed Event Graphs, p. 1, 4, 11, 13, 14, 38

# Chapter 1

## Introduction

Dynamic systems in which the set of states is discrete and the state transitions are observed uniquely at discrete points in time associated with the occurrence of events are called Discrete Event Systems (DESs) [5]. An event is a natural occurrence that leads the system to change its state, *i.e.*, makes the system to transit from a state to another. There are two basic modeling formalisms of DESs: automata and Petri nets.

Petri nets were developed by Carl Adam Petri in 1962 and manipulate events according to specific rules. In Petri nets there are several and explicit conditions under which an event can be enabled, being the reason that they are more suitable to DES whose operation depends on complex control schemes [5]. The basic components of a Petri net graph are transitions, places and arcs connecting them. Events are associated with transitions and the information related to the conditions for a transition to occur is contained in places. Petri net dynamics are defined by moving tokens through the net. This tokens moving is given by the occurrence of transitions. A transition is said to be enabled when it can occur or as commonly used in the Petri net literature “firing”, *i.e. it can fire*. With a Petri net graph, it is possible to describe the logical structure of the modeled system, but not its time evolution. Time has been introduced into Petri nets when it is necessary the temporal performance analysis.

Timed Petri nets are used when it is necessary to make an association with time. This association can be done through transitions (representing transition delays) or places (representing holding times). In this work, time information is associated with places. In this approach, tokens in a place with holding time remain on this place a specific time before they can contribute to the firing of a downstream transition.

Timed Event Graphs (TEGs) are a subclass of timed Petri nets in which every place has a single input arc and a single output arc and all arcs have weight equal to one. TEGs have a dynamic behavior that is characterized by synchronization phenomena, making them suitable to model systems where synchronization

is essential such as transportation networks [6], [7], communication networks [8], and manufacturing assembly lines [9]. The equations describing the dynamics of a TEG are non-linear in conventional algebra. These equations, however, have a linear representation in particular mathematical structures called dioids. Modeling through certain dioids allows adapting concepts of traditional control theory, such as state-space representation and transfer functions, to TEGs, thus paving the way for several control strategies to be introduced. One such strategy is based on state estimation, in which an observer estimates the system's state (*e.g.*, which is not directly measurable) based on the output and feeds this information to the controller, thereby providing insight into the internal behavior of the system. The scalar dioid called max-plus algebra [10] and the dioid of formal power series called  $\mathcal{M}_{in}^{ax}[\gamma, \delta]$  [4] are examples of dioids well established in the literature for modeling TEGs.

Weighted Timed Event Graphs (WTEGs) can be described as extended TEGs in which the weights in arcs can take any value in the set of natural numbers, except zero. The weights are more appropriate for expressing batch/division processes, which makes WTEGs more representative when several occurrences of events are demanded to induce the next event or when one event results in several successive events. Cyclic production systems with batch scheduling, split processes, assembly of products, and buffers of limited capacity are usual in manufacturing systems. Therefore, WTEGs are considered appropriate to model complex assembly lines [11, 12]. In contrast to TEGs, WTEGs have an event-variant behavior and cannot be described by  $\mathcal{M}_{in}^{ax}[\gamma, \delta]$ .

A state feedback controller requires that all states of the system be known. A problem arises when it is not possible to have complete measurement of all the state variables due to lack of sensors. To solve this problem, an observer that provides an estimate of the internal states of a given system by using input/output measurements is used to feed the controller. State estimation is particularly important because it can also be used in fault detection, diagnosis, state-feedback control and to reconstruct the markings of the graph for Petri net[13]. In TEGs, the state trajectories represent the transition firings and their estimations allow the knowledge of the internal properties of the system. A Max-plus Observer for TEG was introduced in [14], in which the observer was used to compute an estimation of state by using the input and output measurements. Recently, in [15], they address the problem of estimating a linear function of the states for a given Max-Plus linear dynamical system. To do so, they use the current and past inputs/outputs of the system to construct a sequence that converges in a finite number of steps to the value given by a linear function of the states, for all initial conditions of the system. They provide necessary and sufficient conditions to solve this general problem. However, it is shown in [15] that the Luenberger approach is better at rejecting the perturbation.

The main contribution of this work is to compute an Observer for WTEGs based on the existing results for ordinary TEGs. There are no results in the literature for observer design for WTEGs. As in [16], the observer in this work, is in analogy with the classical Luenberger observer [17] for linear systems and the Observer Matrix is used to provide information from the system output into the Simulator. In contrast to the [16], the observer realization is obtained modeling the system and the Simulator as a WTEG. The steps for obtaining the observer realization are as follows: firstly, we model the system as a WTEG; secondly, we obtain the TEG from the WTEG using an adaptation of the transformation algorithm to WTEGs proposed in [18]; then, we compute the observer matrix based on TEG since the equations become linear in  $\mathcal{M}_{in}^{ax}[\gamma, \delta]$ ; finally, we size the interfaces. The interface proposed in this work is a specific Petri net which is necessary for obtaining the Observer for WTEGs realization. The inclusion of the interface must ensure that some system properties are preserved. Therefore, the insertion of this structure does not modify the original system.

Another contribution is an algorithm, which converts a WTEG into a TEG. This algorithm is inspired by the algorithm proposed in [18] to convert a Synchronous Dataflow graph (SDF) into a Homogeneous Synchronous Dataflow graph (HSDF). The TEG obtained through the transformation and the original WTEG are equivalent.

This work is organized as follows. In Chapter 2 some fundamentals on Timed Petri nets are presented and an algorithm to convert WTEGs into TEGs is proposed. In Chapter 3 a basic background over dioid theory is introduced. In Chapter 4 a model of the Observer for TEGs is described and design of the Observer for WTEGs is proposed. In Chapter 5 the contributions in this work are summarized and some possible future works are presented.



# Chapter 2

## Modeling preliminaries

In this chapter, the modeling preliminaries about Petri nets are presented. These concepts are fundamental to introduce a transformation algorithm which is fundamental to develop this work. This chapter is organized as follows. In Section 2.1, the theoretical background of Petri nets is presented; in Section 2.2, timed Petri nets are introduced; and in Section 2.3, an algorithm to transform a consistent Weighted Timed Event Graphs (WTEG) in Timed Event Graphs (TEGs) is developed.

### 2.1 Petri nets

Petri nets are a graphical and mathematical modeling tool that can describe behaviors which are characterized as being concurrent, asynchronous, distributed, parallel, nondeterministic, and stochastic. Thus, Petri nets are convenient to model and analyze a variety of discrete event systems [19]. In this section, Petri nets are briefly introduced and the most important and necessary characteristics for this work are described.

#### 2.1.1 Petri net graphs

A Petri net is a particular kind of directed bipartite graph consisting of two kinds of nodes called “places” and “transitions”, where arcs connect transitions to places and places to transitions. Places are graphically represented as circles and contain information related to the states and conditions of the system. Transitions are represented as bars and are associated with the events. Arcs are represented by oriented arrows that define the relations between transitions and places [19]. The formal definition of a Petri net graph is as follows.

**Definition 1 (Petri net graph)** *A Petri net graph is a directed bipartite graph  $\mathcal{N} = (P, T, w)$ , where:*

- $P = \{p_1, p_2, \dots, p_n\}$  is the finite set of places,
- $T = \{t_1, t_2, \dots, t_m\}$  is the finite set of transitions,
- $w : (P \times T) \cup (T \times P) \rightarrow \mathbb{N}_0$  is the weight function.

$A := \{(p_i, t_j) | w(p_i, t_j) > 0\} \cup \{(t_j, p_i) | w(t_j, p_i) > 0\}$  is the arc set. Weights are graphically represented by numbers attached to arcs, and they are typically omitted when equal to 1. Furthermore, the set of upstream and downstream transitions (resp. places) are defined as follows:

- $\bullet p_i := \{t_j \in T | (t_j, p_i) \in A\}$  is the set of upstream transitions of place  $p_i$ ,
- $p_i^\bullet := \{t_j \in T | (p_i, t_j) \in A\}$  is the set of downstream transitions of place  $p_i$ ,
- $\bullet t_j := \{p_i \in P | (p_i, t_j) \in A\}$  is the set of upstream places of transition  $t_j$ ,
- $t_j^\bullet := \{p_i \in P | (t_j, p_i) \in A\}$  is the set of downstream places of transition  $t_j$ .

**Example 1** A simple example of a Petri net graph is shown in Figure 2.1. Its structure is defined by  $P = \{p_1, p_2, p_3\}$ ,  $T = \{t_1, t_2\}$ ,  $w(p_1, t_1) = 1$ ,  $w(p_2, t_2) = 1$ ,  $w(t_1, p_2) = 2$  and  $w(t_2, p_3) = 1$ . The sets of upstream and downstream transitions are:  $\bullet p_1 = \emptyset$ ,  $\bullet p_2 = \{t_1\}$ ,  $\bullet p_3 = \{t_2\}$ ,  $p_1^\bullet = \{t_1\}$ ,  $p_2^\bullet = \{t_2\}$ ,  $p_3^\bullet = \emptyset$ . The sets of upstream and downstream places are:  $\bullet t_1 = \{p_1\}$ ,  $\bullet t_2 = \{p_2\}$ ,  $t_1^\bullet = \{p_2\}$ ,  $t_2^\bullet = \{p_3\}$ .

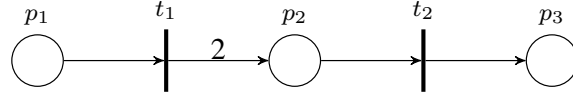


Figure 2.1: Petri net graph of Example 1.

**Definition 2 (Path)** A directed path  $\rho$  is a sequence of transitions  $\{t_1, t_2, \dots, t_{i+1}\}$  and places  $\{p_1, p_2, \dots, p_i\}$ , such that  $\forall j \in \{1, \dots, i\}, w(t_j, p_j) \in A$  and  $w(p_j, t_{j+1}) \in A$ .

## 2.1.2 Petri net dynamics

To each place in a Petri net, a nonnegative integer number of tokens is attached. The marking of a place is determined by the number of tokens in this place. The change in the distribution of tokens among the places reflects the dynamic behavior of the Petri net.

**Definition 3 (Petri net with initial marking)** A Petri net with initial marking is a pair  $(\mathcal{N}, \mathcal{M}^0)$  where  $\mathcal{N} = (P, T, w)$  is a Petri net graph and  $\mathcal{M}^0 \in \mathbb{N}_0^n$  is the initial marking, i.e., the initial distribution of tokens over places in  $\mathcal{N}$ .

**Example 2** A Petri net with initial marking  $\mathcal{M}^0 = [0 \ 2 \ 0]^T$  is represented in Figure 2.2.

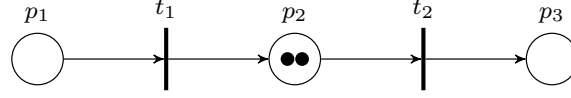


Figure 2.2: Petri net of Example 2 with initial marking  $\mathcal{M}^0 = [0 \ 2 \ 0]^T$ .

In the sequel, we will refer to “firing” when a transition is said to be enabled and it can occur, *i.e.* *it can fire*.

The marking of the Petri net is denoted by  $\mathcal{M} \in \mathbb{N}_0^n$  and changes according to the following (firing) rules [1]:

1. a transition  $t_j$  is said to be enabled if and only if every place  $p_i \in \bullet t_j$  contains at least as many tokens as the weight of the arc from  $p_i$  to  $t_j$ , *i.e.*,  $w(p_i, t_j) \leq \mathcal{M}_i$ .
2. if a transition  $t_j$  fires, the number of tokens in every place  $p_i \in \bullet t_j$  decreases by the weight of the arc connecting  $p_i$  to  $t_j$ , and the number of tokens in every place  $p_i \in t_j^\bullet$  increases by the weight of the arc connecting  $t_j$  to  $p_i$ , *i.e.*,  $\forall p_i \in \bullet t_j, \mathcal{M}'_i = \mathcal{M}_i - w(p_i, t_j)$  and  $\forall p_i \in t_j^\bullet, \mathcal{M}'_i = \mathcal{M}_i + w(t_j, p_i)$ , where  $\mathcal{M}_i$  is the marking before the firing of  $t_j$  and  $\mathcal{M}'_i$  is the marking after the firing of  $t_j$ .

Figure 2.3 shows the distribution of tokens over places after the firing of  $t_1$  of the Petri net of Example 2.

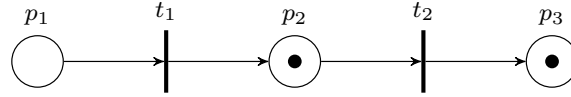


Figure 2.3: Petri net of Example 2 with initial marking  $\mathcal{M}^1 = [0 \ 1 \ 1]^T$ .

**Example 3** In Figure 2.4 a Petri net with  $\mathcal{M}^0 = [2 \ 0]^T$  is shown. Let us consider that transition  $t_1$  can occur and transition  $t_2$  cannot occur. Based on the first firing rule:  $\bullet t_1 = \{p_1\}$  contains 2 tokens and  $w(p_1, t_1) = 1$ , so  $w(p_1, t_1) \leq \mathcal{M}^0_1$ , which means that  $t_1$  is enabled. Besides that,  $\bullet t_2 = \{p_2\}$  does not contain tokens and  $w(p_2, t_2) = 1$ , so  $t_2$  is disabled. Since only  $t_1$  is enabled, considering the second firing rule,  $\mathcal{M}'_1 = 2 - 1 = 1$  and  $\mathcal{M}'_2 = 0 + 1 = 1$ . Therefore, the new marking of this Petri net after  $t_1$  fires is  $\mathcal{M}' = [1 \ 1]^T$ . In other words, when  $t_1$  fires,  $p_1$  loses one token and  $p_2$  gains one token. After the first firing of  $t_1$ ,  $p_2$  contains 1 token and  $w(p_2, t_2) = 1$ , so  $w(p_2, t_2) \leq \mathcal{M}'_2$ , which means that  $t_2$  is enabled.

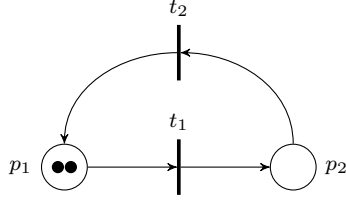


Figure 2.4: Petri net of Example 3 with  $t_1$  enabled and  $t_2$  disabled for  $\mathcal{M}^0 = [2\ 0]^T$ .

### 2.1.3 Properties

Petri nets have behavioral properties which depend on the initial state or marking. These properties are useful for analyzing modeled systems. Here only three of the basic behavioral properties are discussed: reachability, boundedness and liveness.

**Definition 4 (Reachability)** A marking  $\mathcal{M}$  is reachable from a marking  $\mathcal{M}^0$  if there exists a sequence of firings that leads from  $\mathcal{M}^0$  to  $\mathcal{M}$ . The set of all possible markings reachable from  $\mathcal{M}^0$  in a Petri net  $(\mathcal{N}, \mathcal{M}^0)$  is denoted by  $\mathcal{R}(\mathcal{M}^0)$ [19].

**Definition 5 (Boundedness)** A Petri net  $(\mathcal{N}, \mathcal{M}^0)$  is said to be  $k$ -bounded or simply bounded if the number of tokens in each place does not exceed a finite number  $k$  for any marking reachable from  $\mathcal{M}^0$ , i.e.,  $\mathcal{M}_i \leq k$  for every place  $p_i$  and every marking  $\mathcal{M} \in \mathcal{R}(\mathcal{M}^0)$ .

Two Petri nets are presented in Figure 2.5. In Figure 2.5(a), places  $p_1$  and  $p_2$  have at most 2 tokens at all reachable markings, therefore the Petri net is 2-bounded. In Figure 2.5(b), place  $p_3$  receives one token every time  $t_2$  fires and, therefore, can accumulate tokens indefinitely; thus, it is an unbounded Petri net.

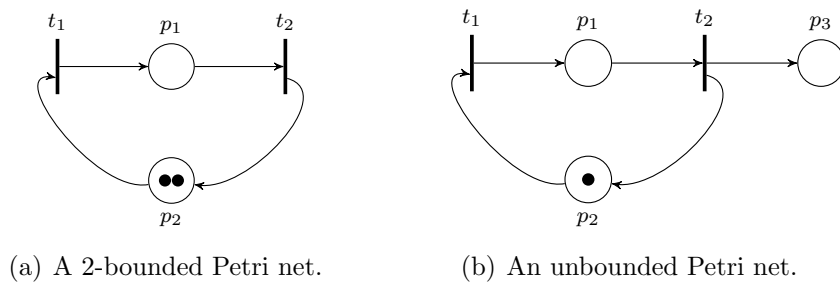


Figure 2.5: (a) a 2-bounded Petri net and (b) an unbounded Petri net.

**Definition 6 (Liveness)** A Petri net  $(\mathcal{N}, \mathcal{M}^0)$  is said to be live if, no matter what marking has been reached from  $\mathcal{M}^0$ , it is possible to ultimately fire any transition of the net by progressing through some further firing sequence.

This means that a live Petri net guarantees deadlock-free operation, no matter what firing sequence is chosen. In Figure 2.6 a live Petri net is shown. It is live because it is always possible to reach a state in which  $t_1$ ,  $t_2$  and  $t_3$  can fire.

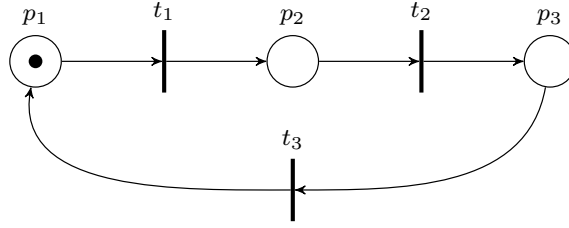
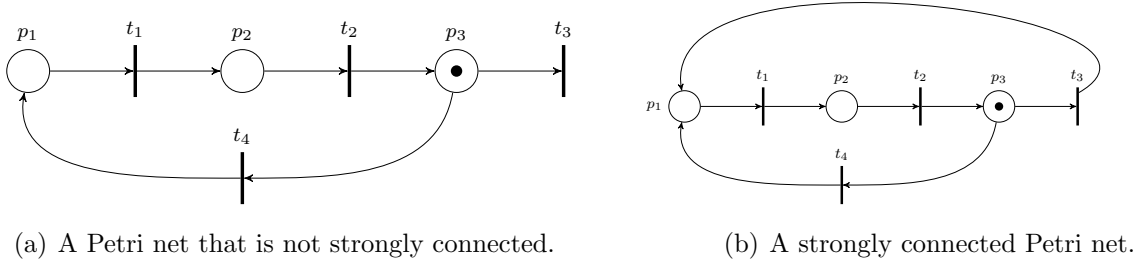


Figure 2.6: A live Petri net.

**Definition 7 (Strong connectedness)** A Petri net  $(P, T, w, \mathcal{M}^0)$  is strongly connected, if there is a directed path from any transition  $t_i$  in  $T$  to any other transition  $t_j$  in  $T$ .

Two Petri nets are shown in Figure 2.7. In Figure 2.7(a), the Petri net is not strongly connected, because there is no directed path from  $t_3$  to the other transitions. In Figure 2.7(b) a Petri net that is strongly connected, because there are directed paths between all transitions.



(a) A Petri net that is not strongly connected.

(b) A strongly connected Petri net.

Figure 2.7: (a) a not strongly connected Petri net and (b) a strongly connected Petri net.

### 2.1.4 Incidence matrix and state equation

An approach to represent Petri nets is through the state equations, which are used to represent their dynamic behavior. The most important element in this procedure is the incidence matrix.

The incidence matrix  $\mathcal{W} \in \mathbb{Z}^{n \times m}$  for a Petri net  $\mathcal{N}$  is an  $n \times m$  matrix of integers where  $n$  represents the number of places and  $m$  represents the number of transitions. The entries of incidence matrix  $\mathcal{W}$  are given by  $\omega_{ij} = w(t_j, p_i) - w(p_i, t_j)$  for all  $i \in \{1, \dots, n\}$  and  $j \in \{1, \dots, m\}$ , where  $w(t_j, p_i)$  and  $w(p_i, t_j)$  are the weights on arcs.

Note that  $\omega_{ij} > 0$  represents the net gain in the number of tokens in place  $p_i$  when transitions  $t_j$  fires and  $\omega_{ij} < 0$  represents the net loss in the number of tokens in place  $p_i$  when transitions  $t_j$  fires.

**Definition 8 (Parikh vector)** Let  $\sigma$  be a finite sequence of transitions in a Petri net  $(P, T, w, \mathcal{M}^0)$ . The Parikh vector of  $\sigma$  is  $\zeta_\sigma \in \mathbb{N}_0^m$  such that  $(\zeta_\sigma)_i$  corresponds to the number of occurrences of  $t_i$  in  $\sigma$ .

The new marking after firing the sequence  $\sigma$  is given by:

$$\mathcal{M}' = \mathcal{M} + \mathcal{W}\zeta_\sigma. \quad (2.1)$$

Given a Parikh vector  $\zeta_\sigma$ , the marking  $\mathcal{M}'$  computed through (2.1), as a general rule, is only potentially reachable because the sequence  $\sigma$  might not be fireable starting from marking  $\mathcal{M}$ .

**Example 4** For the Petri net shown in Figure 2.8, the state equation 2.1 for a trivial firing sequence  $\sigma$  consisting only of one firing of  $t_3$  and starting from  $\mathcal{M}^0$  is displayed as follows:

$$\mathcal{M}' = \begin{bmatrix} 2 \\ 0 \\ 1 \\ 2 \end{bmatrix} + \begin{bmatrix} -2 & 1 & 1 \\ 1 & -1 & 0 \\ 1 & 0 & -1 \\ 0 & 2 & -2 \end{bmatrix} \times \begin{bmatrix} 0 \\ 0 \\ 1 \end{bmatrix} = \begin{bmatrix} 3 \\ 0 \\ 0 \\ 0 \end{bmatrix}$$

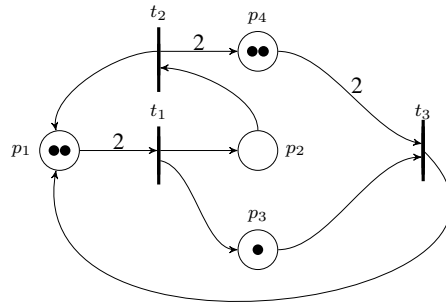


Figure 2.8: Petri net of Example 4.

**Definition 9 (T-semiflow)** A vector  $\xi \in \mathbb{N}^m$  is called T-semiflow if  $\mathcal{W}\xi = 0$ , where 0 indicates the zero vector.

Note that all entries of a T-semiflow  $\xi$  are strictly positive integers.

**Example 5** Let us consider a simple Petri net represented in Figure 2.9 where the incidence matrix is:

$$\mathcal{W} = \begin{bmatrix} 2 & -1 & 0 \\ 0 & 0 & 0 \\ 0 & 1 & -1 \end{bmatrix}.$$

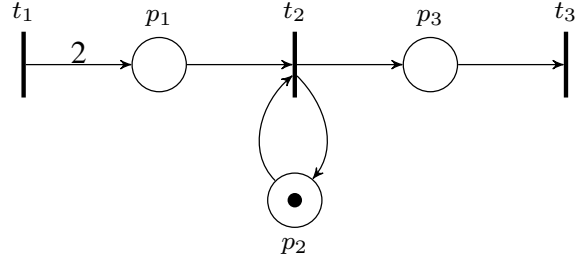


Figure 2.9: Petri net of Example 5.

The element  $\omega_{11}$  represents that place  $p_1$  gains two tokens when  $t_1$  fires. The other elements of the first column are equal to zero because the firing of  $t_1$  does not change the number of tokens in  $p_2$  and  $p_3$ . In the second column,  $\omega_{12}$  is equal to  $-1$  because place  $p_1$  loses one token when  $t_2$  fires. The element  $\omega_{22}$  is zero because  $w(t_2, p_2) = w(p_2, t_2)$ , so the firing of  $t_2$  does not affect the number of tokens in  $p_2$ , and  $\omega_{32}$  is  $1$  because  $p_3$  gains a token when  $t_2$  fires. In the third column, the first two elements are equal to zero given that the firing of  $t_3$  does not change the number of tokens in  $p_1$  and  $p_2$ . The last element  $\omega_{33}$  is equal to  $-1$  since the firing of  $t_3$  results in the loss of one token in  $p_3$ .

Now, computing the  $T$ -semiflow gives:

$$\mathcal{W}\xi = 0,$$

$$\begin{bmatrix} 2 & -1 & 0 \\ 0 & 0 & 0 \\ 0 & 1 & -1 \end{bmatrix} \times \begin{bmatrix} \xi_1 \\ \xi_2 \\ \xi_3 \end{bmatrix} = \begin{bmatrix} 0 \\ 0 \\ 0 \end{bmatrix},$$

$$\xi = \begin{bmatrix} 1 & 2 & 2 \end{bmatrix}^T.$$

Note that the firing of the sequence  $t_1 t_2 t_2 t_3 t_3$  returns to the initial marking  $\mathcal{M}^0 = [0 \ 1 \ 0]^T$ .

## 2.2 Timed Petri nets

Petri nets can be used to model systems in which it is possible for some events to occur currently, although this model may not be complete enough for the study of system performance since no assumption is made on the duration of modeled activities. There are systems for which it is necessary to add timing information for their complete description. The timing information in the approach of Petri nets can be incorporated into the model in two ways: making the association with transitions (representing transition delays) or with places (representing holding times).

### 2.2.1 Timed Petri net

As previously discussed, a Petri net  $(\mathcal{N}, \mathcal{M}^0)$  does not model the actual firing times, but only the ordering of the firings of transitions. When it is necessary to make an association with time, modeling should be done using timed Petri nets. In this work, time is associated with places, as this is the approach most commonly adopted in the literature when dealing with dioids, which play a central role in the results hereby presented. In the association of time with places, tokens in a place  $p_i$  with “holding time” have to be held for a certain time before they contribute to the firing of downstream transitions of  $p_i$ . In this sense, one can then define timed Petri nets.

**Definition 10 (Timed Petri net)** *A timed Petri net with holding times is a triple  $(\mathcal{N}, \mathcal{M}^0, \phi)$ , where  $(\mathcal{N}, \mathcal{M}^0)$  is a Petri net and  $\phi \in \mathbb{N}_0^n$  represents the holding times of the places, i.e.,  $\phi_i$  is the time a token has to remain in place  $p_i$  before it contributes to the firing of a transition in  $p_i^\bullet$ . Holding times are graphically represented by numbers attached to places.*

**Example 6** *The timed Petri net is represented in Figure 2.10. The token in  $p_1$  has to be held for 2 time units before enabling  $t_2$ . The holding times are  $\phi_1 = 2$  and  $\phi_2 = 0$ .*

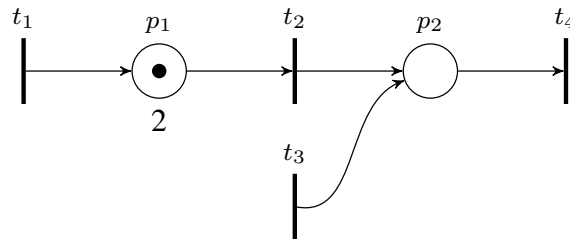


Figure 2.10: Timed Petri net of Example 6.

### 2.2.2 Weighted Timed Event Graphs

There is a subclass of timed Petri nets called Weighted Timed Event Graphs (WTEGs) which can be formally defined as follows.

**Definition 11 (Weighted Timed Event Graphs)** *A timed Petri net  $(\mathcal{N}, \mathcal{M}^0, \phi)$  is called a Weighted Timed Event Graph (WTEG), if every place has exactly one upstream and one downstream transition, i.e.,  $\forall p_i \in P : |p_i^\bullet| = |\bullet p_i| = 1$ .*

**Example 7** *Figure 2.11 represents a WTEG, where,  $|p_i^\bullet| = |\bullet p_i| = 1, i = 1, 2, 3$ . Note that, to contribute to the firing of  $t_2$ , the token in  $p_2$  needs to be held for 2 time instants.*



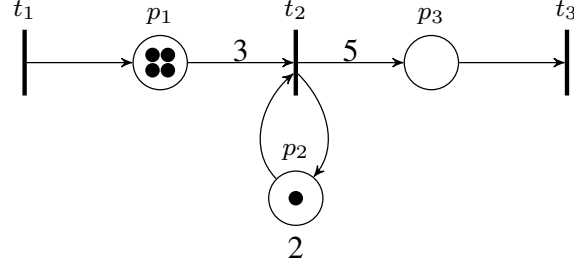


Figure 2.11: WTEG with initial marking  $\mathcal{M}^0 = [4\ 1\ 0]^T$ .

If  $t_2$  fires,  $p_1$  loses 3 tokens and  $p_3$  gains 5 tokens. In Figure 2.12 the new marking is shown.

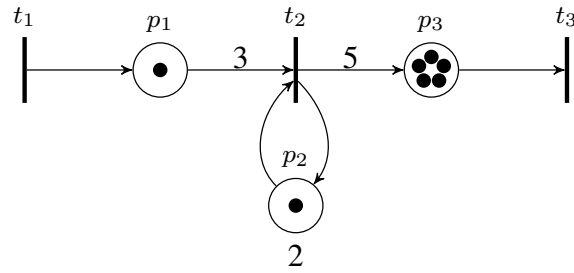


Figure 2.12: WTEG after the firing of  $t_2$ , with marking  $\mathcal{M}^1 = [1\ 1\ 5]^T$ .

**Definition 12 (Basic Path)** A basic directed path,  $\pi_i = t_i \rightarrow p_i \rightarrow t_j$  of a WTEG is such that  $t_i \in \bullet p_i$  and  $t_j \in p_i^\bullet$ . As  $|p_i^\bullet| = |\bullet p_i| = 1 \forall p_i \in P$ , each place appears in precisely one basic directed path.

In Figure 2.11 there are the following basic paths:  $\pi_1 = t_1 \rightarrow p_1 \rightarrow t_2$ ,  $\pi_2 = t_2 \rightarrow p_3 \rightarrow t_3$  and  $\pi_3 = t_2 \rightarrow p_2 \rightarrow t_2$ .

**Definition 13 (Gain of a basic path)** The gain of  $\pi_i$  is defined by  $\Gamma(\pi_i) = \Gamma(t_i, p_i, t_j) = \frac{w(t_i, p_i)}{w(p_i, t_j)}$ .

In Figure 2.11 the gain of the basic paths are:  $\Gamma(\pi_1) = 1/3$ ,  $\Gamma(\pi_2) = 5$  and  $\Gamma(\pi_3) = 1$ .

**Definition 14 (Consistent Weighted Timed Event Graphs)** A WTEG is consistent if and only if it has a unique minimal T-semiflow.

A T-semiflow is said to be minimal when the greatest common divisor of its elements is one and when the set of nonzero components is not a proper superset of any other [20]. In Figure 2.11, the WTEG is consistent, since it has a unique minimal T-semiflow  $\xi = [3\ 1\ 5]^T$ .

### 2.2.3 Timed Event Graphs

Timed Event Graphs (TEGs) are directed bipartite graphs in which each place has exactly one incoming arc and one outgoing arc and the weight of all arcs is one. A TEG is formally defined as follows:

**Definition 15 (Timed Event Graphs)** *An ordinary Timed Event Graph (TEG) is a WTEG, where all arcs have weight 1, i.e.,  $\forall (p_i, t_j), (t_j, p_i) \in A, w(p_i, t_j) = w(t_j, p_i) = 1$ .*

In a TEG, when all input places of a given transition received their  $k$ -th token and their relative holding times have elapsed, the transition is able to fire for the  $k$ -th time. Part of a general TEG with holding times is shown in Figure 2.13. When  $t_r$  fires,  $p_i$  gets one token and it has to spend  $v_i$  time units before being able to contribute to the firing of transition  $t_j$  [1].

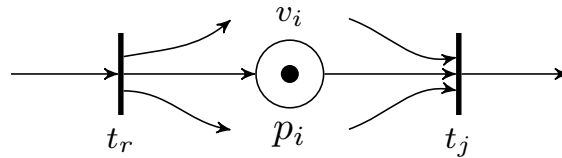


Figure 2.13: Part of a general TEG with holding times [1].

**Example 8** *Consider the TEG showed in Figure 2.14. Transitions  $t_1$  and  $t_2$  can fire autonomously given that they do not have input places. Once  $t_1$  fires,  $p_1$  gains one token and this token has to stay two time units in  $p_1$  before being able to contribute to the firing of  $t_3$ . Once  $t_2$  fires  $p_2$  gains one token and this token has to stay five time units in  $p_2$  before being able to contribute to the firing of  $t_3$ .*

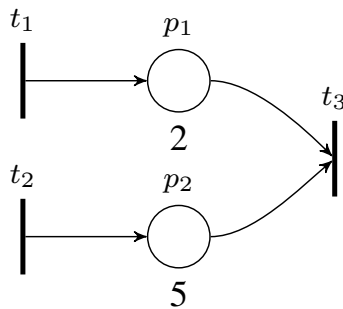


Figure 2.14: TEG with holding times.

Denoting  $x_i(k)$  as the earliest possible time instant of the  $k$ -th firing of transition  $t_i$  (i.e., of the  $k$ -th occurrence of event  $x_i$ ), in Figure 2.14 the time of the  $k$ -th firing of transition  $t_3$  satisfies the inequality below:

$$x_3(k) \geq \max(x_1(k) + 2, x_2(k) + 5). \quad (2.2)$$

**Definition 16 (Earliest firing rule)** *The earliest firing rule of a TEG consists in firing transitions as soon as they are enabled.*

**Remark 1** *In Petri nets, even if the transition is enabled to fire, it might not actually do so. However, in this work, it is assumed that a transition fires as soon as it is enabled, i.e., the earliest firing rule applies. This assumption is very weak since by definition there are no conflicting transitions in TEGs. For example, inequality (2.2) in Example 8 turns into equality supposing that the TEG operates according to the earliest firing rule.*

The equations used to determine the firing instants of transitions in a TEG are clearly non-linear in conventional algebra. However, there is a mathematical structure in which these equations have a linear representation; in the so-called Max-plus algebra, it is possible to model a TEG as a linear system, as will be discussed in more detail in Section 3.5 [10].

## 2.3 Transformation Algorithm

The weights on the arcs in WTEGs allow the modeling of a larger class of DES, such as when multiple occurrences of events are needed to induce the subsequent event or when one event can result in multiple subsequent events. In other words, WTEGs have an event-variant behavior, which for instance allows to model phenomena such as group/ungroup processes in manufacturing lines. However, its analysis and control are complex. One method to analyze WTEGs is to model their time behavior by TEGs because they can be modeled as a linear system. From this perspective, an algorithm to convert consistent WTEGs into TEGs is introduced.

### 2.3.1 Algorithm to Convert WTEGs into TEGs

An “equivalent” TEG can be obtained by the transformation of a consistent WTEG, where by “equivalent” we mean that this TEG obtained by the transformation has an equivalent transition firing order to the WTEG. The equivalent TEG can be computed by a strategy inspired on the algorithm to convert a Synchronous Dataflow graph (SDF), which are an equivalent representation of WTEGs [21], into a Homogeneous Synchronous Dataflow graph (HSDF) [18]. A similar algorithm for strongly connected WTEGs was introduced in [22] and [18]. In the following, an adaptation to WTEGs of the transformation algorithm proposed in [18] is presented.

---

**Algorithm 1** *Convert consistent WTEG to TEG [18]*

---

**Input:** *Consistent WTEG  $(P, T, w, \mathcal{M}^0, \phi)$*

**Output:**  $TEG (P', T', w', \mathcal{M}^0, \phi')$

1: Compute the  $T$ -semiflow vector  $\xi$

2: Let  $\xi(t_l)$  be the corresponding entry in  $\xi$  of transition  $t_l$  in the WTEG

2.1: **for** each entry  $\xi(t_l)$  in  $\xi$ :

add  $\xi(t_l)$  transitions to the transition set  $T'$  of TEG using index  $t_l^1, t_l^2 \dots t_l^{\xi(t_l)}$

**end for**

3: **for** each basic path  $t_l \rightarrow p_m \rightarrow t_g$  in the WTEG:

3.1: **for** each  $i$  such that  $1 \leq i \leq \xi(t_l)$

**for** each  $k$  such that  $1 \leq k \leq w(t_l, p_m)$

$$\text{Let } j = \left\lfloor \frac{(\mathcal{M}^0(p_m) + (i-1)w(t_l, p_m) + k - 1) \bmod (w(p_m, t_g)\xi(t_g))}{w(p_m, t_g)} \right\rfloor + 1$$

Add place  $p'_{l_i, g_j}$  to place set  $P'$  of TEG

Set:

$$\begin{cases} w'(t'_l, p'_{l_i, g_j}) = 1 \\ w'(p'_{l_i, g_j}, t'_{g_j}) = 1 \\ \mathcal{M}^0(p'_{l_i, g_j}) = \left\lfloor \frac{(\mathcal{M}^0(p_m) + (i-1)w(t_l, p_m) + k - 1)}{w(p_m, t_g)\xi(t_g)} \right\rfloor \\ \phi'(p'_{l_i, g_j}) = \phi(p_m) \end{cases}$$

**end for**

**end for**

**end for**

4: **for** each entry  $\xi(t_l) \neq 1$  in  $\xi$

4.1: **for** each  $i$  such that  $1 \leq i < \xi(t_l)$

Add place  $(p'_{l_i, l_{i+1}})$  to place set  $P'$  of TEG

Set:

$$\begin{cases} w'(t'_l, p'_{l_i, l_{i+1}}) = 1 \\ w'(p'_{l_i, l_{i+1}}, t'_{l_{i+1}}) = 1 \\ \mathcal{M}^0(p'_{l_i, l_{i+1}}) = 0 \\ \phi'(p'_{l_i, l_{i+1}}) = 0 \end{cases}$$

**end for**

4.2: Add place  $(p'_{l_{\xi(t_l),l_1}})$  to place set  $P'$  of TEG

$$\text{Set: } \begin{cases} w'(t'_{l_{\xi(t_l),l_1}}, p'_{l_{\xi(t_l),l_1}}) = 1 \\ w'(p'_{l_{\xi(t_l),l_1}}, t'_{l_1}) = 1 \\ \mathcal{M}^{0'}(p'_{l_{\xi(t_l),l_1}}) = 1 \\ \phi'(p'_{l_{\xi(t_l),l_1}}) = 0 \end{cases}$$

**end for**

5: All weights  $w'$  which were not explicitly defined in Step 3 and Step 4 are considered 0

Summarizing the steps of Algorithm 1, in the second step, each transition in the consistent WTEG is duplicated by its corresponding entry in the T-semiflow. That is, for each transition  $t_l$  in WTEG, the TEG contains  $\xi(t_l)$  copies (or instances) of  $t_l$ .

Then, in the third step, considering each basic path in the consistent WTEG, the weights, the initial marking, the holding times and the places of the set  $P'$  to be added on TEG are determined.

To enforce a firing order on the internal duplicated transitions without self-loops, in the fourth step, a loop between them is defined. In Step 4.1, the downstream arc for the first duplicated transition is connected to the upstream arc for the next transition, and so on, up to the last duplicated transition. In Step 4.2, the downstream arc for the last duplicated transition is connected to the upstream arc for the first duplicated transition. Moreover, in Steps 4.1 and 4.2, the weights, the initial marking and the holding times that will be fixed in the loop are determined.

An example is given for an illustration of Algorithm 1,

**Example 9** Consider the consistent WTEG shown in Figure 2.15.

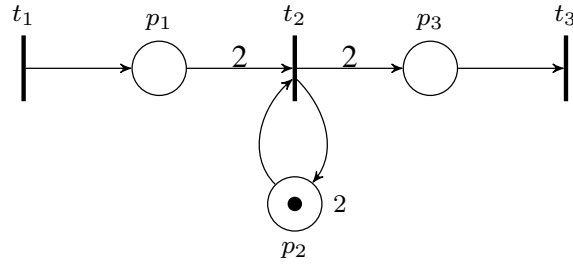


Figure 2.15: Consistent WTEG.

Following Algorithm 1 steps, we have:

Step 1: Computing the  $T$ -semiflow vector  $\xi$ :

$$\begin{aligned} \mathcal{W}\xi &= 0 \\ \begin{bmatrix} 1 & -2 & 0 \\ 0 & 0 & 0 \\ 0 & 2 & -1 \end{bmatrix} \times \begin{bmatrix} \xi_1 \\ \xi_2 \\ \xi_3 \end{bmatrix} &= \begin{bmatrix} 0 \\ 0 \\ 0 \end{bmatrix} \\ \xi &= \begin{bmatrix} 2 & 1 & 2 \end{bmatrix}^T \end{aligned}$$

Step 2: The transition set  $T'$  of TEG is:  $T' = \{t_1^1, t_1^2, t_2^1, t_3^1, t_3^2\}$ .

Therefore, each transition in the WTEG is duplicated by its corresponding entry in the  $T$ -semiflow.

Step 3: For each basic path in WTEG:

**Basic Path 1** ( $t_1, p_1, t_2$ ):

$$1 \leq i \leq 2$$

$$1 \leq k \leq 1$$

**for**  $i = 1$

$$j = \left\lfloor \frac{(0+(1-1)\times 1)+1-1}{2} \bmod(2\times 1) \right\rfloor + 1 = 1$$

Add place  $p'_{11,21}$  to place set  $P'$  of TEG.

Set:

$$\begin{cases} w'(t'_1, p'_{11,21}) = 1 \\ w'(p'_{11,21}, t'_2) = 1 \\ \mathcal{M}^{0'}(p'_{11,21}) = \left\lfloor \frac{(0+(1-1)\times 1)+1-1}{2\times 1} \right\rfloor = 0 \\ \phi'(p'_{11,21}) = \phi(p_1) = 0 \end{cases}$$

**for**  $i = 2$

$$j = \left\lfloor \frac{(0+(2-1)\times 1)+1-1}{2} \bmod(2\times 1) \right\rfloor + 1 = 1$$

Add place  $p'_{12,21}$  to place set  $P'$  of TEG.

Set:

$$\begin{cases} w'(t'_2, p'_{12,21}) = 1 \\ w'(p'_{12,21}, t'_2) = 1 \\ \mathcal{M}^{0'}(p'_{12,21}) = \left\lfloor \frac{(0+(2-1)\times 1)+1-1}{2\times 1} \right\rfloor = 0 \\ \phi'(p'_{12,21}) = \phi(p_1) = 0 \end{cases}$$

**Basic Path 2** ( $t_2, p_2, t_2$ ):

$$1 \leq i \leq 1$$

$$1 \leq k \leq 1$$

$$j = \left\lfloor \frac{(1+(1-1) \times 1) + 1 - 1}{1} \bmod (1 \times 1) \right\rfloor + 1 = 1$$

Add place  $p'_{2_1,2_1}$  to place set  $P'$  of TEG.

Set:

$$\begin{cases} w'(t'_{2_1}, p'_{2_1,2_1}) = 1 \\ w'(p'_{2_1,2_1}, t'_{2_1}) = 1 \\ \mathcal{M}^{0'}(p'_{2_1,2_1}) = \left\lfloor \frac{(1+(1-1) \times 1 + 1 - 1)}{1 \times 1} \right\rfloor = 1 \\ \phi'(p'_{2_1,2_1}) = \phi(p_2) = 2 \end{cases}$$

**Basic Path 3**  $(t_2, p_3, t_3)$ :

$$1 \leq i \leq 1$$

$$1 \leq k \leq 2$$

**for**  $k = 1$

$$j = \left\lfloor \frac{(0+(1-1) \times 2) + 1 - 1}{1} \bmod (1 \times 2) \right\rfloor + 1 = 1$$

Add place  $p'_{2_1,3_1}$  to place set  $P'$  of TEG.

Set:

$$\begin{cases} w'(t'_{2_1}, p'_{2_1,3_1}) = 1 \\ w'(p'_{2_1,3_1}, t'_{3_1}) = 1 \\ \mathcal{M}^{0'}(p'_{2_1,3_1}) = \left\lfloor \frac{(0+(1-1) \times 2 + 1 - 1)}{1 \times 2} \right\rfloor = 0 \\ \phi'(p'_{2_1,3_1}) = \phi(p_3) = 0 \end{cases}$$

**for**  $k = 2$

$$j = \left\lfloor \frac{(0+(1-1) \times 1) + 2 - 1}{1} \bmod (1 \times 2) \right\rfloor + 1 = 2$$

Add place  $p'_{2_1,3_2}$  to place set  $P'$  of TEG.

Set:

$$\begin{cases} w'(t'_{2_1}, p'_{2_1,3_2}) = 1 \\ w'(p'_{2_1,3_2}, t'_{3_2}) = 1 \\ \mathcal{M}^{0'}(p'_{2_1,3_2}) = \left\lfloor \frac{(0+(1-1) \times 2 + 2 - 1)}{1 \times 2} \right\rfloor = 0 \\ \phi'(p'_{2_1,3_2}) = \phi(p_3) = 0 \end{cases}$$

Step 4: Loop between duplicated transitions:

**for**  $\xi(t_1)$

**for**  $1 \leq i < 2$

Add place  $(p'_{1_1,1_2})$  to place set  $P'$  of TEG

Set:

$$\begin{cases} w'(t'_1, p'_{1_1,1_2}) = 1 \\ w'(p'_{1_1,1_2}, t'_1) = 1 \\ \mathcal{M}^{0'}(p'_{1_1,1_2}) = 0 \\ \phi'(p'_{1_1,1_2}) = 0 \end{cases}$$

Add place  $(p'_{1_2,1_1})$  to place set  $P'$  of TEG

Set:

$$\begin{cases} w'(t'_{1_2}, p'_{1_2,1_1}) = 1 \\ w'(p'_{1_2,1_1}, t'_{1_1}) = 1 \\ \mathcal{M}^{0'}(p'_{1_2,1_1}) = 1 \\ \phi'(p'_{1_2,1_1}) = 0 \end{cases}$$

**for**  $\xi(t_3)$

**for**  $1 \leq i < 2$

Add place  $(p'_{3_1,3_2})$  to place set  $P'$  of TEG

Set:

$$\begin{cases} w'(t'_{3_1}, p'_{3_1,3_2}) = 1 \\ w'(p'_{3_1,3_2}, t'_{3_2}) = 1 \\ \mathcal{M}^{0'}(p'_{3_1,3_2}) = 0 \\ \phi'(p'_{3_1,3_2}) = 0 \end{cases}$$

Add place  $(p'_{3_2,3_1})$  to place set  $P'$  of TEG

Set:

$$\begin{cases} w'(t'_{3_2}, p'_{3_2,3_1}) = 1 \\ w'(p'_{3_2,3_1}, t'_{3_1}) = 1 \\ \mathcal{M}^{0'}(p'_{3_2,3_1}) = 1 \\ \phi'(p'_{3_2,3_1}) = 0 \end{cases}$$

Figure 2.16 shows the TEG corresponding to the consistent WTEG of Figure 2.15. Transition  $t_1$  in Figure 2.15 is duplicated twice. It corresponds to transitions  $t_1^1$  and  $t_1^2$  of the corresponding TEG in Figure 2.16. Similarly, transition  $t_2$  corresponds to transition  $t_2^1$  and transition  $t_3$  is also duplicated twice and corresponds to transitions  $t_3^1$  and  $t_3^2$ .



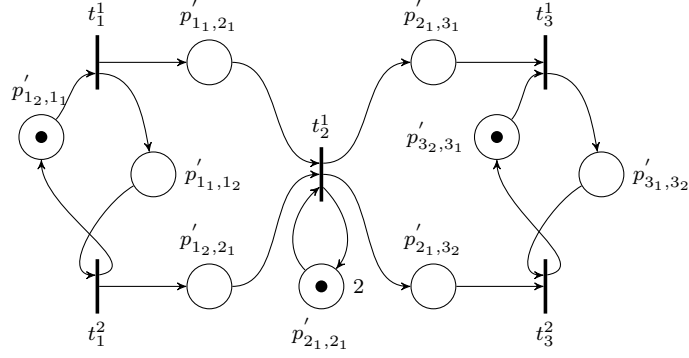


Figure 2.16: TEG corresponding to the consistent WTEG of Figure 2.15.

The associations of the number of firings with the firing times of each transition for the consistent WTEG and for the “equivalent” TEG are shown in Table 2.1 and Table 2.2, respectively. In both, it is assumed that they operate under the earliest firing rule. The firing times of the internal and output transitions are therefore uniquely determined based on the firing times of the input transitions. Here, the firing times of  $t_1$  on Table 2.1 have been arbitrarily chosen for the purpose of illustration, and those of  $t_1^1$  and  $t_1^2$  on Table 2.2, have then been determined accordingly.

Firing Times			
Firing	Input	Internal Transitions	Output
Count	$t_1$	$t_2$	$t_3$
1	0	1	1
2	1	3	1
3	2	—	3
4	3	—	3

Table 2.1: Firing Table for the consistent WTEG of Figure 2.15.

Firing Times					
Firing	Input		Internal Transitions	Output	
Count	$t_1^1$	$t_1^2$	$t_2^1$	$t_3^1$	$t_3^2$
1	0	1	1	1	1
2	2	3	3	3	3

Table 2.2: Firing Table for the TEG of Figure 2.16.

Comparing the two tables, note that the firing times of  $t_1$  in the WTEG correspond to the firing times of the input transitions in the TEG; the firing times of  $t_3$

in the WTEG correspond to the firing times of the output transitions in the TEG, and the firing times of  $t_2$  in the WTEG correspond to the firing times of  $t_2^1$  in the TEG. Therefore, the firing of a duplicated transition in the TEG corresponds to the firing of the original transition in the WTEG [23]. Moreover, note that, even though two transitions may fire (or the same transition may fire twice) “simultaneously” in terms of our digital time scale, the firings are logically sequenced. In our example, from Table 2.1 one can see that  $t_2$  and  $t_3$  can both fire at time 1; however, from the WTEG of Figure 2.15 it is clear that the firing of  $t_2$  must logically precede that of  $t_3$ . Similarly, although each firing of  $t_3^1$  and  $t_3^2$  in the TEG of Figure 2.16 corresponds to a firing of  $t_3$  in the WTEG of Figure 2.15 and, as shown in Table 2.2,  $t_3^1$  and  $t_3^2$  may fire at the same time instant (which corresponds to two firings of  $t_3$  at the same time instant), logically  $t_3^1$  and  $t_3^2$  fire alternately. So, for instance, the first firing of  $t_3^1$  at time 1 (Table 2.2) corresponds to the first firing of  $t_3$  at time 1 (Table 2.1), whereas the first firing of  $t_3^2$  at time 1 corresponds to the second firing of  $t_3$  at time 1.

An example is given now for illustrating the case in which internal transitions are duplicated.

**Example 10** Consider the consistent WTEG shown in Figure 2.17.

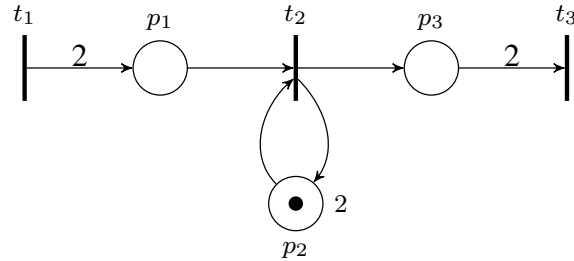


Figure 2.17: Consistent WTEG.

Following the algorithm steps.

Step 1: Computing the  $T$ -semiflow vector  $\xi$ :

$$\mathcal{W}\xi = 0$$

$$\begin{bmatrix} 2 & -1 & 0 \\ 0 & 0 & 0 \\ 0 & 1 & -2 \end{bmatrix} \times \begin{bmatrix} \xi_1 \\ \xi_2 \\ \xi_3 \end{bmatrix} = \begin{bmatrix} 0 \\ 0 \\ 0 \end{bmatrix}$$

$$\xi = \begin{bmatrix} 1 & 2 & 1 \end{bmatrix}^T$$

Step 2: The transition set  $T'$  of TEG is:  $T' = \{t_1^1, t_2^1, t_2^2, t_3^1\}$ .

Step 3: **for** each basic path in the WTEG:

**Basic Path 1**  $(t_1, p_1, t_2)$ :

$$1 \leq i \leq 1$$

$$1 \leq k \leq 2$$

**for**  $k = 1$

$$j = \left\lfloor \frac{(0+(1-1) \times 2) + 1 - 1}{1} \bmod (1 \times 2) \right\rfloor + 1 = 1$$

Add place  $p'_{1,2_1}$  to place set  $P'$  of TEG.

Set:

$$\begin{cases} w'(t'_1, p'_{1,2_1}) = 1 \\ w'(p'_{1,2_1}, t'_{2_1}) = 1 \\ \mathcal{M}^{0'}(p'_{1,2_1}) = \left\lfloor \frac{(0+(1-1) \times 2 + 1 - 1)}{1 \times 2} \right\rfloor = 0 \\ \phi'(p'_{1,2_1}) = \phi(p_1) = 0 \end{cases}$$

**for**  $k = 2$

$$j = \left\lfloor \frac{(0+(1-1) \times 2) + 2 - 1}{1} \bmod (1 \times 2) \right\rfloor + 1 = 2$$

Add place  $p'_{1,2_2}$  to place set  $P'$  of TEG.

Set:

$$\begin{cases} w'(t'_1, p'_{1,2_2}) = 1 \\ w'(p'_{1,2_2}, t'_{2_2}) = 1 \\ \mathcal{M}^{0'}(p'_{1,2_2}) = \left\lfloor \frac{(0+(1-1) \times 2 + 2 - 1)}{1 \times 2} \right\rfloor = 0 \\ \phi'(p'_{1,2_2}) = \phi(p_1) = 0 \end{cases}$$

**Basic Path 2**  $(t_2, p_2, t_2)$ :

$$1 \leq i \leq 2$$

$$1 \leq k \leq 1$$

**for**  $i = 1$

$$j = \left\lfloor \frac{(1+(1-1) \times 1) + 1 - 1}{1} \bmod (1 \times 2) \right\rfloor + 1 = 2$$

Add place  $p'_{2,2_2}$  to place set  $P'$  of TEG.

Set:

$$\begin{cases} w'(t'_2, p'_{2,2_2}) = 1 \\ w'(p'_{2,2_2}, t'_{2_2}) = 1 \\ \mathcal{M}^{0'}(p'_{2,2_2}) = \left\lfloor \frac{(1+(1-1) \times 1 + 1 - 1)}{1 \times 2} \right\rfloor = 0 \\ \phi'(p'_{2,2_2}) = \phi(p_2) = 2 \end{cases}$$

**for**  $i = 2$

$$j = \left\lfloor \frac{(1+(2-1)\times 1)+1-1}{1} \bmod (1\times 2) \right\rfloor + 1 = 1$$

Add place  $p'_{2_2,2_1}$  to place set  $P'$  of TEG.

Set:

$$\begin{cases} w'(t'_{2_2}, p'_{2_2,2_1}) = 1 \\ w'(p'_{2_2,2_1}, t'_{2_1}) = 1 \\ \mathcal{M}^{0'}(p'_{2_2,2_1}) = \left\lfloor \frac{(1+(2-1)\times 1)+1-1}{1\times 2} \right\rfloor = 1 \\ \phi'(p'_{1_1,2_2}) = \phi(p_2) = 2 \end{cases}$$

**Basic Path 3**  $(t_2, p_3, t_3)$ :

$$1 \leq i \leq 2$$

$$1 \leq k \leq 1$$

**for**  $i = 1$

$$j = \left\lfloor \frac{(0+(1-1)\times 1)+1-1}{2} \bmod (2\times 1) \right\rfloor + 1 = 1$$

Add place  $p'_{2_1,3_1}$  to place set  $P'$  of TEG.

Set:

$$\begin{cases} w'(t'_{2_1}, p'_{2_1,3_1}) = 1 \\ w'(p'_{2_1,3_1}, t'_{3_1}) = 1 \\ \mathcal{M}^{0'}(p'_{2_1,3_1}) = \left\lfloor \frac{(0+(1-1)\times 1)+1-1}{2\times 1} \right\rfloor = 0 \\ \phi'(p'_{2_1,3_1}) = \phi(p_3) = 0 \end{cases}$$

**for**  $i = 2$

$$j = \left\lfloor \frac{(0+(2-1)\times 1)+1-1}{2} \bmod (2\times 1) \right\rfloor + 1 = 1$$

Add place  $p'_{2_2,3_1}$  to place set  $P'$  of TEG.

Set:

$$\begin{cases} w'(t'_{2_2}, p'_{2_2,3_1}) = 1 \\ w'(p'_{2_2,3_1}, t'_{3_1}) = 1 \\ \mathcal{M}^{0'}(p'_{2_2,3_1}) = \left\lfloor \frac{(0+(2-1)\times 1)+1-1}{2\times 1} \right\rfloor = 0 \\ \phi'(p'_{2_1,3_2}) = \phi(p_3) = 0 \end{cases}$$

In this Example step 4 is not necessary.

Figure 2.18 shows the TEG corresponding to the consistent WTEG of Figure 2.17.

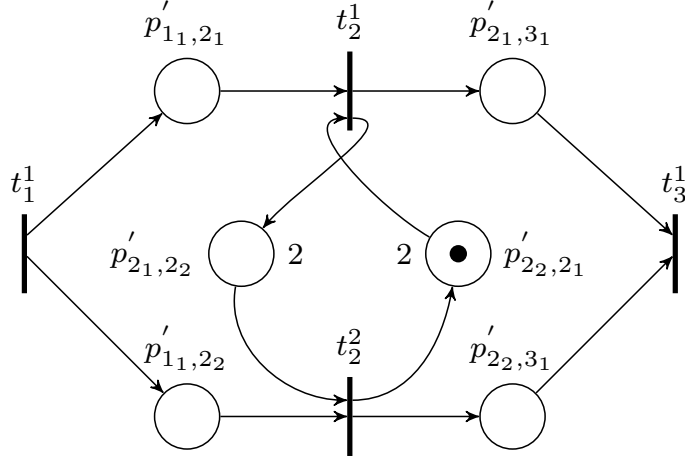


Figure 2.18: TEG corresponding to the consistent WTEG of Figure 2.17.

The firing tables of the consistent WTEG of Figure 2.15 and of the equivalent TEG of Figure 2.18 are shown in Table 2.3 and Table 2.4, respectively. In both, it is assumed that they operate under the earliest firing rule.

		Firing Times		
Firing Count	Input	Internal Transitions		Output
	$t_1$	$t_2$	$t_3$	
1	0	0	2	2
2	1	2	6	6
3	—	4	—	—
4	—	6	—	—

Table 2.3: Firing Table for the WTEG of Figure 2.17.

		Firing Times		
Firing Count	Input	Internal Transitions		Output
	$t_1^1$	$t_2^1$	$t_2^2$	$t_3^1$
1	0	0	2	2
2	1	4	6	6

Table 2.4: Firing Table for the TEG of Figure 2.18.

Comparing the two tables, note that the firing times of  $t_1$  in the WTEG correspond to the firing times of  $t_1^1$  in the TEG; the firing times of  $t_3$  in the WTEG correspond to the firing times of  $t_3^1$  in the TEG and the firing times of  $t_2$  in the WTEG correspond to the firing times of  $t_2^1$  and  $t_2^2$  in the TEG.

Additionally, in our example, from Table 2.3, one can see that  $t_1$  and  $t_2$  can both fire at time 0; however, from the WTEG of Figure 2.17 it is clear that the firing of  $t_1$  must logically precede that of  $t_2$ . Similarly, each firing of  $t_2^1$  and  $t_2^2$  in the TEG of Figure 2.18 corresponds to a firing of  $t_2$  in the WTEG of Figure 2.17 as shown in Table 2.4. However,  $t_2^1$  and  $t_2^2$  may not fire at the same time instant (because there are holding times in the loop). So, for instance, the first firing of  $t_2^1$  at time 0 (Table 2.4) corresponds to the first firing of  $t_2$  at time 0 (Table 2.3), whereas the first firing of  $t_2^2$  at time 2 corresponds to the second firing of  $t_2$  at time 2.

# Chapter 3

## Algebraic background

The computation of the earliest possible firing times for transitions in TEGs can be done iteratively; however, to optimize this process, some algebraic concepts to obtain a linear representation of the transitions' firing instants are used. This chapter summarizes these algebraic settings. In order to do so, it is divided into five sections: in Section 3.1, the basic notions about dioids are presented; in Section 3.2, matrix dioids are introduced; in Section 3.3, some concepts about mapping defined over dioids are described; in Section 3.4, the residuation theory is presented; and in Section 3.5, dioid models of TEGs are introduced.

### 3.1 Dioids

In the first place, a few basic notions from ordered sets are listed, with the main purpose of clarifying some technical terms that are used in dioid theory. For a deeper understanding of the subject, the interested reader may refer to [10].

**Definition 17 (Order relation)** *A binary relation (denoted  $\preceq$ ) on a set  $\mathcal{C}$  which  $\forall a, b, c \in \mathcal{C}$  is:*

- reflexive ( $a \preceq a$ ),
- antisymmetric ( $(a \preceq b \text{ and } b \preceq a) \Rightarrow a = b$ ),
- transitive ( $(a \preceq b \text{ and } b \preceq c) \Rightarrow a \preceq c$ ).

**Definition 18 (Ordered set)** *An ordered set, denoted by  $(\mathcal{C}, \preceq)$ , is defined as a set  $\mathcal{C}$  endowed with an order relation  $\preceq$ . If, for each pair of elements  $a, b \in \mathcal{C}$ , the order relation holds true either for  $a, b$  or for  $b, a$ , or otherwise established, if  $a$  and  $b$  are comparable, the order is total. If not,  $(\mathcal{C}, \preceq)$  is said to be partially ordered.*

**Example 11** *Classical examples of totally ordered sets are real  $(\mathbb{R}, \leq)$  and integer numbers  $(\mathbb{Z}, \leq)$  with respect to the classical “less or equal” order relation. In contrast, the ordered set  $(\mathbb{Z}^{2 \times 1}, \preceq)$ , where  $v_1 = [x_1 \ x_2]^T$  and  $v_2 = [y_1 \ y_2]^T$  are ordered, i.e.,  $v_1 \preceq v_2$ , if  $x_1 \leq y_1$  and  $x_2 \leq y_2$ , is only partially ordered, because it is not possible to compare all pairs of  $v_1$  and  $v_2$  with integer entries.*

**Definition 19 (Bounds on ordered set)** *An element  $c \in \mathcal{C}$ , given a non-empty subset  $\mathcal{B} \subseteq \mathcal{C}$ , is called an upper bound of  $\mathcal{B}$  if  $\forall b \in \mathcal{B} : b \preceq c$ . In the same way, an element  $a \in \mathcal{C}$  is called a lower bound of  $\mathcal{B}$  if  $\forall b \in \mathcal{B} : a \preceq b$ . If  $\mathcal{B}$  has an upper bound, its least upper bound (if it exists) is denoted  $\bigvee \mathcal{B}$ . If  $\mathcal{B}$  has a lower bound, its greatest lower bound (if it exists) is denoted  $\bigwedge \mathcal{B}$ .*

**Definition 20 (Diod)** *A dioid or idempotent semiring, denoted  $(\mathcal{D}, \oplus, \otimes)$ , is a set  $\mathcal{D}$  endowed with two binary operations  $\oplus$  and  $\otimes$ , for which the following axioms hold:*

- *Associativity of addition :  $\forall a, b, c \in \mathcal{D}$ ,*  

$$(a \oplus b) \oplus c = a \oplus (b \oplus c) .$$
- *Commutativity of addition:  $\forall a, b \in \mathcal{D}$ ,*  

$$(a \oplus b) = (b \oplus a) .$$
- *Associativity of multiplication:  $\forall a, b, c \in \mathcal{D}$ ,*  

$$(a \otimes b) \otimes c = a \otimes (b \otimes c) .$$
- *Distributivity of multiplication with respect to addition:  $\forall a, b, c \in \mathcal{D}$ ,*  

$$(a \oplus b) \otimes c = (a \otimes c) \oplus (b \otimes c),$$

$$c \otimes (a \oplus b) = (c \otimes a) \oplus (c \otimes b) .$$
- *Existence of a zero element:  $\exists \varepsilon \in \mathcal{D} : \forall a \in \mathcal{D}$ ,*  

$$a \oplus \varepsilon = a .$$
- *Absorbing zero element per multiplication:  $\forall a \in \mathcal{D}$ ,*  

$$a \otimes \varepsilon = \varepsilon \otimes a = \varepsilon .$$
- *Existence of an identity element:  $\exists e \in \mathcal{D} : \forall a \in \mathcal{D}$ ,*  

$$a \otimes e = e \otimes a = a .$$
- *Idempotency of addition:  $\forall a \in \mathcal{D}$ ,*  

$$a \oplus a = a .$$

**Remark 2** *A dioid  $(\mathcal{D}, \oplus, \otimes)$  is said to be commutative, if the operation  $\otimes$  commutes, i.e.,  $\forall a, b \in \mathcal{D}, ab = ba$ .*



**Remark 3** The symbol  $\otimes$  is usually omitted, as in conventional algebra.

**Remark 4** Note that the symbol  $\bigoplus$  refers to the sum in the corresponding dioid, in direct analogy to the summation symbol  $\Sigma$  in conventional algebra. E.g.,

$$\bigoplus_{i=1}^5 a_i = a_1 \oplus a_2 \oplus a_3 \oplus a_4 \oplus a_5.$$

**Definition 21 (Canonical order relation)** A canonical order in a dioid  $(\mathcal{D}, \oplus, \otimes)$  is naturally defined by the  $\oplus$  operation, i.e.,  $a \preceq b \Leftrightarrow a \oplus b = b$ .

**Definition 22 (Complete dioid)** A dioid is called complete if it is closed for infinite sums and if  $\otimes$  distributes over infinite sums, i.e., if  $\forall c \in \mathcal{D}$  and  $\forall \chi \subseteq \mathcal{D}$ :

$$c \otimes \left( \bigoplus_{x \in \chi} x \right) = \bigoplus_{x \in \chi} c \otimes x.$$

In a complete dioid  $(\mathcal{D}, \oplus, \otimes)$ , one can define the top element  $\top$  as the sum of all elements in the dioid, i.e.,  $\top = \bigoplus_{x \in \mathcal{D}} x$ .  $\top$  is absorbing for  $\oplus$  ( $\forall a \in \mathcal{D}, \top \oplus a = \top$ ) and we have  $\top \otimes \varepsilon = \varepsilon \otimes \top = \varepsilon$ .

**Definition 23 (Greatest lower bound)** The greatest lower bound of  $a, b \in \mathcal{D}$ , where  $(\mathcal{D}, \oplus, \otimes)$  is a complete dioid, is defined as

$$a \wedge b = \bigoplus_{x \preceq a, x \preceq b} x,$$

where  $\wedge$  is associative, commutative and idempotent. Moreover, the following equivalences hold:

$$a \preceq b \Leftrightarrow b = a \oplus b \Leftrightarrow a = a \wedge b. \quad (3.1)$$

**Example 12 (Max-plus algebra)** The Max-plus algebra is a complete dioid denoted  $(\bar{\mathbb{Z}}_{max}, \oplus, \otimes)$ . It is defined over the set  $\bar{\mathbb{Z}}_{max} = \mathbb{Z} \cup \{-\infty, +\infty\}$  with the following binary operations:

- addition:  $a \oplus b := \max(a, b), \forall a, b \in \bar{\mathbb{Z}}_{max}$ ,
- multiplication:  $a \otimes b := a + b, \forall a, b \in \bar{\mathbb{Z}}_{max}$ .

The zero element is defined as  $\varepsilon = -\infty$ , the unit element is  $e = 0$ ,  $a \wedge b = \min(a, b)$  and the top element is  $\top = +\infty$ . In Max-plus algebra the order relation  $\preceq$  induced by  $\oplus$  corresponds to the natural order on  $\mathbb{Z}$ . Hence, for two elements  $a = 6$  and  $b = 2$ ,  $a \oplus b = 6 \oplus 2 = 6$ , which indicates that  $6 \succeq 2$  in  $\bar{\mathbb{Z}}_{max}$ .

**Example 13** *The following numerical examples illustrates the binary operations in Max-plus algebra:*

$$3 \oplus 5 = \max(3, 5) = 5,$$

$$2 \otimes 7 = 2 + 7 = 9,$$

$$3 \oplus \varepsilon = \max(3, -\infty) = 3,$$

$$2 \otimes \varepsilon = 2 - \infty = -\infty = \varepsilon,$$

$$3 \oplus e = \max(3, 0) = 3,$$

$$5 \otimes -8 \oplus 4 \otimes 1 = -3 \oplus 5 = 5.$$

To solve implicit inequalities and equations over a complete dioid  $(\mathcal{D}, \oplus, \otimes)$ , the following theorem is presented:

**Theorem 1** ([10] and [3]) *The implicit equation  $x = ax \oplus b$  and the implicit inequality  $x \succeq ax \oplus b$ , given  $a$  and  $b$  elements in a complete dioid  $(\mathcal{D}, \oplus, \otimes)$ , admit  $x = a^*b$  as the least solution, where  $a^* = \bigoplus_{i \geq 0} a^i$  (Kleene star operator).*

On a complete dioid, the Kleene star operator is defined by:

$$a^* = e \oplus a \oplus a^2 \oplus \dots = \bigoplus_{i \in \mathbb{N}_0} a^i.$$

Some properties of the Kleene star operator (\*) are summarized bellow. These properties hold for any complete dioid. The following equalities are taken from [3]:

1.  $(a \oplus b)^* = (a^*b)^*a^* = (b^*a)^*b$ ,
2.  $a^*a^* = a^*$ ,
3.  $(a^*)^* = a^*$ ,
4.  $a(ba)^* = (ab)^*a$ ,
5.  $(ab^*)^* = e \oplus a(a \oplus b)^*$ ,
6.  $a^* \preceq b^* \Leftrightarrow a^*b^* = b^*$ ,
7.  $ax \preceq x \Leftrightarrow a^*x = x$ .

## 3.2 Matrix dioids

In analogy to conventional algebra, addition and multiplication can be extended to matrices (of correct dimensions) with entries in a dioid  $(\mathcal{D}, \oplus, \otimes)$ , that is:

$$(A \oplus B)_{ij} = a_{ij} \oplus b_{ij}, \quad A, B \in \mathcal{D}^{m \times n}, \quad (3.2)$$

$$(C \otimes D)_{ik} = \bigoplus_{j=1}^n (c_{ij} \otimes d_{jk}), \quad C \in \mathcal{D}^{m \times n}, D \in \mathcal{D}^{n \times p}. \quad (3.3)$$

A (partial) order on the set of matrices with entries in  $\mathcal{D}$  is induced by the element-wise order  $\preceq$  on  $\mathcal{D}$ . This means that, for matrices  $A, B \in \mathcal{D}^{m \times n}$ , the following equivalence holds:

$$A \preceq B \Leftrightarrow a_{ij} \preceq b_{ij} \quad \forall i \in [1, m], \forall j \in [1, n]. \quad (3.4)$$

A (complete) dioid is formed by the set of square  $(n \times n)$  matrices with entries in a (complete) dioid  $\mathcal{D}$  jointly with the operations  $\oplus$  and  $\otimes$  described above.

The identity matrix (one element) of  $\mathcal{D}^{n \times n}$  has entries equal to  $e$  on the diagonal and  $\varepsilon$  elsewhere; it is denoted  $\mathcal{I}_n$ . The zero matrix (zero element) of  $\mathcal{D}^{n \times n}$  has all entries equal to  $\varepsilon$  and it is simply denoted  $\varepsilon$ . Moreover, the order defined in (3.4) is consistent with Definition 21, *i.e.*:

$$A \preceq B \Leftrightarrow A \oplus B = B.$$

The Kleene star operation can be extended to square matrices with entries in a complete dioid. Let  $A \in \mathcal{D}^{n \times n}$  be such a matrix, so:

$$A^* = \bigoplus_{i \geq 0} A^i$$

where  $A^0 = \mathcal{I}_n$  is equal to the identity matrix.

**Lemma 1** ([24]) *For  $a \in \mathcal{D}^{n \times n}$  partitioned into four blocks, that is to say:*

$$a = \begin{bmatrix} a_{11} & a_{12} \\ a_{21} & a_{22} \end{bmatrix},$$

$$a^* = \begin{bmatrix} a_{11}^* \oplus a_{11}^* a_{12} (a_{21} a_{11}^* a_{12} \oplus a_{22})^* a_{21} a_{11}^* & a_{11}^* a_{12} (a_{21} a_{11}^* a_{12} \oplus a_{22})^* \\ (a_{21} a_{11}^* a_{12} \oplus a_{22})^* a_{21} a_{11}^* & (a_{21} a_{11}^* a_{12} \oplus a_{22})^* \end{bmatrix}.$$

In [3], an algorithm for the computation of  $A^*$ , with  $A \in \mathcal{D}^{n \times n}$  and  $\mathcal{D}$  being a complete dioid, was developed, and it is a straightforward application of Lemma 1.

### 3.3 Mappings

This section describes some concepts about mappings defined over dioids.

**Definition 24 (Isotone, antitone, monotone)** *Let  $\Pi : \mathcal{D} \rightarrow \mathcal{C}$  be a mapping from a dioid  $(\mathcal{D}, \oplus, \otimes)$  into another dioid  $(\mathcal{C}, \oplus, \otimes)$ :*

- *mapping  $\Pi$  is isotone if it is order preserving, i.e.,  $\forall x, x' \in \mathcal{D}$  the following implication holds:  $x \preceq x' \Rightarrow \Pi(x) \preceq \Pi(x')$ ,*
- *mapping  $\Pi$  is antitone if it is order reversing, i.e.,  $\forall x, x' \in \mathcal{D}$  the following implication holds:  $x \preceq x' \Rightarrow \Pi(x) \succeq \Pi(x')$ ,*
- *mapping  $\Pi$  is monotone if it is isotone or antitone.*

**Remark 5** *If a mapping  $\Pi$  from a dioid  $(\mathcal{D}, \oplus, \otimes)$  into another dioid  $(\mathcal{C}, \oplus, \otimes)$  is isotone, the following inequalities hold:*

$$\Pi(x \oplus x') \succeq \Pi(x) \oplus \Pi(x') \quad \forall x, x' \in \mathcal{D},$$

$$\Pi(x \wedge x') \preceq \Pi(x) \wedge \Pi(x') \quad \forall x, x' \in \mathcal{D}.$$

### 3.4 Residuation Theory

Generally, multiplication in dioids does not admit an inverse. However, residuation theory provides a pseudo inversion for specific mappings defined over ordered sets. For details about this theory, one can consult [25]. Using residuation theory, it is possible to compute the greatest solution of inequalities of the form  $f(x) \preceq b$ .

**Definition 25 (Residuated mapping and Residual)** *Let  $f : \mathcal{D} \rightarrow \mathcal{C}$  be an isotone mapping, with  $\mathcal{D}$  and  $\mathcal{C}$  being complete dioids. If for all  $y \in \mathcal{C}$  the inequality  $f(x) \preceq y$  has a greatest solution in  $\mathcal{D}$ ,  $f$  is a residuated mapping. This greatest solution is denoted by  $f^\sharp(y)$ .*

*The mapping  $f^\sharp : \mathcal{C} \rightarrow \mathcal{D}, y \mapsto \bigoplus \{x \in \mathcal{D} \mid f(x) \preceq y\}$  is called the residual of  $f$ .*

$f^\sharp(y)$  provides the greatest solution of equality  $f(x) = y$ , if the equality is solvable.

For a residuated mapping  $f : \mathcal{D} \rightarrow \mathcal{C}$ , the following equalities hold:

$$f \circ f^\sharp \circ f = f,$$

$$f^\sharp \circ f \circ f^\sharp = f^\sharp.$$

In Figure 3.1, an illustration of these properties taken from [2] is given :

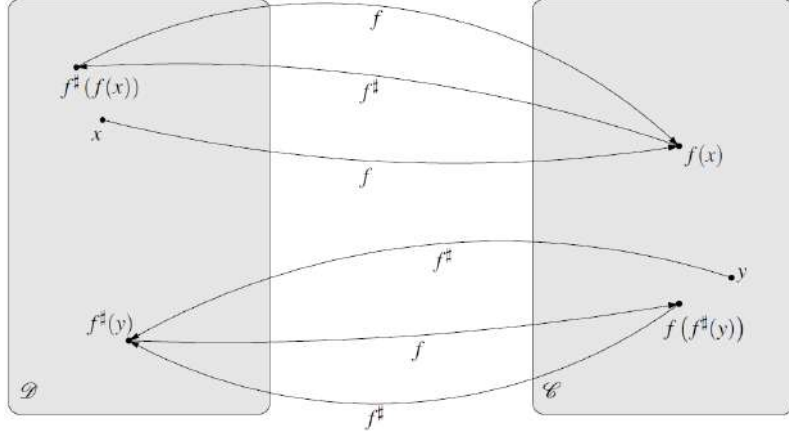


Figure 3.1: Properties of residuated mapping  $f : \mathcal{D} \rightarrow \mathcal{C}$  and the corresponding residual mapping  $f^\# : \mathcal{C} \rightarrow \mathcal{D}$  [2].

### 3.4.1 Residual of right and left product

Two elementary mappings in a complete dioid  $(\mathcal{D}, \oplus, \otimes)$ , namely the left and right multiplication by a constant, are residuated mappings, *i.e.*:

$$L_a : \mathcal{D} \rightarrow \mathcal{D}$$

$$x \mapsto a \otimes x$$

$$R_a : \mathcal{D} \rightarrow \mathcal{D}$$

$$x \mapsto x \otimes a$$

The corresponding residual mappings are denoted:

$$L_a^\#(x) = a \backslash x$$

$$R_a^\#(x) = x / a$$

The greatest solution for  $a \otimes x \preceq b$  is  $L_a^\#(b) = a \backslash b = \bigoplus_{x \in \mathcal{D}} \{x \mid ax \preceq b\}$ .

The greatest solutions of matrix inequalities can also be obtained using residuation theory. The order relation  $\preceq$  is interpreted element-wise. Given matrices  $A, D \in \mathcal{D}^{m \times n}$ ,  $B \in \mathcal{D}^{m \times p}$  and  $C \in \mathcal{D}^{n \times p}$ , the greatest solution of inequality  $A \otimes X \preceq B$  is given by  $C = A \backslash B$  and the greatest solution of inequality  $X \otimes C \preceq B$  is given by  $D = B / C$ . The entries of  $C$  and  $D$  are determined as follows:

$$C_{ij} = \bigwedge_{k=1}^m (A_{ki} \setminus B_{kj}), \quad \forall i \in [1, n], \forall j \in [1, p],$$

$$D_{ij} = \bigwedge_{k=1}^p (B_{ik} \setminus C_{jk}), \quad \forall i \in [1, m], \forall j \in [1, n].$$

### 3.5 Dioid models of TEGs

The dynamics of a TEG can be modelled by linear equations in the Max-plus algebra. For this, a dater function  $d : \mathbb{Z} \rightarrow \bar{\mathbb{Z}}_{max}$  is associated to each transition such that  $\forall k \in \mathbb{Z}$ ,  $d(k)$  represents the time of the  $k$ -th firing of the related transition. By convention,  $d(k) = -\infty$  for any  $k \leq 0$ , and  $d(k) = +\infty$  if the  $k$ -th firing never takes place. The set of dater functions is denoted by  $\Sigma$ . The set of transitions of a TEG is partitioned into:

- internal transitions: a set of transitions  $x_i, i = 1, \dots, n$ , with both upstream and downstream places;
- output transitions: a set of transitions  $y_i, i = 1, \dots, m$ , with only upstream places;
- input transitions: a set of transitions with only downstream places that is divided as:
  - controllable input transitions: a set of input transitions  $u_i, i = 1, \dots, p$ , with freely assignable firing times.
  - uncontrollable input transitions: a set of input transitions  $w_i, i = 1, \dots, l$ , with unknown firing times, that can be interpreted as disturbances.

A TEG operating under the earliest firing rule can be described by the following Max-plus linear system:

$$x(k) = \bigoplus_{j=0}^{N_a} A_j x(k-j) \oplus \bigoplus_{j=0}^{N_b} B_j u(k-j) \oplus R_0 w(k), \quad (3.5)$$

$$y(k) = C_0 x(k), \quad (3.6)$$

where the vector function  $x : \mathbb{Z} \rightarrow \bar{\mathbb{Z}}_{max}^n$  are the internal dater functions; the vector function  $u : \mathbb{Z} \rightarrow \bar{\mathbb{Z}}_{max}^p$  are the controllable input dater functions; the vector function  $w : \mathbb{Z} \rightarrow \bar{\mathbb{Z}}_{max}^l$  are the uncontrollable input dater functions and the vector function  $y : \mathbb{Z} \rightarrow \bar{\mathbb{Z}}_{max}^m$  are the output dater functions. The integer number  $N_a$  (respectively

$N_b$ ) is equal to the maximal number of tokens initially available in places between internal transitions (respectively in places between controllable input transitions and internal transitions). Matrices  $A_j \in \bar{\mathbb{Z}}_{max}^{n \times n}$ ,  $B_j \in \bar{\mathbb{Z}}_{max}^{n \times p}$ ,  $R_0 \in \bar{\mathbb{Z}}_{max}^{n \times l}$  and  $C_0 \in \bar{\mathbb{Z}}_{max}^{m \times n}$ , represent the structure of the TEG.

**Remark 6** *In this modeling, it is assumed, that each input transition and each output transition are linked to only one internal transition, which results in that each column of matrix  $B_j$  has one entry equal to  $e$  and the others equal to  $\varepsilon$  and each row of matrix  $C_0$  has one entry equal to  $e$  and the others equal to  $\varepsilon$ .*

Example 14 withdraws from [3] demonstrates how to model a TEG as a Max-plus linear system.

**Example 14** *Figure 3.2 depicts a TEG with controllable input transition  $p = 1$ , uncontrollable input transitions  $l = 2$  and measurable output transition  $m = 1$ . The maximal number of tokens initially in places between internal transitions is  $N_a = 2$  and the maximal number of tokens initially in places between controllable input transitions and internal transitions is  $N_b = 0$ .*

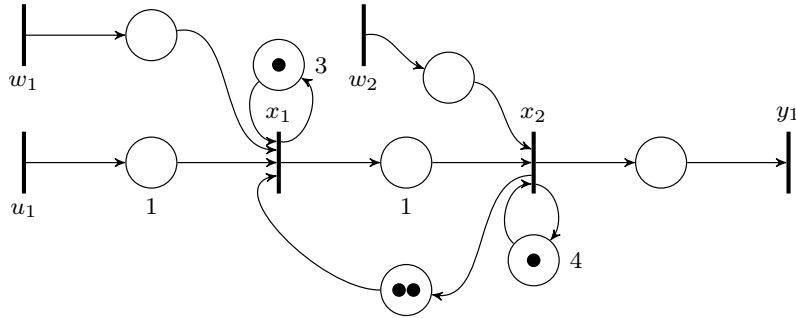


Figure 3.2: TEG with one controllable input transition ( $u_1$ ), two uncontrollable input transitions ( $w_1, w_2$ ) and one measurable output transition ( $y_1$ ).

*The system matrices of the TEG model by the Max-plus linear system in Equations (3.5) and (3.6) are:*

$$A_0 = \begin{bmatrix} \varepsilon & \varepsilon \\ 1 & \varepsilon \end{bmatrix}, A_1 = \begin{bmatrix} 3 & \varepsilon \\ \varepsilon & 4 \end{bmatrix},$$

$$A_2 = \begin{bmatrix} \varepsilon & e \\ \varepsilon & \varepsilon \end{bmatrix}, B_0 = \begin{bmatrix} 1 \\ \varepsilon \end{bmatrix},$$

$$C_0 = \begin{bmatrix} \varepsilon & e \end{bmatrix}, R_0 = \begin{bmatrix} e & \varepsilon \\ \varepsilon & e \end{bmatrix}.$$

The matrix  $A_i$ ,  $i = 0, 1, 2$  represents the holding times between the internal transitions  $x_1$  and  $x_2$ , where  $i$  is the number of initial tokens contained in the places. For instance, in matrix  $A_1$ , we are considering all internal transitions which are connected to places that contain one token. The entry  $(A_1)_{11} = 3$  represents the connection of the internal transition  $x_1$  with itself which has a holding time of 3 time units. The entries  $(A_1)_{12} = (A_1)_{21} = \varepsilon$ , because there is no place with a single token between  $x_1$  and  $x_2$  and between  $x_2$  and  $x_1$ , respectively. The entry  $(A_1)_{22} = 4$  represents the connection of the internal transition  $x_2$  with itself which has a holding time of 4 time units. Note that  $e$  in  $A_2$  represents that the place between  $x_2$  and  $x_1$  has two tokens and no holding time. The matrix  $B_0$  represents the holding times between the input transition  $u_1$  and the internal transitions  $x_1$  and  $x_2$ . The matrix  $C_0$  represents the holding times between the output transition  $y_1$  and the internal transitions  $x_1$  and  $x_2$ . The matrix  $R_0$  represents the holding times between the disturbances  $w_1$  and  $w_2$  and the internal transitions  $x_1$  and  $x_2$ . Note that  $R_0$  is equal to the identity matrix in  $\bar{\mathbb{Z}}_{max}$ , thus the internal transitions  $x_1$  and  $x_2$  are affected by the disturbances  $w_1$  and  $w_2$ , respectively.

The specific dioid on formal power series called  $\mathcal{M}_{in}^{ax}[\gamma, \delta]$  is suitable to obtain transfer functions for TEGs. For more details about the dioid  $\mathcal{M}_{in}^{ax}[\gamma, \delta]$  see Appendix A. In dioid  $\mathcal{M}_{in}^{ax}[\gamma, \delta]$  the variable  $\gamma$  is associated to the event-shift operator, *i.e.*,  $\forall x \in \Sigma: (\gamma^n x)(k) = x(k - n)$ , and the variable  $\delta$  is associated to the time-shift operator, *i.e.*,  $\forall x \in \Sigma: (\delta^\tau x)(k) = x(k) + \tau$ .

Figure 3.3 represents the model of a TEG in  $\mathcal{M}_{in}^{ax}[\gamma, \delta]$ , where  $\mathcal{M}_1^0$  is the initial marking of  $p_1$  and  $\phi_1$  is the holding time of  $p_1$ . Then, the earliest firing relation, shown in Definition 16, between transitions  $t_1$  and  $t_2$  of the following path is  $x_2 = \gamma^{\mathcal{M}_1^0} \delta^{\phi_1} x_1$ , where  $x_1, x_2$  are dater functions associated to transitions  $t_1$  and  $t_2$ ,  $\gamma$  is associated to initial marking and  $\delta$  is associated to holding times, and both form the dioid  $\mathcal{M}_{in}^{ax}[\gamma, \delta]$ .

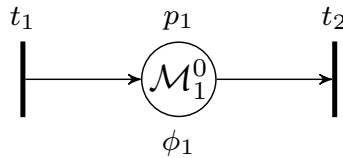


Figure 3.3: Model of a TEG in  $\mathcal{M}_{in}^{ax}[\gamma, \delta]$ .

Complete TEGs can be modeled in the following form:

$$x = Ax \oplus Bu \oplus Rw \tag{3.7}$$

$$y = Cx \tag{3.8}$$



where  $x \in \mathcal{M}_{in}^{ax}[[\gamma, \delta]]^n$  is the state,  $u \in \mathcal{M}_{in}^{ax}[[\gamma, \delta]]^p$  is the controllable input,  $y \in \mathcal{M}_{in}^{ax}[[\gamma, \delta]]^m$  is the output and  $w \in \mathcal{M}_{in}^{ax}[[\gamma, \delta]]^l$  are the disturbances.  $A \in \mathcal{M}_{in}^{ax}[[\gamma, \delta]]^{n \times n}$ ,  $B \in \mathcal{M}_{in}^{ax}[[\gamma, \delta]]^{n \times p}$ ,  $C \in \mathcal{M}_{in}^{ax}[[\gamma, \delta]]^{m \times n}$  and  $R \in \mathcal{M}_{in}^{ax}[[\gamma, \delta]]^{m \times l}$  are matrices which represent the influence of transitions on one another.

**Example 15** *The TEG showed in Figure 3.2 can be described in  $\mathcal{M}_{in}^{ax}[[\gamma, \delta]]$  using the Equations (3.7) and (3.8). The system matrices are given as:*

$$A = \begin{bmatrix} \delta^3\gamma^1 & \delta^0\gamma^2 \\ \delta^1\gamma^0 & \delta^4\gamma^1 \end{bmatrix}, B = \begin{bmatrix} \delta^1\gamma^0 \\ \varepsilon \end{bmatrix},$$

$$C = \begin{bmatrix} \varepsilon & e \end{bmatrix}, R = \begin{bmatrix} e & \varepsilon \\ \varepsilon & e \end{bmatrix}.$$

The entry  $a_{11} = \delta^3\gamma^1$  represents the place linking transition  $t_1$  to itself and indicates that this place has a holding time of 3 time units and initially contains one token.

**Theorem 2** ([3]) *Considering Theorem 1, under the earliest functioning rule, a solution for (3.7) and (3.8) can be obtained and the state and output trajectories can be rewritten as:*

$$x = A^*Bu \oplus A^*Rw \quad (3.9)$$

$$y = CA^*Bu \oplus CA^*Rw \quad (3.10)$$

where  $CA^*B \in \mathcal{M}_{in}^{ax}[[\gamma, \delta]]^{m \times p}$  is the input/output matrix and  $CA^*R \in \mathcal{M}_{in}^{ax}[[\gamma, \delta]]^{m \times l}$  is the disturbance/output matrix.

In other words,  $CA^*B$  and  $CA^*R$  are the transfer function matrices. They represent the earliest behavior of the system. The uncontrollable input vector  $w$  is only able to delay the firing times of internal and output transitions, *i.e.*, to delay the occurrence of the corresponding events.

**Example 16** *The input-output transfer function matrix of the system shown in Figure 3.2 is equal to:*

$$H = CA^*B = \begin{bmatrix} \varepsilon & e \end{bmatrix} A^* \begin{bmatrix} \delta^1\gamma^0 \\ \varepsilon \end{bmatrix} = \delta^2\gamma^0(\delta^4\gamma^1)^*$$

where  $H$  is called the transfer function matrix of the TEG.  $H = \delta^2\gamma^0(\delta^4\gamma^1)^*$  describes the transfer relation between the controllable input  $u_1$  and the output  $y_1$  of the TEG shown in Figure 3.2. The transfer relation represents the impulse response of a system, as in control theory. Ultimately, if the TEG operates under the earliest

firing rule and if the uncontrollable input does not slow down the system, given a sequence of firing times of  $u$ ,  $y = CA^*Bu \in \mathcal{M}_{in}^{ax}[[\gamma, \delta]]$  encodes the sequence of firing times of  $y$ . In our example, applying an impulse at the input, i.e.,  $u = \delta^0\gamma^0$ ,  $y = CA^*B = \delta^2\gamma^0(\delta^4\gamma^1)^*$ . Thus, the impulse response represents the fastest system behavior.

$H$  is computed using the toolbox *MinMaxGD*, a C++ library developed in order to handle periodic series (see [26, 27]).  $A^*$  can be determined using the algorithm developed in [3]:

$$A^* = \begin{bmatrix} e \oplus \delta^3\gamma^1 \oplus \delta^6\gamma^2 \oplus \delta^9\gamma^3 \oplus \delta^{12}\gamma^4 \oplus \delta^{15}\gamma^5 \oplus \delta^{18}\gamma^6 \delta^{21}\gamma^7 (\delta^4\gamma^4)^* & \delta^0\gamma^2(\delta^4\gamma^1)^* \\ & \delta^1\gamma^0(\delta^4\gamma^1)^* & (\delta^4\gamma^1)^* \end{bmatrix}.$$

In this chapter, we resume the algebraic settings about dioids theory and its application in the modeling of TEGs. In the following, we present observer design for timed Petri nets. First, we introduce the Observer for TEGs. Then, it is shown how to obtain the Observer for WTEGs. Finally, we show how to implement the Observer for WTEGs in a final example.

# Chapter 4

## Observer Design for Timed Petri nets

Since the modeling preliminaries about Timed Petri nets were presented in Chapter 2 and the background theory about dioids was presented in Chapter 3, the observer design for timed Petri nets can be determined. In this Chapter, the Observer for TEGs is presented in Section 4.1. In Section 4.2, based on the algorithm to convert WTEGs into TEGs introduced in Section 2.3, the Observer for WTEGs is proposed. In Section 4.3, the implementation of the Observer for WTEGs following every step of the presented method is described and to better illustrate this work an example is shown.

### 4.1 Observer for TEGs

Let  $x$  be referred to as a state of the model in Equations (3.7) and (3.8) and  $\hat{x}$  be referred to as a estimated state. As described in Section 3.5,  $x$  is the vector of dater functions which are associated with the firing times of the internal transitions in the TEG. Usually, the state is not measurable for two main reasons: (i) it can be inaccessible, and (ii) the high cost required for measurement. For this reason, the state estimation is an important problem for DES. A way to solve this problem is an observer structure directly inspired by the Luenberger observer in classical linear systems theory [17] that is considered in [14] and [28]. For instance, this structure allows detecting a possible machine breakdown in the manufacturing line. Based on a TEG model, on the measured firing times of the output transitions and on the known controllable input transitions, the firing times of internal transitions are estimated. The observer structure is illustrated in Figure 4.1 and is composed of two parts:

1. simulator,

2. observer matrix  $L$ .

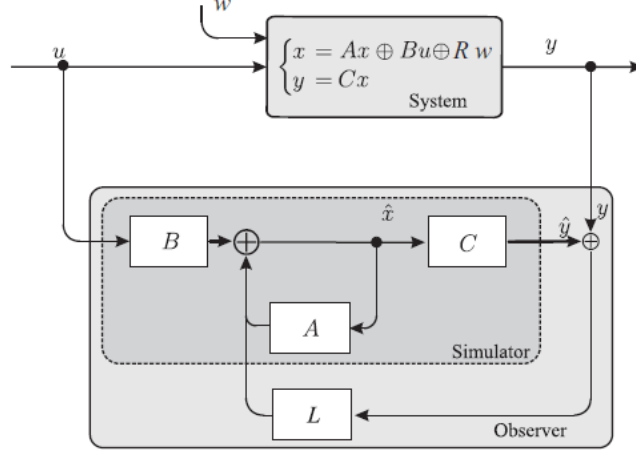


Figure 4.1: The observer structure of Max-plus linear systems [3].

The Simulator  $\mathcal{S}(P, T, w, \mathcal{M}^0, \phi)$  is described by the system model by Equations (3.7) and (3.8), except for the disturbance term  $Rw$ , as disturbances are uncontrollable and a priori unknown, the Simulator does not take them into account. It is characterized by the matrices  $A \in \mathcal{M}_{in}^{ax}[\gamma, \delta]^{n \times n}$ ,  $B \in \mathcal{M}_{in}^{ax}[\gamma, \delta]^{n \times p}$  and  $C \in \mathcal{M}_{in}^{ax}[\gamma, \delta]^{m \times n}$ . By assumption, the entries of matrix  $C \in \mathcal{M}_{in}^{ax}[\gamma, \delta]^{m \times n}$  are in  $\{\varepsilon, e\}$  and precisely in each row, one entry is equal to  $e$ . Note that this representation corresponds to the fastest behavior of the real system and, therefore, the disturbances can only delay its behavior [16].

The Observer Matrix  $L \in \mathcal{M}_{in}^{ax}[\gamma, \delta]^{n \times m}$  is used to provide information from the measurable system output into the Simulator to take the action of the disturbances  $w$  into account. To compute the Optimal Observer, the matrix  $L \in \mathcal{M}_{in}^{ax}[\gamma, \delta]^{n \times m}$  is chosen to be the greatest matrix, in the order of  $\mathcal{M}_{in}^{ax}[\gamma, \delta]$ , to achieve the constraint  $\hat{x} \preceq x$ . In other words, the estimated state  $\hat{x}_i$  gives an estimate for the firing times of the internal transition  $t_i$ , such that this estimate is as late as possible, but earlier than or at the same time as the firing time of the internal transition  $t_i$ .

Matrices  $A, B, C$  and  $R$  are assumed to be known, and they represent the system model. The system trajectories are given by Equations (3.9) and (3.10). According to Figure 4.1, the observer equations are given by:

$$\begin{aligned}
 \hat{x} &= A\hat{x} \oplus Bu \oplus L(\hat{y} \oplus y) \\
 &= A\hat{x} \oplus Bu \oplus LC\hat{x} \oplus LCx \\
 &= (A \oplus LC)\hat{x} \oplus Bu \oplus LCx
 \end{aligned} \tag{4.1}$$

Using Theorem 1 in Equation 4.1, we obtain:

$$\begin{aligned}\hat{x} &= (A \oplus LC)^*Bu \oplus (A \oplus LC)^*LCx \\ &= (A \oplus LC)^*Bu \oplus (A \oplus LC)^*LC(A^*Bu \oplus A^*Rw)\end{aligned}$$

By doing the algebraic manipulations described in [16] and [3], the observer model may be written as follows:

$$\hat{x} = (A \oplus LC)^*Bu \oplus (A \oplus LC)^*LCA^*Rw \quad (4.2)$$

The main objective is to compute the greatest observer matrix  $L$ , denoted as  $L_{opt}$ , such that the estimated state vector is smaller than or equal to the state, *i.e.*,  $\hat{x} \preceq x$ , where  $\hat{x}$  is represented in Equation 4.2. Formally, finding the greatest  $L$  satisfying the following inequality  $\forall u, w$ :

$$(A \oplus LC)^*Bu \oplus (A \oplus LC)^*LCA^*Rw \preceq A^*Bu \oplus A^*Rw \quad (4.3)$$

Equivalently, the following two conditions are required:

$$(A \oplus LC)^*B \preceq A^*B, \text{ and} \quad (4.4)$$

$$(A \oplus LC)^*LCA^*R \preceq A^*R. \quad (4.5)$$

Two Lemmas provide and produce conditions for the greatest observer matrices such that the Equations (4.4) and (4.5) hold.

**Lemma 2** ([3, 14]) *The following equivalence holds:*

$$(A \oplus LC)^*B = A^*B \Leftrightarrow L \preceq L_1 = (A^*B)\phi(CA^*B)$$

**Lemma 3** ([3, 14]) *The following equivalence holds:*

$$(A \oplus LC)^*LCA^*R \preceq A^*R \Leftrightarrow L \preceq L_2 = (A^*R)\phi(CA^*R)$$

The mathematical proofs of the lemmas described above can be checked in [3]. A direct consequence of Lemmas 1 and 2 is that the greatest observer matrix  $L$  that satisfies Equations (4.4) and (4.5) is  $L_1 \wedge L_2$ . Hence, the following proposition holds.

**Proposition 1** ([3, 14])  *$L_1 \wedge L_2$  is the greatest observer matrix  $L$  such that  $\forall(u, w)$ :*

$$\hat{x} = A\hat{x} \oplus Bu \oplus Ly \preceq x = Ax \oplus Bu \oplus Rw.$$

The following corollary is about the relation between the real output and its

estimated.

**Corollary 1** ([3, 14]) *The greatest causal observer that allows  $y = \hat{y}$  is  $L_{opt+} = \text{Pr}_+(L_{opt})$ , where  $L_{opt} = L_1 \wedge L_2$ .*

In other words, the equality between the estimated output  $\hat{y}$  and the measured output  $y$  is ensured, when the Optimal Observer  $L_{opt+}(P_l, T_l, w_l, \mathcal{M}_l^0, \phi_l)$  is considered, where  $L_{opt+}$  is the causal projection presented in Appendix A in Theorem 3.

To illustrate the observer design process for TEGs, the Example 17 is presented. This example is taken from [3].

**Example 17** *Let us consider the TEG shown in Figure 4.2. The structure is defined by two controllable transitions  $u_1, u_2$ , one measurable output transition  $y_1$ , six uncontrollable transitions  $w_1, w_2, w_3, w_4, w_5, w_6$  and six internal transitions  $x_1, x_2, x_3, x_4, x_5, x_6$ . Besides that, it is assumed that all transitions fires as soon as they are enabled.*

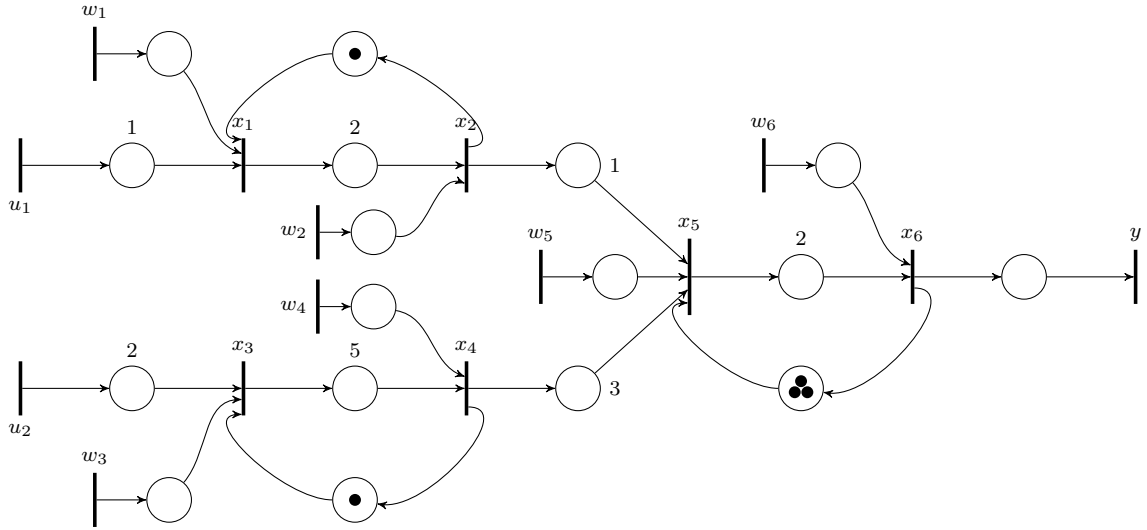


Figure 4.2: TEG model [3].

*The state space representation in  $\mathcal{M}_{in}^{ax}[\gamma, \delta]$  of the TEG is given as:*

$$\begin{aligned} x &= Ax \oplus Bu \oplus Rw, \\ y &= Cx. \end{aligned}$$

$$A = \begin{bmatrix} \varepsilon & \delta^0\gamma^1 & \varepsilon & \varepsilon & \varepsilon & \varepsilon \\ \delta^2\gamma^0 & \varepsilon & \varepsilon & \varepsilon & \varepsilon & \varepsilon \\ \varepsilon & \varepsilon & \varepsilon & \delta^0\gamma^1 & \varepsilon & \varepsilon \\ \varepsilon & \varepsilon & \delta^5\gamma^0 & \varepsilon & \varepsilon & \varepsilon \\ \varepsilon & \delta^1\gamma^0 & \varepsilon & \delta^3\gamma^0 & \varepsilon & \delta^0\gamma^3 \\ \varepsilon & \varepsilon & \varepsilon & \varepsilon & \delta^2\gamma^0 & \varepsilon \end{bmatrix}, \quad B = \begin{bmatrix} \delta^1\gamma^0 & \varepsilon \\ \varepsilon & \varepsilon \\ \varepsilon & \delta^2\gamma^0 \\ \varepsilon & \varepsilon \\ \varepsilon & \varepsilon \\ \varepsilon & \varepsilon \end{bmatrix},$$

$$C = \begin{bmatrix} \varepsilon & \varepsilon & \varepsilon & \varepsilon & \varepsilon & e \end{bmatrix}, \quad R = \begin{bmatrix} e & \varepsilon & \varepsilon & \varepsilon & \varepsilon & \varepsilon \\ \varepsilon & e & \varepsilon & \varepsilon & \varepsilon & \varepsilon \\ \varepsilon & \varepsilon & e & \varepsilon & \varepsilon & \varepsilon \\ \varepsilon & \varepsilon & \varepsilon & e & \varepsilon & \varepsilon \\ \varepsilon & \varepsilon & \varepsilon & \varepsilon & e & \varepsilon \\ \varepsilon & \varepsilon & \varepsilon & \varepsilon & \varepsilon & e \end{bmatrix}$$

Note that,  $(A)_{12} = \delta^0\gamma^1$  represents that there is a place between  $x_2$  and  $x_1$  with one token and no delay of time and  $(B)_{32} = \delta^2\gamma^0$  demonstrates that there is a place between  $x_3$  and  $u_2$  with no token and a delay of 2 time units. The entry  $e$  in the  $C$  matrix represents that there is a place between  $x_6$  and  $y_1$  with no token and no delay of time. The entries  $e$  in the  $R$  matrix correspond to the disturbances.

The transfer function  $H = CA^*B$  of this TEG is computed using the toolbox *MinMaxGD* (see [26, 27]) and is given by:

$$H = \begin{bmatrix} \delta^6\gamma^0(\delta^2\gamma^1)^* & \delta^{12}\gamma^0(\delta^5\gamma^1)^* \end{bmatrix}.$$

The observer matrix  $L_{opt} = L_1 \wedge L_2 = (A^*B)\phi(CA^*B) \wedge (A^*R)\phi(CA^*R)$  is computed using the toolbox *MinMaxGD*:

$$L_{opt} = \begin{bmatrix} \varepsilon & \varepsilon & \varepsilon & \varepsilon & \delta^0\gamma^3(\delta^2\gamma^3)^* & (\delta^2\gamma^3)^* \end{bmatrix}^T.$$

As  $L_{opt}$  is causal, so  $L_{opt+} = \text{Pr}_+(L_{opt}) = L_{opt}$ . To obtain the observer equations, they can be rewrite as:

$$\hat{x} = A\hat{x} \oplus Bu \oplus L_{opt}l,$$

$$\beta = L_{opt}l.$$

Therefore

$$\hat{x} = A\hat{x} \oplus Bu \oplus [\varepsilon \ \varepsilon \ \varepsilon \ \varepsilon \ \beta_5 \ \beta_6]^T, \quad (4.6)$$

$$\begin{bmatrix} \beta_1 \\ \beta_2 \\ \beta_3 \\ \beta_4 \\ \beta_5 \\ \beta_6 \end{bmatrix} = \begin{bmatrix} \varepsilon \\ \varepsilon \\ \varepsilon \\ \varepsilon \\ \delta^0\gamma^3(\delta^2\gamma^3)^* \\ (\delta^2\gamma^3)^* \end{bmatrix} l. \quad (4.7)$$

The entry  $(L_{opt})_5 = \delta^0\gamma^3(\delta^2\gamma^3)^*$ , where  $(\delta^2\gamma^3)^*$  represents the cyclic component in  $\beta_5$  with 3 tokens and a delay of 2 time units, and  $\delta^0\gamma^3$  represents a relation between  $\beta_5$  and  $l_1$  with 3 tokens and no delay of time. The entry  $(L_{opt})_6 = (\delta^2\gamma^3)^*$ , where  $(\delta^2\gamma^3)^*$  represents the cyclic component in  $\beta_6$  with 3 tokens and a delay of 2 time units. The relation between  $\beta_6$  and  $l_1$  can be represented by  $e$ , because there is 0 tokens and no delay of time. Therefore, Equation 4.8 is a solution of Equation 4.7. The realization of  $L_{opt+}$  is shown in Figure 4.3.

$$\begin{bmatrix} \beta_1 \\ \beta_2 \\ \beta_3 \\ \beta_4 \\ \beta_5 \\ \beta_6 \end{bmatrix} = \begin{bmatrix} \varepsilon & \varepsilon & \varepsilon & \varepsilon & \varepsilon & \varepsilon \\ \varepsilon & \varepsilon & \varepsilon & \varepsilon & \varepsilon & \varepsilon \\ \varepsilon & \varepsilon & \varepsilon & \varepsilon & \varepsilon & \varepsilon \\ \varepsilon & \varepsilon & \varepsilon & \varepsilon & \varepsilon & \varepsilon \\ \varepsilon & \varepsilon & \varepsilon & \varepsilon & \delta^2\gamma^3 & \varepsilon \\ \varepsilon & \varepsilon & \varepsilon & \varepsilon & \varepsilon & \delta^2\gamma^3 \end{bmatrix} \begin{bmatrix} \beta_1 \\ \beta_2 \\ \beta_3 \\ \beta_4 \\ \beta_5 \\ \beta_6 \end{bmatrix} \oplus \begin{bmatrix} \varepsilon \\ \varepsilon \\ \varepsilon \\ \varepsilon \\ \gamma^3 \\ e \end{bmatrix} l. \quad (4.8)$$

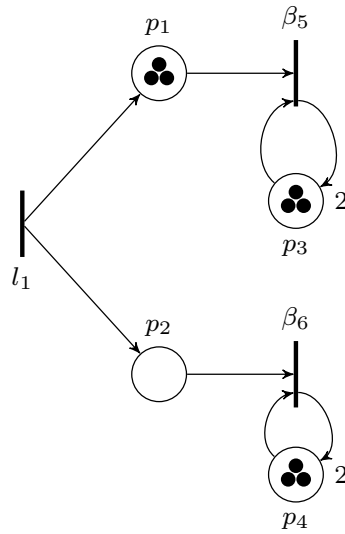


Figure 4.3: The realization of  $L_{opt+}$ .

Note that, the relation between  $\beta_5$  and  $l_1$  is represented by the place  $p_1$  as described



in Equation 4.8 by  $\gamma^3$ . The relation between  $\beta_6$  and  $l_1$  is represented by the place  $p_2$  as described in Equation 4.8 by  $e$ . The observer can be written as the following set of difference equations in the Max-plus algebra, considering that  $\gamma$  is the backward shift operator.

$$\begin{aligned}\beta_5(k) &= 2\beta_5(k-3) \oplus y(k-3), \\ \beta_6(k) &= 2\beta_6(k-3) \oplus y(k), \\ \hat{x}_1(k) &= \hat{x}_2(k-1) \oplus 1u_1(k), \\ \hat{x}_2(k) &= 2\hat{x}_1(k), \\ \hat{x}_3(k) &= \hat{x}_4(k-1) \oplus 2u_2(k), \\ \hat{x}_4(k) &= 5\hat{x}_3(k), \\ \hat{x}_5(k) &= 1\hat{x}_2(k) \oplus 3\hat{x}_4(k) \oplus \hat{x}_6(k-3) \oplus \beta_5(k), \\ \hat{x}_6(k) &= 2\hat{x}_5(k) \oplus \beta_6(k).\end{aligned}$$

The system, the  $L_{opt+}$  realization and the Simulator represent the observer and are shown in Figure 4.4. Note that, the Simulator is a replica of the system model, unless for the disturbance terms  $w_1, w_2, w_3, w_4, w_5, w_6$ . The observer will compute an estimation of the current state by using the input and the output measurements.

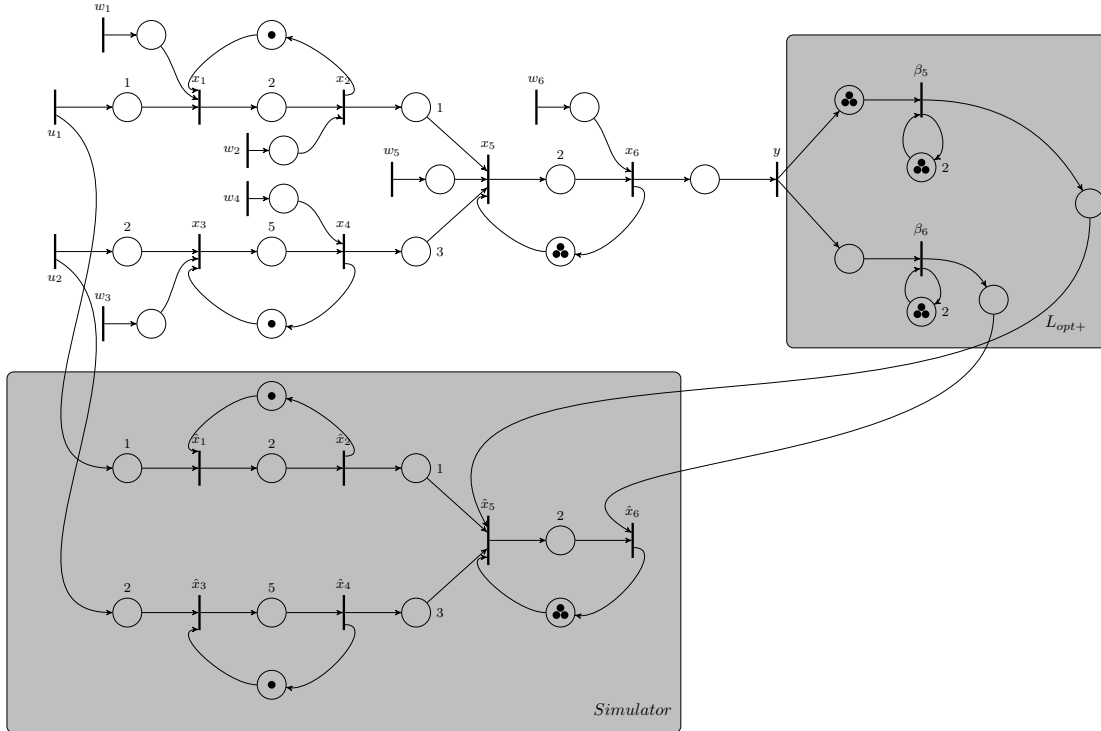


Figure 4.4: The observer for TEG of Figure 4.2.

**Remark 7** In order to calculate  $L_{opt+}$  to design the Observer for WTEGs, it is

required that the “equivalent” TEG has the following structure:

- the places between input or output transitions and internal transitions have no holding times and have no initial marking,
- input or output transitions are connected only to internal transitions.

When these two conditions are not satisfied, it is necessary to add Artificial Transitions to TEG. Each artificial transition inserted consist of a sequence of one transition and one place (or one place and one transition) in which  $\gamma^0\delta^0$ , i.e., the place do not have tokens and do not have holding times. For this reason, artificial transitions do not change the firing order of the input/output transitions. The artificial transitions are inserted only with the purpose to calculate  $L_{opt+}$ . After to compute it, they are removed.

In Example 17, it can be noted that the structure of the “equivalent” TEG conforms to the requirements of the Remark 7, so it was not necessary to add artificial transitions. Algorithm 2 summarized the steps in order to obtain  $L_{opt+}$  realization.

---

**Algorithm 2**  $L_{opt+}$  realization

---

**Input:** “Equivalent” TEG  $(P', T', w', \mathcal{M}^0, \phi')$

**Output:**  $L_{opt+}(P_l, T_l, w_l, \mathcal{M}_l^0, \phi_l)$

- 1: Compute matrices  $A \in \mathcal{M}_{in}^{ax}[\gamma, \delta]^{n \times n}$ ,  $B \in \mathcal{M}_{in}^{ax}[\gamma, \delta]^{n \times p}$ ,  $C \in \mathcal{M}_{in}^{ax}[\gamma, \delta]^{m \times n}$  and  $R \in \mathcal{M}_{in}^{ax}[\gamma, \delta]^{n \times l}$
  - 2: Compute the matrix:  $L_{opt} = L_1 \wedge L_2 = (A^*B)\#(CA^*B) \wedge (A^*R)\#(CA^*R)$ .  $\triangleright$  using Toolbox *MinMaxGD*
  - 3: Compute The Optimal Observer  $L_{opt+}$ :  $L_{opt+} = Pr_+(L_{opt}) = L_{opt}$ .  $\triangleright$  using Toolbox *MinMaxGD*
  - 4: Obtain  $L_{opt+}$  realization
- 

## 4.2 Observer for WTEGs

In the previous section, the Observer for TEGs introduced in [14] was presented. In this section, the Observer for WTEGs  $Obs(WTEG)(P_o, T_o, w_o, \mathcal{M}_o^0, \phi_o)$  is designed through the connection between: (i) the original WTEG, (ii) the Observer

Matrix  $L_{opt+}$  and (iii) the Simulator. First of all, the Algorithm 1 to transform the consistent WTEG into a TEG was developed in Section 2.3. Then, in order to estimate the firing times of internal transitions of a WTEG, it is necessary to compute the Observer Matrix using the “equivalent” TEG as presented in Section 4.1. The Simulator is constructed based on the original system as shown in Section 4.1. To build the Observer for WTEGs it is necessary to insert the Interface which is the connections between (i), (ii) and (iii) and it is defined as follow.

### 4.2.1 Interface

The Interface is a specific Petri net and it is used to connect the WTEG to the Observer Matrix and to the Simulator. For this, two types of interfaces are proposed: Input Interface and Output Interface. The size  $n$  of the Interface, *i.e.*, the number of transitions of the Interface, is determined by entries in the T-semiflow. In Figure 4.5 the Interface insertion in Observer for WTEGs realization is depicted, where  $\mathcal{I}_i$  refers to the Input Interface and  $\mathcal{O}_i$  to the Output Interface.

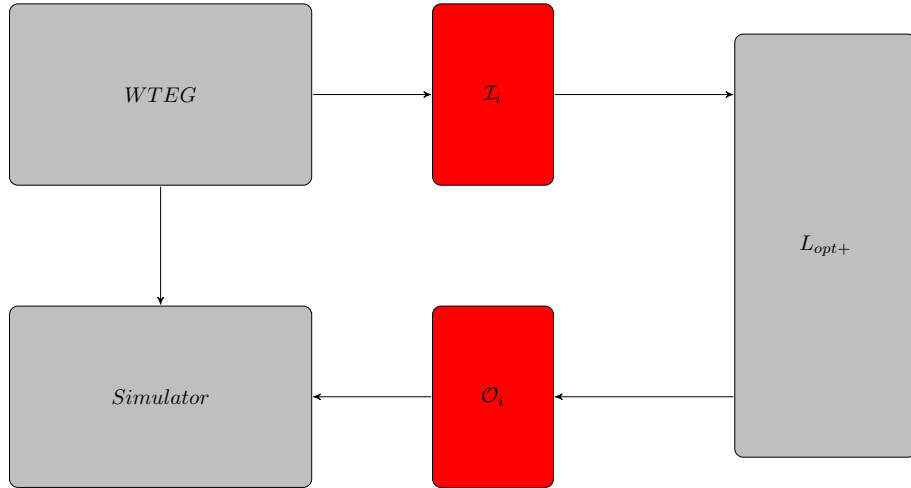


Figure 4.5: Interface insertion in Observer for WTEGs realization.

The first connection is the Input Interface which is made between the output of WTEG and the input of  $L_{opt+}$  realization. The size of the Interface to be inserted depends on the size of the entries of T-semiflow that corresponds to the WTEG output transitions. For example, if the WTEG has only one output transition with T-semiflow entry equal to 4, the size of the Interface will be  $n = 4$ . Input Interface is defined as follows.

**Definition 26 (Input Interface)** *The Input Interface of size  $n$  is a particular Petri net  $\mathcal{I}_i = (P, T, w, \mathcal{M}^0)$ , where:*

- $P = \{p_1, \dots, p_n\}$  is the finite set of places,

- $T = \{u_0, \dots, u_n\}$  is the finite set of transitions,
- $w(u_0, p_i) = 1$  and  $w(p_i, u_i) = n, \forall i \in \{1, \dots, n\}$  are the weight function,
- $\mathcal{M}^0(p_i) = n - i, \forall i \in \{1, \dots, n\}$  is the initial marking.

When operating under the earliest firing rule, it can be observed that the firing of transitions  $u_1, \dots, u_n$  are ordered. This firing order is obtained through the weights  $w(p_i, u_i) = n$  and the initial marking of the Input Interface. Thus, the order is given by:

$$u_i(k) \leq u_{i+1}(k) \leq u_i(k+1), \forall i = 1, \dots, n-1,$$

where, the  $k$ -th firing of  $u_{i+1}$  is not earlier than the  $k$ -th firing of  $u_i, \forall i = 1, \dots, n-1$ .

To illustrate the Input Interface, Example 18 is presented.

**Example 18** Let us consider that the size of the Interface is  $n = 2$ , therefore, it has two transitions  $u_1$  and  $u_2$ . The Input Interface is depicted in Figure 4.6. In this input Interface:  $P = \{p_1, p_2\}$ ,  $T = \{u_0, u_1, u_2\}$ ,  $w(u_0, p_1) = w(u_0, p_2) = 1$  and  $w(p_1, u_1) = w(p_2, u_2) = 2$ .  $\mathcal{M}^0(p_1) = 1$  and  $\mathcal{M}^0(p_2) = 0$ . Note that  $w(p_1, u_1) = w(p_2, u_2) = 2$  because the size of the Interface in  $n = 2$ . The firing order of the Input Interface is based on the initial marking. For instance, as  $\mathcal{M}^0(p_1) = 1$  and  $\mathcal{M}^0(p_2) = 0$ , so  $u_1(k) \leq u_2(k)$ , i.e., the firing of transition  $u_1$  occurs before the firing of  $u_2$ .

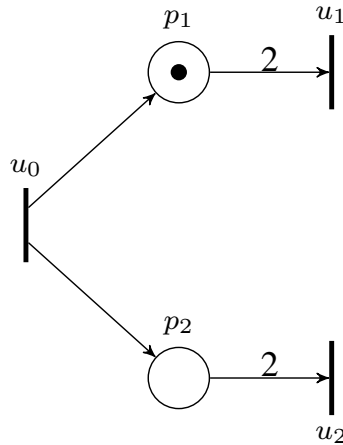


Figure 4.6: Input Interface for  $n = 2$ .

The second connection is the Output Interface which is made between the output of  $L_{opt+}$  realization and the Simulator. The size of the Interface to be inserted depends on the size of the entries of the T-semiflow that corresponds to the WTEG internal transitions. Output Interface is defined as follows.

**Definition 27 (Output Interface)** The Output Interface of size  $n$  is a particular Petri net  $\mathcal{O}_i = (P, T, w, \mathcal{M}^0)$ , where:

- $P = \{p_n, \dots, p_1\}$  is the finite set of places,
- $T = \{y_n, \dots, y_0\}$  is the finite set of transitions,
- $w(y_n, p_i) = n$  and  $w(p_i, y_0) = 1, \forall i \in \{n, \dots, 1\}$  are the weight function,
- $\mathcal{M}^0(p_i) = n - i, \forall i \in \{n, \dots, 1\}$  is the initial marking.

With the purpose to demonstrate the Output Interface the Example 19 is presented:

**Example 19** Let us consider that the size of the Interface is  $n = 3$ , therefore, there are three transitions  $y_1, y_2$  and  $y_3$ . The Output Interface is depicted in Figure 4.7. In this Output Interface:  $P = \{p_1, p_2, p_3\}$ ,  $T = \{y_0, y_1, y_2, y_3\}$ ,  $w(y_1, p_1) = w(y_2, p_2) = w(y_3, p_3) = 3$  and  $w(p_1, y_0) = w(p_2, y_0) = w(p_3, y_0) = 1$ .  $\mathcal{M}^0(p_1) = 0$ ,  $\mathcal{M}^0(p_2) = 1$  and  $\mathcal{M}^0(p_3) = 2$ . Note that  $w(y_1, p_1) = w(y_2, p_2) = w(y_3, p_3) = 3$  because the size of the Interface is  $n = 3$ . The firing of  $y_1$  leads to the first firing of  $y_0$ , the firing of  $y_2$  leads to the second firing of  $y_0$  and, the firing of  $y_3$  leads to the third firing of  $y_0$ .

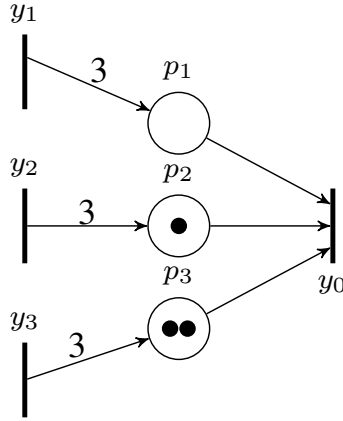


Figure 4.7: Output Interface for  $n = 3$ .

The Input Interface leads to an expansion in the number of transitions and the Output Interface leads to a reduction in the number of transitions. The index  $i$  refers to the number of Interfaces that will be inserted to allow the connection between the systems. Algorithm 3 shown the procedure for obtaining Interfaces realization.

---

**Algorithm 3** *Interface*

---

**Input:** Consistent WTEG  $(P, T, w, \mathcal{M}^0, \phi)$

**Output:** Input Interface  $\mathcal{I}_i(P, T, w, \mathcal{M}^0, \phi)$ , Output Interface  $\mathcal{O}_i(P, T, w, \mathcal{M}^0, \phi)$

- 1: Compute  $T$ -semiflow  $\xi$

2: **for** each entry  $\xi_{(t_i)} \in \xi$

2.1: **if**  $\xi_{(t_i)}$  corresponds to the **output transitions** and  $\xi_{(t_i)} \neq 1$ :

2.1.1: Compute the size  $n$  of Input Interface  $\mathcal{I}_i$   $\triangleright$  WTEG  $\rightarrow L_{opt+}$

2.1.2: Obtain Input Interface  $\mathcal{I}_i(P, T, w, \mathcal{M}^0, \phi)$   $\triangleright$  Definition 26

2.2: **if**  $\xi_{(t_i)}$  corresponds to the **internal transitions** and  $\xi_{(t_i)} \neq 1$ :

2.2.1: Compute the size  $n$  of Output Interface  $\mathcal{O}_i$   $\triangleright$   $L_{opt+} \rightarrow$  Simulator

2.1.2: Obtain Output Interface  $\mathcal{O}_i(P, T, w, \mathcal{M}^0, \phi)$   $\triangleright$  Definition 27

**end for**

---

## 4.2.2 Input/Output behavior

In this section, we propose an Optimal Observer built through the conversion algorithm from WTEG to TEG. Thus, for the implementation of the Observer for WTEGs, it is necessary to connect the output of the WTEG to the input of the Optimal Observer and the output of the Optimal Observer to the Simulator. The joining of all these structures is done through the insertion of the Interface. In the following, we explain why the Optimal Observer designed as a TEG is a valid observer for the plant model which is given by a WTEG based on previous works in the literature.

**1.** [23] *functional perspective: the total number of tokens consumed and produced by the firing transitions in TEG is equals the number of tokens consumed and produced by the firing of corresponding transitions in WTEG.*

As mentioned in Section 2.3, the transformation SDF into a HSDF is equivalent to the transformation WTEG into a TEG. According to result **1**, the firing order of the duplicated transitions in TEG corresponds to the firing order in WTEG.

**2.** [18] *Even the firing transition  $A$  produces all  $n_A$  tokens onto place  $(A, B)$  simultaneously according to the WTEG model, the  $n_A$  generated tokens have a fixed relative order in which they are generated on the place  $(A, B)$ . This is because each place  $(A, B)$  is essentially a first-in-first-out buffer.*

This means that the order in which tokens are generated on their related places in WTEG is also maintained for “equivalent” TEG.

**3.** [22] *Assume that  $\Sigma = (N, m_0)$  is a live and bounded WTEG. There exists a live and bounded marking for a WTEG if and only if it is strongly connected and consistent (i.e.,  $\exists \mathbf{X} > 0$  such that  $C\mathbf{X} = 0$ ).*

The result **3** is applied in the transformation algorithm, which requires that the WTEG is consistent to ensure that there is a unique minimal T-semiflow.

4. [22] *The Petri net languages<sup>1</sup> of the WTEG and the TEG are the same when all transitions  $t_i^j$  in the TEG are considered as  $t_i$  in the original WTEG.*

In this work, all the duplicated transitions in “equivalent” TEG are considered as a single transition in original WTEG. Thus, one can assume that the firing sequence of WTEG and “equivalent” TEG are the same since  $t_i^j$  in TEG are considered as  $t_i$  in original WTEG.

In order to illustrate the fact that the input/output behavior of WTEG and of TEG with Interface are the same, the Example 20 is described:

**Example 20** *Let us consider consistent WTEG shown in Figure 4.8 and “equivalent” TEG obtained using the Algorithm 1 shown in Figure 4.9. In Figure 4.8,  $w(t_1, p_1) = w(t_2, p_2) = w(p_2, t_2) = w(p_3, t_3) = 1$  and  $w(p_1, t_2) = w(t_2, p_3) = 2$ . In Figure 4.9 all arcs have weight 1. Note that the token in  $p_2$  and in  $p'_{2_1, 2_1}$  needs to be held for 2 time instants to contribute to the firing of  $t_2$  and  $t_2^1$ , respectively.*

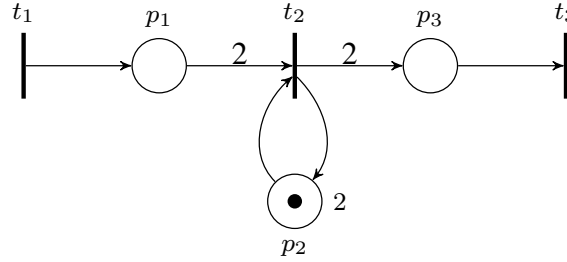


Figure 4.8: Consistent WTEG.

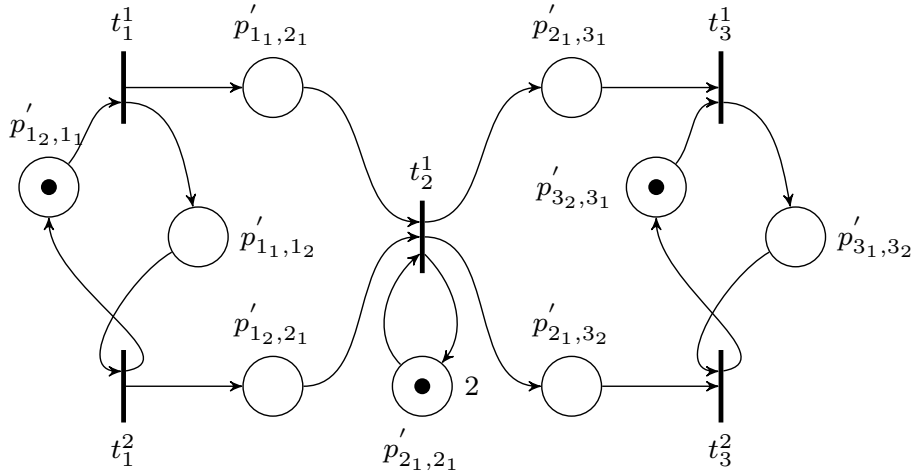


Figure 4.9: “Equivalent” TEG corresponding to the WTEG of Figure 4.8.

*In this example, two interfaces will be connected to the TEG, one in the input and one in the output.  $\xi = [2 \ 1 \ 2]^T$  as calculated in Example 9. To build the*

<sup>1</sup>here, by “language” it is meant the set of all firing sequences from the initial marking.

interfaces it is necessary to analyze the input transition  $t_1$  and the output transition  $t_3$ . The first and the last entries of the  $T$ -semiflow, that correspond to transitions  $t_1$  and  $t_3$  in the WTEG, respectively, are equal to 2, so, the interface that will be connected to the input and to the output have the same size,  $n = 2$ . In Figure 4.10(a) and 4.10(b) the interfaces that will be connected to the input and to the output to the TEG are depicted, respectively.

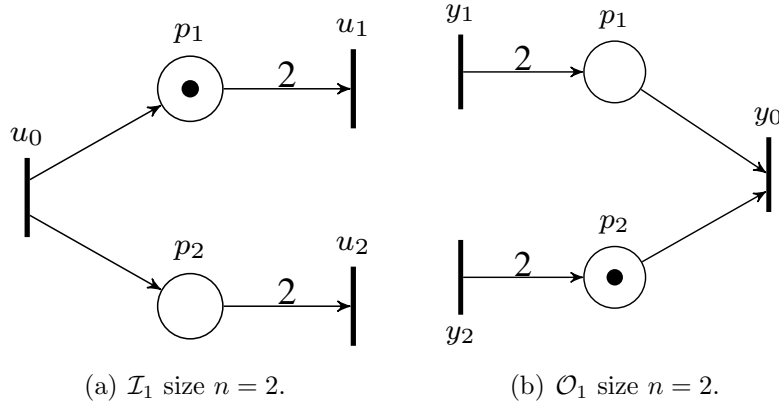


Figure 4.10: Interfaces that will be connected to the input and to the output of the TEG.

After design the interfaces, they are connected to the input and output of the TEG. The interfaces are shown in red in Figure 4.11.

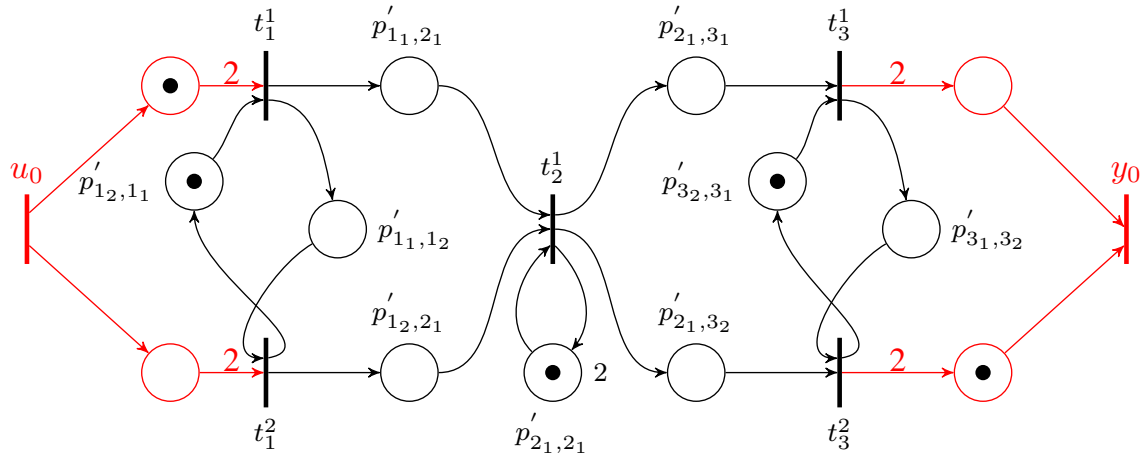


Figure 4.11: TEG with Input and Output Interface.

To demonstrate the performance of the input/output of the WTEG and of TEG with the insertion of interfaces, let us consider the dater function as follows:



$$d(k) = \begin{cases} -\infty, & \text{for } k < 1 \\ 0, & \text{if } k = 1 \\ 1, & \text{if } k = 2 \\ 2, & \text{if } k = 3 \\ 3, & \text{if } k = 4 \\ +\infty, & \text{else.} \end{cases}$$

This dataer functions can be interpreted as follows. There is no firing before time 0. The first firing occurs at the time 0. The second firing occurs at time 1, the third firing occurs at time 2 and the fourth firing occurs at time 3. After time 3, there is no additional firing. Table 4.1 shows the firing times for WTEG operating under the earliest firing rule, as shown in Definition 16, where  $t_i$  denotes the dataer associated with transition  $t_i, i = 1, 2, 3$ . Notice that the first firing of the input transition  $t_1$  is at  $t = 0$ , the second firing at  $t = 1$ , the third firing at  $t = 2$  and the fourth firing at  $t = 3$ , as seen in the second column of Table 4.1. The first firing of the internal transition  $t_2$  is at  $t = 1$ , as shown in the third column of Table 4.1, because  $w(p_1, t_2) = 2$ . The second firing of  $t_2$  is at  $t = 3$ , because the token remains in  $p_2$  2 time units before it can contribute to the next firing of  $t_2$ . The first and the second firing of the output transition  $t_3$  are at  $t = 1$ , because in the first fire of  $t_2$ ,  $p_3$  receives 2 tokens. The third and fourth firing are at  $t = 3$ , because in the second fire of  $t_2$ ,  $p_3$  receives 2 tokens.

		Firing Times		
Firing	Input	Internal Transitions	Output	
Count k	$t_1(k) = d(k)$	$t_2(k)$	$t_3(k)$	
1	0	1	1	
2	1	3	1	
3	2	$+\infty$	3	
4	3	$+\infty$	3	
5	$+\infty$	$+\infty$	$+\infty$	

Table 4.1: Firing Table WTEG of Figure 4.8.

Table 4.2 shows the firing times for the TEG with Interface. Notice that the first firing of the input transition  $u_0$  is at  $t = 0$ , the second firing at  $t = 1$ , the third firing at  $t = 2$  and the fourth firing at  $t = 3$ , as seen in the second column of Table 4.2. Analyzing the firing of the internal transitions, note that the first firing of  $t_1^1$  and of  $t_1^2$  occur at  $t = 0$  and  $t = 1$ , respectively, and the second firing of them occur at  $t = 2$  and  $t = 3$ , respectively. Notice that the firing of  $t_1^1$  and  $t_1^2$  occur alternately as shown in the third and fourth column of Table 4.2. The first firing of  $t_2^1$  occurs at

$t = 1$ , because it is necessary to wait the first firing of  $t_1^1$  and  $t_1^2$  to occur. The second firing of  $t_2^1$  occurs at  $t = 3$ , because the token remains in  $p_{2_1,2_1}'$  2 time units before it can contribute to the next firing of  $t_2^1$ . The first firing of  $t_3^1$  and  $t_3^2$  occur at  $t = 1$  after the first firing of  $t_2^1$ . The second firing of them occur at  $t = 3$  after the second firing of  $t_2^1$ . Finally, the first firing and the second firing of the output transition  $y_0$  occur at  $t = 1$ , after the first firing of  $t_3^1$  and  $t_3^2$ . The third and the fourth firing of  $y_0$  occur at  $t = 3$ , after the second firing of  $t_3^1$  and  $t_3^2$ .

Firing Count k	Firing Times						
	Input $u_0(k) = d(k)$	Internal Transitions					Output $y_0(k)$
		$t_1^1(k)$	$t_1^2(k)$	$t_2^1(k)$	$t_3^1(k)$	$t_3^2(k)$	
1	0	0	1	1	1	1	1
2	1	2	3	3	3	3	1
3	2	$+\infty$	$+\infty$	$+\infty$	$+\infty$	$+\infty$	3
4	3	$+\infty$	$+\infty$	$+\infty$	$+\infty$	$+\infty$	3
5	$+\infty$	$+\infty$	$+\infty$	$+\infty$	$+\infty$	$+\infty$	$+\infty$

Table 4.2: Firing Table for TEG with Interface of Figure 4.11.

Comparing the information obtained with both tables 4.1 and 4.2, notice that the firing times of  $t_1^1$  and  $t_1^2$  in the TEG with Interface merged are the same as the firing times of  $t_1$  in WTEG. The firing times of  $t_2^1$  in the TEG + Interface are the same as the firing times of  $t_2$  in WTEG. The firing times of  $t_3^1$  and of  $t_3^2$  in the TEG with Interface merged are the same as the firing times of  $t_3$  in WTEG. Therefore, it is concluded that the input/output behavior of the WTEG is the same as the input/output behavior of the TEG with Interface. As required, the output of the WTEG and the output of the TEG + Interface are equal, i.e.,  $t_3(k) = y_0(k)$ .

### 4.3 Implementation of Observer for WTEGs

In this section, an algorithm for the Observer for WTEGs design is proposed. In order to implement  $Obs(WTEG)$ , five main steps are required. First, compute the “equivalent” TEG through consistent WTEG as showed in Algorithm 1. Second, obtain the  $L_{opt+}$  realization using Max-plus approach, which is based on algebraic results related to dioid, as described in Algorithm 2. Third, get the Input and Output Interface realization, as described in Algorithm 3. Fourth, obtain the Simulator that is equal to the system model, excluding for the disturbance terms. Fifth, the system’s parts are connected via Interfaces. Algorithm 4 summarized all these steps.

---

**Algorithm 4** *Observer for WTEGs*

---

**Input:** *Consistent WTEG*  $(P, T, w, \mathcal{M}^0, \phi)$

**Output:**  $Obs(WTEG)(P_o, T_o, w_o, \mathcal{M}_o^0, \phi_o)$

- 1: Call Algorithm 1 ▷ Compute TEG  $(P', T', w', \mathcal{M}^0, \phi')$
  - 2: Call Algorithm 2 ▷ Compute  $L_{opt+}(P_l, T_l, w_l, \mathcal{M}_l^0, \phi_l)$
  - 3: Call Algorithm 3 ▷ Compute  $\mathcal{I}_i(P, T, w, \mathcal{M}^0)$  and  $\mathcal{O}_i(P, T, w, \mathcal{M}^0)$
  - 4: Built the Simulator ▷ Compute  $\mathcal{S}(P, T, w, \mathcal{M}^0, \phi)$ , see Section 4.1
  - 5: Observer for WTEG realization  $Obs(WTEG)$ 
    - 5.1: Connect WTEG input  $\rightarrow \mathcal{S}$  input
    - 5.2: Connect WTEG output  $\rightarrow L_{opt+}$  input using  $\mathcal{I}_i$
    - 5.3: Connect  $L_{opt+}$  output  $\rightarrow \mathcal{S}$  internal transitions using  $\mathcal{O}_i$
- 

Figure 4.5 depicts the Observer for WTEGs realization  $Obs(WTEG)$ . Following, an example illustrating step by step the application of Algorithm 4 to obtain  $Obs(WTEG)$  is presented.

**Example 21** *To illustrate this work, let us consider an example to obtain the Observer for WTEGs. In order to do so, we will use the consistent WTEG shown in Figure 4.12. This consistent WTEG is defined as follows:*

- set of places:  $P = \{p_1, p_2, p_3, p_4, p_5, p_6, p_7\}$ ;
- set of transitions:  $T = \{t_1, t_2, t_3, t_4, t_5, t_6\}$ ;
- weights:  $w(t_1, p_1) = w(p_1, t_3) = w(t_3, p_3) = w(t_2, p_2) = w(p_2, t_4) = w(p_4, t_3) = w(p_5, t_5) = w(t_5, p_7) = w(p_7, t_6) = 1$ ,  $w(t_4, p_5) = w(p_6, t_4) = 2$  and  $w(p_3, t_5) = w(t_5, p_4) = 3$ ;
- holding times:  $\phi_3 = 4$  and  $\phi_5 = 3$ ;
- initial marking:  $\mathcal{M}^0 = \left[ 0 \ 0 \ 0 \ 3 \ 0 \ 2 \ 0 \right]^T$ ;
- disturbances:  $w_1, w_2, w_3$ .

*This consistent WTEG can be transformed into an “equivalent” TEG, which is obtained through the transformation Algorithm 1 described in Section 2.3.*

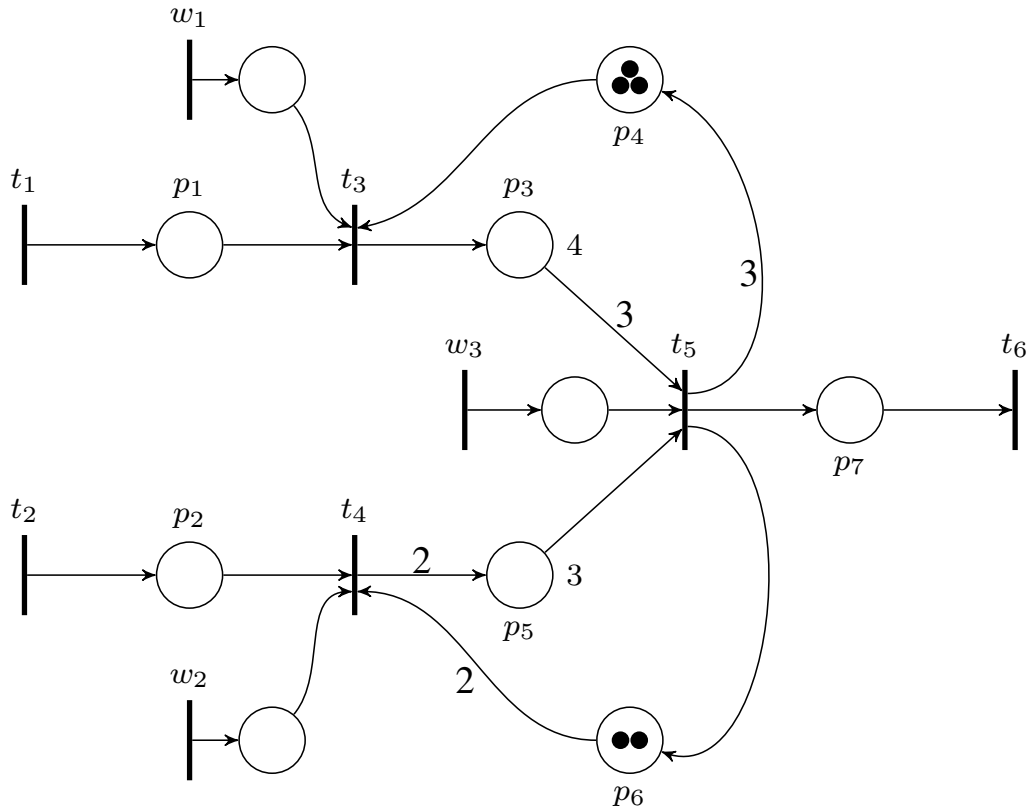


Figure 4.12: Consistent WTEG.

**Remark 8** The steps of the algorithm do not take into account the disturbances. It is enough, after obtaining the “equivalent” TEG, to duplicate the transitions related to the disturbances and to connect them to the corresponding TEG transitions.

Let us present step by step Algorithm 4 to obtain  $\text{Obs}(WTEG)$ .

**Step 1**

In Step 1 of Algorithm 4, that is convert consistent WTEG into “equivalent” TEG, we have the following steps of Algorithm 1.

1: Computing T-semiflow vector  $\xi$ :

$$\mathcal{W}\xi = 0$$

$$\begin{bmatrix} 1 & 0 & -1 & 0 & 0 & 0 \\ 0 & 1 & 0 & -1 & 0 & 0 \\ 0 & 0 & 1 & 0 & -3 & 0 \\ 0 & 0 & -1 & 0 & 3 & 0 \\ 0 & 0 & 0 & 2 & -1 & 0 \\ 0 & 0 & 0 & -2 & 1 & 0 \\ 0 & 0 & 0 & 0 & 1 & -1 \end{bmatrix} \times \begin{bmatrix} \xi_1 \\ \xi_2 \\ \xi_3 \\ \xi_4 \\ \xi_5 \\ \xi_6 \end{bmatrix} = \begin{bmatrix} 0 \\ 0 \\ 0 \\ 0 \\ 0 \\ 0 \\ 0 \end{bmatrix}$$

$$\xi = \left[ \begin{array}{cccccc} 6 & 1 & 6 & 1 & 2 & 2 \end{array} \right]^T$$

2: The transition set  $T'$  of TEG is:

$$T' = \{t_1^1, t_1^2, t_1^3, t_1^4, t_1^5, t_1^6, t_2^1, t_3^1, t_3^2, t_3^3, t_3^4, t_3^5, t_3^6, t_4^1, t_5^1, t_5^2, t_6^1, t_6^2\}.$$

3: For each basic path in WTEG:

**Basic Path 1** ( $t_1, p_1, t_3$ ):

1) Add place  $p'_{11,31}$  to place set  $P'$  of TEG.

$$\text{Set:} \begin{cases} w'(t'_{11}, p'_{11,31}) = 1 \\ w'(p'_{11,31}, t'_{31}) = 1 \\ \mathcal{M}^{0'}(p'_{11,31}) = 0 \\ \phi'(p'_{11,31}) = \phi(p_1) = 0 \end{cases}$$

2) Add place  $p'_{12,32}$  to place set  $P'$  of TEG.

$$\text{Set:} \begin{cases} w'(t'_{12}, p'_{12,32}) = 1 \\ w'(p'_{12,32}, t'_{32}) = 1 \\ \mathcal{M}^{0'}(p'_{12,32}) = 0 \\ \phi'(p'_{12,32}) = \phi(p_1) = 0 \end{cases}$$

3) Add place  $p'_{13,33}$  to place set  $P'$  of TEG.

$$\text{Set:} \begin{cases} w'(t'_{13}, p'_{13,33}) = 1 \\ w'(p'_{13,33}, t'_{33}) = 1 \\ \mathcal{M}^{0'}(p'_{13,33}) = 0 \\ \phi'(p'_{13,33}) = \phi(p_1) = 0 \end{cases}$$

4) Add place  $p'_{14,34}$  to place set  $P'$  of TEG.

$$\text{Set:} \begin{cases} w'(t'_{14}, p'_{14,34}) = 1 \\ w'(p'_{14,34}, t'_{34}) = 1 \\ \mathcal{M}^{0'}(p'_{14,34}) = 0 \\ \phi'(p'_{14,34}) = \phi(p_1) = 0 \end{cases}$$

5) Add place  $p'_{15,35}$  to place set  $P'$  of TEG.

Set:

$$\begin{cases} w'(t'_{15}, p'_{15,35}) = 1 \\ w'(p'_{15,35}, t'_{35}) = 1 \\ \mathcal{M}^{0'}(p'_{15,35}) = 0 \\ \phi'(p'_{15,35}) = \phi(p_1) = 0 \end{cases}$$

6) Add place  $p'_{16,36}$  to place set  $P'$  of TEG.

Set:

$$\begin{cases} w'(t'_{16}, p'_{16,36}) = 1 \\ w'(p'_{16,36}, t'_{36}) = 1 \\ \mathcal{M}^{0'}(p'_{16,36}) = 0 \\ \phi'(p'_{16,36}) = \phi(p_1) = 0 \end{cases}$$

**Basic Path 2** ( $t_3, p_3, t_5$ ):

1) Add place  $p'_{31,51}$  to place set  $P'$  of TEG.

Set:

$$\begin{cases} w'(t'_{31}, p'_{31,51}) = 1 \\ w'(p'_{31,51}, t'_{51}) = 1 \\ \mathcal{M}^{0'}(p'_{31,51}) = 0 \\ \phi'(p'_{31,51}) = \phi(p_3) = 4 \end{cases}$$

2) Add place  $p'_{32,51}$  to place set  $P'$  of TEG.

Set:

$$\begin{cases} w'(t'_{32}, p'_{32,51}) = 1 \\ w'(p'_{32,51}, t'_{51}) = 1 \\ \mathcal{M}^{0'}(p'_{32,51}) = 0 \\ \phi'(p'_{32,51}) = \phi(p_3) = 4 \end{cases}$$

3) Add place  $p'_{33,51}$  to place set  $P'$  of TEG.

Set:

$$\begin{cases} w'(t'_{33}, p'_{33,51}) = 1 \\ w'(p'_{33,51}, t'_{51}) = 1 \\ \mathcal{M}^{0'}(p'_{33,51}) = 0 \\ \phi'(p'_{33,51}) = \phi(p_3) = 4 \end{cases}$$

4) Add place  $p'_{34,52}$  to place set  $P'$  of TEG.

Set:

$$\begin{cases} w'(t'_{34}, p'_{34,52}) = 1 \\ w'(p'_{34,52}, t'_{52}) = 1 \\ \mathcal{M}^{0'}(p'_{34,52}) = 0 \\ \phi'(p'_{34,52}) = \phi(p_3) = 4 \end{cases}$$

5) Add place  $p'_{35,52}$  to place set  $P'$  of TEG.

Set:

$$\begin{cases} w'(t'_{35}, p'_{35,52}) = 1 \\ w'(p'_{35,52}, t'_{52}) = 1 \\ \mathcal{M}^{0'}(p'_{35,52}) = 0 \\ \phi'(p'_{35,52}) = \phi(p_3) = 4 \end{cases}$$

6) Add place  $p'_{36,52}$  to place set  $P'$  of TEG.

Set:

$$\begin{cases} w'(t'_{36}, p'_{36,52}) = 1 \\ w'(p'_{36,52}, t'_{52}) = 1 \\ \mathcal{M}^{0'}(p'_{36,52}) = 0 \\ \phi'(p'_{36,52}) = \phi(p_3) = 4 \end{cases}$$

**Basic Path 3** ( $t_5, p_4, t_3$ ):

1) Add place  $p'_{51,34}$  to place set  $P'$  of TEG.

Set:

$$\begin{cases} w'(t'_{51}, p'_{51,34}) = 1 \\ w'(p'_{51,34}, t'_{34}) = 1 \\ \mathcal{M}^{0'}(p'_{51,34}) = 0 \\ \phi'(p'_{51,34}) = \phi(p_4) = 0 \end{cases}$$

2) Add place  $p'_{51,35}$  to place set  $P'$  of TEG.

Set:

$$\begin{cases} w'(t'_{51}, p'_{51,35}) = 1 \\ w'(p'_{51,35}, t'_{35}) = 1 \\ \mathcal{M}^{0'}(p'_{51,35}) = 0 \\ \phi'(p'_{51,35}) = \phi(p_4) = 0 \end{cases}$$

3) Add place  $p'_{51,36}$  to place set  $P'$  of TEG.

Set:

$$\begin{cases} w'(t'_{51}, p'_{51,36}) = 1 \\ w'(p'_{51,36}, t'_{36}) = 1 \\ \mathcal{M}^{0'}(p'_{51,36}) = 0 \\ \phi'(p'_{51,36}) = \phi(p_4) = 0 \end{cases}$$

4) Add place  $p'_{52,31}$  to place set  $P'$  of TEG.

Set:

$$\begin{cases} w'(t'_{52}, p'_{52,31}) = 1 \\ w'(p'_{52,31}, t'_{31}) = 1 \\ \mathcal{M}^{0'}(p'_{52,31}) = 1 \\ \phi'(p'_{52,31}) = \phi(p_4) = 0 \end{cases}$$

5) Add place  $p'_{52,32}$  to place set  $P'$  of TEG.

$$\begin{cases} w'(t'_{52}, p'_{52,32}) = 1 \\ w'(p'_{52,32}, t'_{32}) = 1 \\ \mathcal{M}^{0'}(p'_{52,32}) = 1 \\ \phi'(p'_{52,32}) = \phi(p_4) = 0 \end{cases}$$

6) Add place  $p'_{52,33}$  to place set  $P'$  of TEG.

$$\begin{cases} w'(t'_{52}, p'_{52,33}) = 1 \\ w'(p'_{52,33}, t'_{33}) = 1 \\ \mathcal{M}^{0'}(p'_{52,33}) = 1 \\ \phi'(p'_{52,33}) = \phi(p_4) = 0 \end{cases}$$

**Basic Path 4**  $(t_2, p_2, t_4)$ :

1) Add place  $p'_{21,41}$  to place set  $P'$  of TEG.

$$\begin{cases} w'(t'_{21}, p'_{21,41}) = 1 \\ w'(p'_{21,41}, t'_{41}) = 1 \\ \mathcal{M}^{0'}(p'_{21,41}) = 0 \\ \phi'(p'_{21,41}) = \phi(p_2) = 0 \end{cases}$$

**Basic Path 5**  $(t_4, p_5, t_5)$ :

1) Add place  $p'_{41,51}$  to place set  $P'$  of TEG.

$$\begin{cases} w'(t'_{41}, p'_{41,51}) = 1 \\ w'(p'_{41,51}, t'_{51}) = 1 \\ \mathcal{M}^{0'}(p'_{41,51}) = 0 \\ \phi'(p'_{41,51}) = \phi(p_5) = 3 \end{cases}$$

2) Add place  $p'_{41,52}$  to place set  $P'$  of TEG.

Set:



$$\begin{cases} w'(t'_{41}, p'_{41,52}) = 1 \\ w'(p'_{41,52}, t'_{52}) = 1 \\ \mathcal{M}^{0'}(p'_{41,52}) = 0 \\ \phi'(p'_{41,52}) = \phi(p_5) = 3 \end{cases}$$

**Basic Path 6** ( $t_5, p_6, t_4$ ):

1) Add place  $p'_{51,41}$  to place set  $P'$  of TEG.

$$\begin{array}{l} \text{Set:} \\ \begin{cases} w'(t'_{51}, p'_{51,41}) = 1 \\ w'(p'_{51,41}, t'_{41}) = 1 \\ \mathcal{M}^{0'}(p'_{51,41}) = 1 \\ \phi'(p'_{51,41}) = \phi(p_6) = 0 \end{cases} \end{array}$$

2) Add place  $p'_{52,41}$  to place set  $P'$  of TEG.

$$\begin{array}{l} \text{Set:} \\ \begin{cases} w'(t'_{52}, p'_{52,41}) = 1 \\ w'(p'_{52,41}, t'_{41}) = 1 \\ \mathcal{M}^{0'}(p'_{52,41}) = 1 \\ \phi'(p'_{52,41}) = \phi(p_6) = 0 \end{cases} \end{array}$$

**Basic Path 7** ( $t_5, p_7, t_6$ ):

1) Add place  $p'_{51,61}$  to place set  $P'$  of TEG.

$$\begin{array}{l} \text{Set:} \\ \begin{cases} w'(t'_{51}, p'_{51,61}) = 1 \\ w'(p'_{51,61}, t'_{61}) = 1 \\ \mathcal{M}^{0'}(p'_{51,61}) = 0 \\ \phi'(p'_{51,61}) = \phi(p_7) = 0 \end{cases} \end{array}$$

2) Add place  $p'_{52,62}$  to place set  $P'$  of TEG.

$$\begin{array}{l} \text{Set:} \\ \begin{cases} w'(t'_{52}, p'_{52,62}) = 1 \\ w'(p'_{52,62}, t'_{62}) = 1 \\ \mathcal{M}^{0'}(p'_{52,62}) = 0 \\ \phi'(p'_{52,62}) = \phi(p_7) = 0 \end{cases} \end{array}$$

4: Loop between duplicated transitions:

$\xi(\mathbf{t}_1)$  :

1) Add places  $(p'_{11,12}, p'_{12,13}, p'_{13,14}, p'_{14,15}, p'_{15,16})$  to place set  $P'$  of TEG

$$\left\{ \begin{array}{l} w'(t'_{11}, p'_{11,12}) = w'(t'_{12}, p'_{12,13}) = w'(t'_{13}, p'_{13,14}) = w'(t'_{14}, p'_{14,15}) = \\ = w'(t'_{15}, p'_{15,16}) = 1 \\ w'(p'_{11,12}, t'_{12}) = w'(p'_{12,13}, t'_{13}) = w'(p'_{13,14}, t'_{14}) = w'(p'_{14,15}, t'_{15}) = \\ = w'(p'_{15,16}, t'_{16}) = 1 \\ \mathcal{M}^{0'}(p'_{11,12}) = \mathcal{M}^{0'}(p'_{12,13}) = \mathcal{M}^{0'}(p'_{13,14}) = \mathcal{M}^{0'}(p'_{14,15}) = \\ = \mathcal{M}^{0'}(p'_{15,16}) = 0 \\ \phi'(p'_{11,12}) = \phi'(p'_{12,13}) = \phi'(p'_{13,14}) = \phi'(p'_{14,15}) = \phi'(p'_{15,16}) = 0 \end{array} \right.$$

2) Add place  $(p'_{16,11})$  to place set  $P'$  of TEG

$$\left\{ \begin{array}{l} \text{Set:} \\ w'(t'_{16}, p'_{16,11}) = 1 \\ w'(p'_{16,11}, t'_{11}) = 1 \\ \mathcal{M}^{0'}(p'_{16,11}) = 1 \\ \phi'(p'_{16,11}) = 0 \end{array} \right.$$

$\xi(\mathbf{t}_3)$  :

1) Add places  $(p'_{31,32}, p'_{32,33}, p'_{33,34}, p'_{34,35}, p'_{35,36})$  to place set  $P'$  of TEG

$$\left\{ \begin{array}{l} w'(t'_{31}, p'_{31,32}) = w'(t'_{32}, p'_{32,33}) = w'(t'_{33}, p'_{33,34}) = w'(t'_{34}, p'_{34,35}) = \\ = w'(t'_{35}, p'_{35,36}) = 1 \\ w'(p'_{31,32}, t'_{32}) = w'(p'_{32,33}, t'_{33}) = w'(p'_{33,34}, t'_{34}) = w'(p'_{34,35}, t'_{35}) = \\ = w'(p'_{35,36}, t'_{36}) = 1 \\ \mathcal{M}^{0'}(p'_{31,32}) = \mathcal{M}^{0'}(p'_{32,33}) = \mathcal{M}^{0'}(p'_{33,34}) = \mathcal{M}^{0'}(p'_{34,35}) = \\ = \mathcal{M}^{0'}(p'_{35,36}) = 0 \\ \phi'(p'_{31,32}) = \phi'(p'_{32,33}) = \phi'(p'_{33,34}) = \phi'(p'_{34,35}) = \phi'(p'_{35,36}) = 0 \end{array} \right.$$

2) Add place  $(p'_{36,31})$  to place set  $P'$  of TEG

$$\left\{ \begin{array}{l} w'(t'_{36}, p'_{36,31}) = 1 \\ w'(p'_{36,31}, t'_{31}) = 1 \\ \mathcal{M}^{0'}(p'_{36,31}) = 1 \\ \phi'(p'_{36,31}) = 0 \end{array} \right.$$

$\xi(\mathbf{t}_5)$  :

1) Add place  $(p'_{51,52})$  to place set  $P'$  of TEG

$$\begin{cases} w'(t'_{51}, p'_{51,52}) = 1 \\ w'(p'_{51,52}, t'_{52}) = 1 \\ \mathcal{M}^{0'}(p'_{51,52}) = 0 \\ \phi'(p'_{51,52}) = 0 \end{cases}$$

2) Add place  $(p'_{52,51})$  to place set  $P'$  of TEG

$$\begin{cases} w'(t'_{52}, p'_{52,51}) = 1 \\ w'(p'_{52,51}, t'_{51}) = 1 \\ \mathcal{M}^{0'}(p'_{52,51}) = 1 \\ \phi'(p'_{52,51}) = 0 \end{cases}$$

$\xi(\mathbf{t}_6)$  :

1) Add place  $(p'_{61,62})$  to place set  $P'$  of TEG

$$\begin{cases} w'(t'_{61}, p'_{61,62}) = 1 \\ w'(p'_{61,62}, t'_{62}) = 1 \\ \mathcal{M}^{0'}(p'_{61,62}) = 0 \\ \phi'(p'_{61,62}) = 0 \end{cases}$$

2) Add place  $(p'_{62,61})$  to place set  $P'$  of TEG

$$\begin{cases} w'(t'_{62}, p'_{62,61}) = 1 \\ w'(p'_{62,61}, t'_{61}) = 1 \\ \mathcal{M}^{0'}(p'_{62,61}) = 1 \\ \phi'(p'_{62,61}) = 0 \end{cases}$$

Figure 4.13 shows the “equivalent” TEG corresponding to the consistent WTEG of Figure 4.12. Transition  $t_1$  in Figure 4.12 is duplicated in  $t_1^1, t_1^2, t_1^3, t_1^4, t_1^5, t_1^6$  in Figure 4.13. Transition  $t_2$  in Figure 4.12 is equivalent to transition  $t_2^1$  in Figure 4.13. Transition  $t_3$  in Figure 4.12 is duplicated in  $t_3^1, t_3^2, t_3^3, t_3^4, t_3^5, t_3^6$  in Figure 4.13. Transition  $t_4$  in Figure 4.12 is equivalent to transition  $t_4^1$  in Figure 4.13. Transition  $t_5$  in Figure 4.12 is duplicated in  $t_5^1, t_5^2$  in Figure 4.13. Transition  $t_6$  in Figure 4.12 is duplicated in  $t_6^1, t_6^2$  in Figure 4.13. The loop on the duplicated transitions enforce a firing order. For example, the loop between  $t_5^1, t_5^2$  in Figure 4.13, ensures that  $t_5^1$  fires strictly before that  $t_5^2$ . The disturbance  $w_1$  in Figure 4.12 is duplicated in  $w_1^1, w_1^2, w_1^3, w_1^4, w_1^5, w_1^6$  in Figure 4.13. The disturbance  $w_2$  in Figure 4.12 is equivalent to  $w_2^1$  in Figure 4.13. The disturbance  $w_3$  in Figure 4.12 is duplicated in  $w_3^1, w_3^2$  in Figure 4.13.

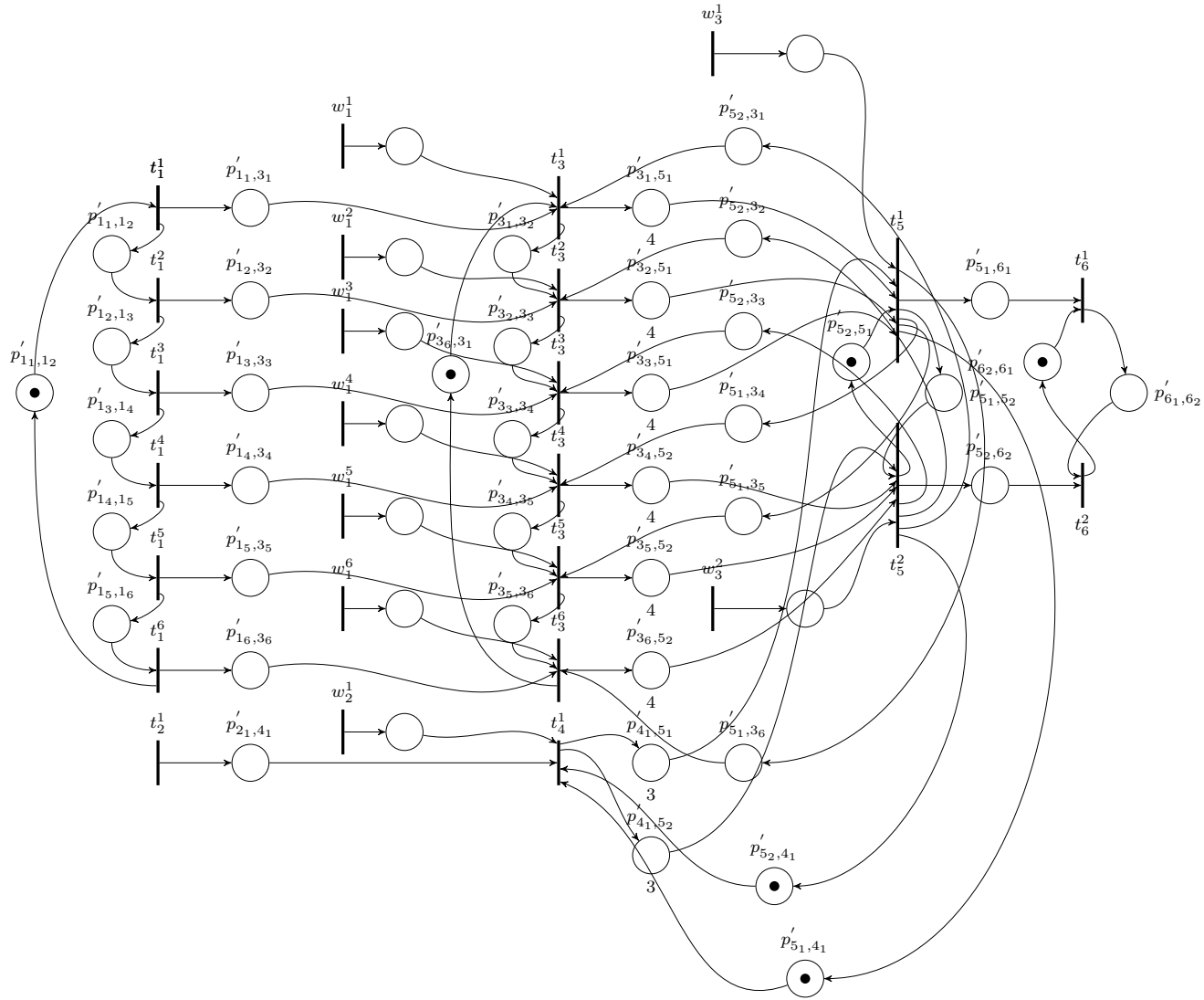


Figure 4.13: “Equivalent” TEG corresponding to the WTEG of Figure 4.12.

### ***Insertion of Artificial Transitions***

As mentioned in Remark 7, it is necessary to verify in Figure 4.13, if both structure conditions for TEGs are satisfied to calculate  $L_{opt+}$ . In Figure 4.13 it can be observed that the places between the input transitions  $t_1^1, t_1^2, t_1^3, t_1^4, t_1^5, t_1^6, t_2^1$  and the internal transitions  $t_3^1, t_3^2, t_3^3, t_3^4, t_3^5, t_3^6, t_4^1$  have no holding times and have no initial marking. The same occurs with the output transitions  $t_6^1, t_6^2$  and the internal transitions  $t_5^1, t_5^2$ . Therefore, the first requirement hold.

However, the input transition  $t_1^1$  is connected to  $t_1^2$ ,  $t_1^2$  is connected to  $t_1^3$ ,  $t_1^3$  is connected to  $t_1^4$ ,  $t_1^4$  is connected to  $t_1^5$ ,  $t_1^5$  is connected to  $t_1^6$  and  $t_1^6$  is connected to  $t_1^1$ . Besides that, the output transition  $t_6^1$  is connected to  $t_6^2$  and  $t_6^2$  is also connected to  $t_6^1$  through the loop. In other words, input and output transitions are not connected only to internal transitions. Thus, it is necessary to insert Artificial Transitions to calculate  $L_{opt+}$ .

Figure 4.14 shows the “equivalent” TEG with the artificial transitions  $u_1, u_2, u_3, u_4, u_5, u_6, y_1, y_2$  in blue. Without loss of generality, artificial transitions are inserted in Figure 4.13, without changing the firing order, as  $\gamma^0\delta^0$ , i.e., they do not have tokens and do not have holding times.

The artificial transitions are considered for the purpose of the computation of the  $L_{opt+}$ . After obtaining  $L_{opt+}$ , when the Interfaces are connected, the artificial transitions are removed.

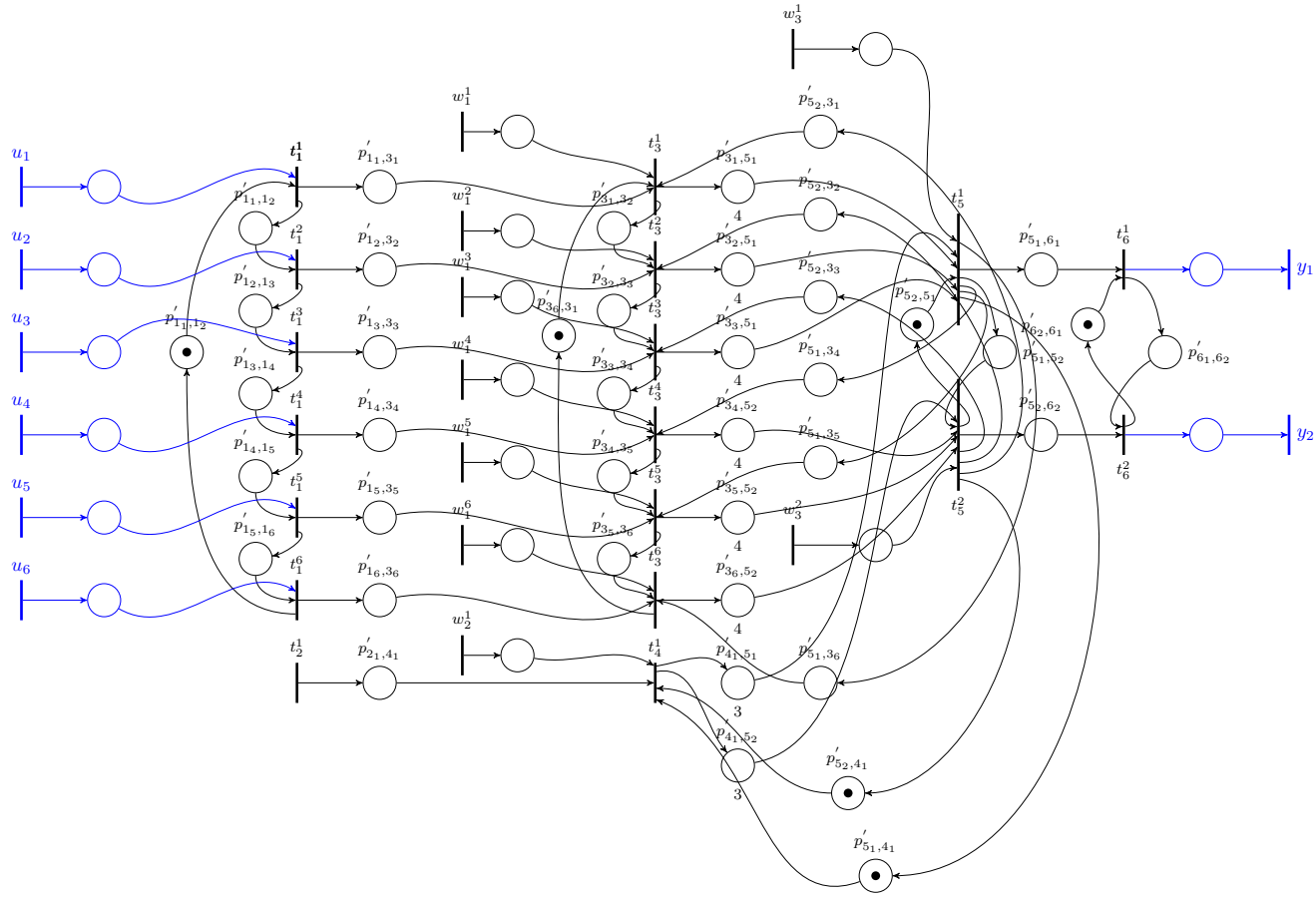


Figure 4.14: “Equivalent” TEG corresponding to the WTEG of Figure 4.12 with Artificial Transitions.







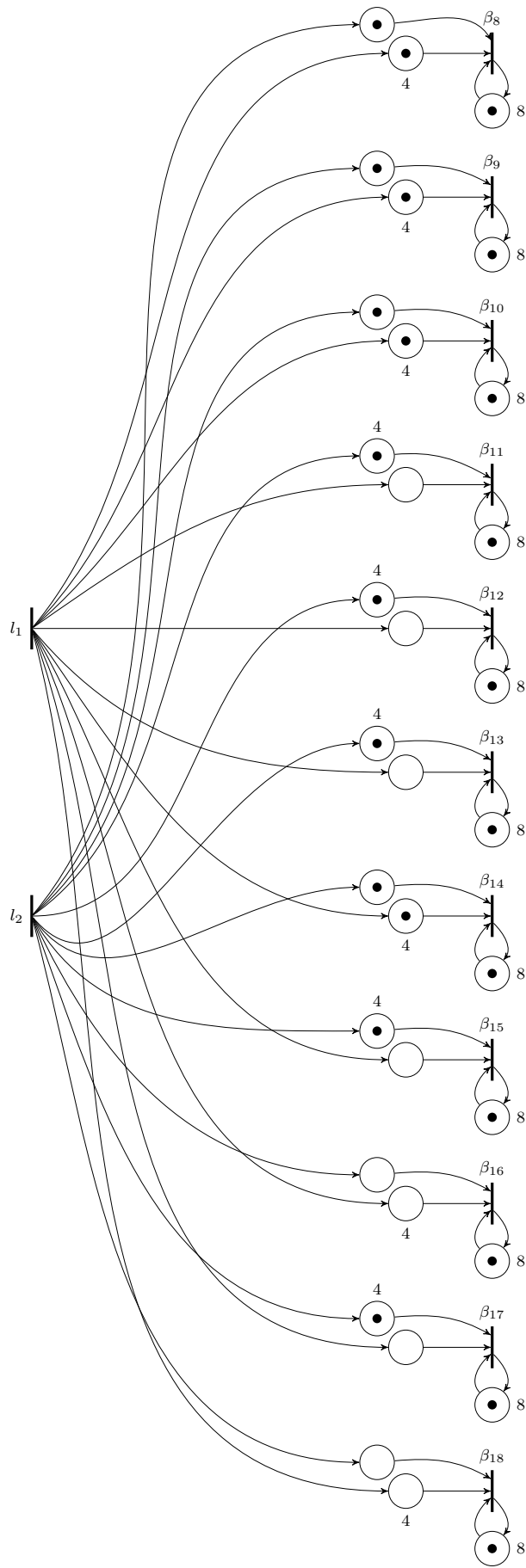


Figure 4.15: The  $L_{opt+}$  realization corresponding to the TEG of Figure 4.12.

### Step 3

In Step 3 of Algorithm 4, that is Interfaces realization, we have following steps of Algorithm 3.

1: T-semiflow of WTEG is  $\xi = \begin{bmatrix} 6 & 1 & 6 & 1 & 2 & 2 \end{bmatrix}^T$ , as showed in **Step 1**.

2: **for**  $\xi_{(t_i)}, i = 1, 2, 3, 4, 5, 6$

2.1:  $\xi_{(t_6)}$  The size of the Interfaces is determined by entries in T-semiflow. The WTEG has one output transition  $t_6$  and the  $L_{opt+}$  realization has two input transitions  $l_1$  and  $l_2$ . Thus it is necessary to insert an Input Interface to connect them. This Input Interface leads to an expansion in the number of transitions which allows the connection between WTEG and  $L_{opt+}$  realization. As  $\xi_{(t_6)} = 2$ , the size of the Input Interface is  $n = 2$ . In Figure 4.16 the Input Interface is shown.

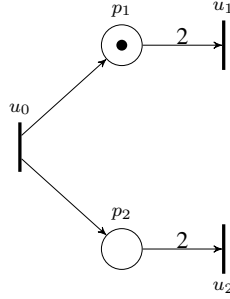
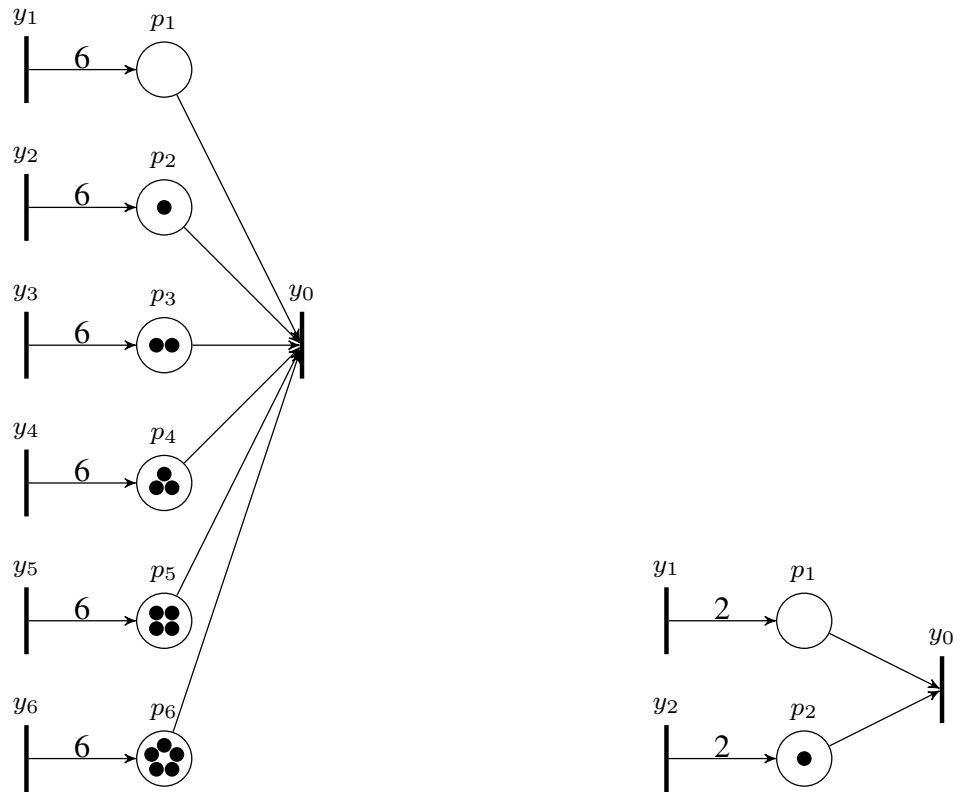


Figure 4.16:  $\mathcal{I}_1$  to connect WTEG  $\rightarrow L_{opt+}$ .

2.2: The entries of T-semiflow that correspond to the internal transitions are  $\xi_{(t_3)} = 6$  and  $\xi_{(t_5)} = 2$ . It is necessary to add two Output Interfaces, which lead to a reduction in the number of transitions. The size of the Output Interface for  $t_3$  is  $n = 6$  and the size of the Output Interface for  $t_5$  is  $n = 2$ .

To connect the realization of  $L_{opt+}$  into the WTEG Simulator, it is necessary to insert the Interfaces. The realization of  $L_{opt+}$  has eleven output transitions  $\beta_8, \beta_9, \beta_{10}, \beta_{11}, \beta_{12}, \beta_{13}, \beta_{14}, \beta_{15}, \beta_{16}, \beta_{17}$  and  $\beta_{18}$ .

With the insertion of these Interfaces, the connection between  $L_{opt+}$  realization and WTEG Simulator is possible. In Figure 4.17 the Output Interfaces are shown.



(a)  $\mathcal{O}_1$  to connect  $L_{opt+}$  to  $\hat{t}_3$  in Simulator.

(b)  $\mathcal{O}_2$  to connect  $L_{opt+}$  to  $\hat{t}_5$  in Simulator.

Figure 4.17: (a)  $\mathcal{O}_1$  with size  $n = 6$  and (b)  $\mathcal{O}_2$  with size  $n = 2$ .

#### Step 4

Step 4 of Algorithm 4 is built Simulator  $\mathcal{S}$ , which is a copy of the original system without the disturbance terms. Figure 4.18 depicts  $\mathcal{S}$ .

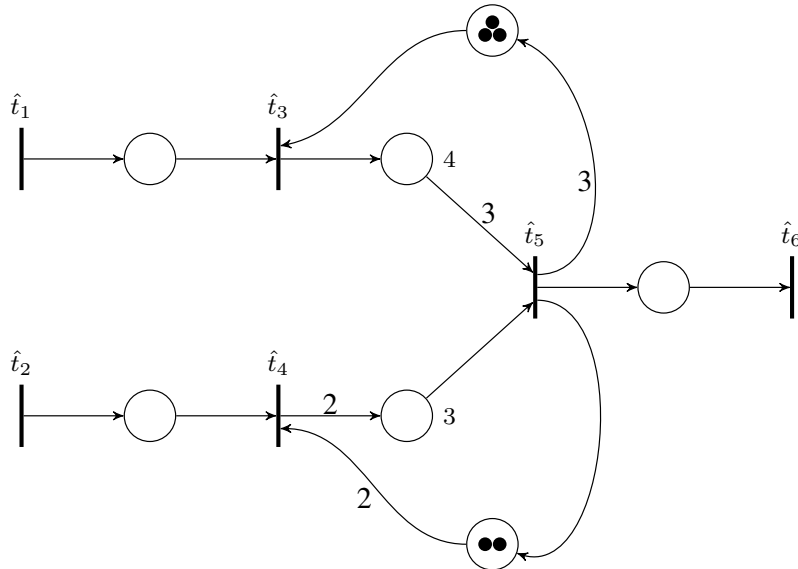


Figure 4.18: Simulator  $\mathcal{S}$  to WTEG of Figure 4.12

### Step 5

In Step 5 of Algorithm 4, we build  $\text{Obs}(WTEG)$ .

The system realization can be modeled by the connection of the WTEG to  $L_{opt+}$  using the Input Interface, the connection of  $L_{opt+}$  to WTEG Simulator using the Output Interfaces and the connection WTEG to WTEG Simulator. The Interfaces proposed to ensure the connections without changing the properties of the system.

5.1 Input transition  $t_1$  of WTEG is connected to internal transition  $\hat{t}_3$  in Simulator, and input transition  $t_2$  of WTEG is connected to internal transition  $\hat{t}_4$  in Simulator.

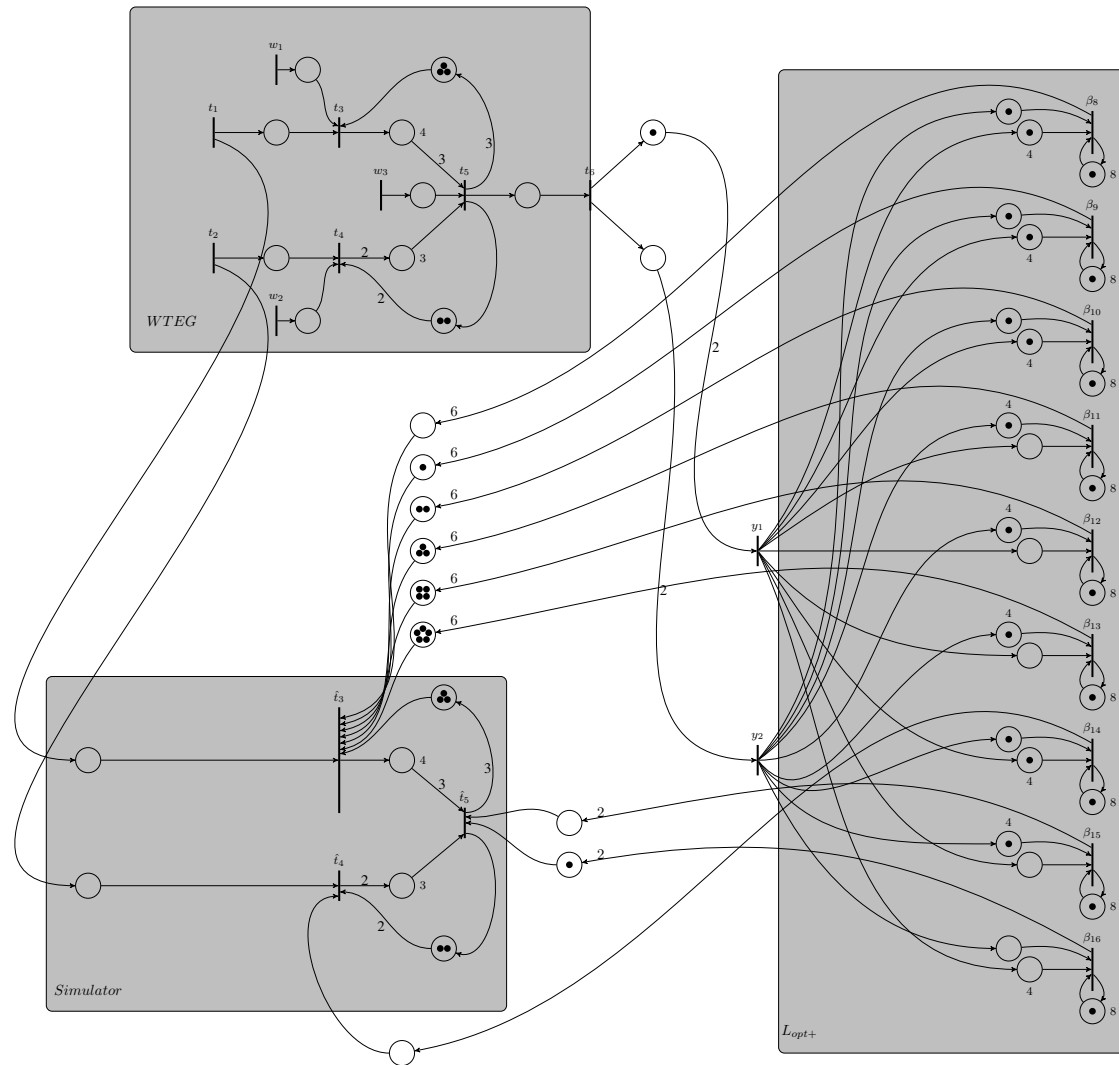
5.2 WTEG output has one output transition  $t_6$ . To connect to the input transitions of  $L_{opt+}$  realization, it is necessary to add the Input Interface  $n = 2$ , to expand the number of transitions. Thus, the input transitions of  $L_{opt+}$  realization:  $l_1$  and  $l_2$ , now they are called  $y_1$  and  $y_2$ . The  $L_{opt+}$  realization has eleven output transitions:  $\beta_8, \beta_9, \beta_{10}, \beta_{11}, \beta_{12}, \beta_{13}, \beta_{14}, \beta_{15}, \beta_{16}, \beta_{17}$  and  $\beta_{18}$ . The Simulator has three internal transitions  $\hat{t}_3, \hat{t}_4$  and  $\hat{t}_5$ .

5.3 To connect the  $L_{opt+}$  realization to the Simulator it is necessary to add two Output Interfaces: one  $n = 6$  and another  $n = 2$ , to reduce the number of transitions.

Figure 4.19 depict the Observer for WTEGs realization. The WTEG is connected through an Input Interface to the  $L_{opt+}$  realization. The  $L_{opt+}$  realization is connected to the Simulator through an Output Interface.

After the connections,  $L_{opt+y}$  can be written in the event domain by considering max-plus algebra as follows.

$$\begin{aligned}
\beta_8(k) &= 8\beta_8(k-1) \oplus 4y_1(k-1) \oplus y_2(k-1) \\
\beta_9(k) &= 8\beta_9(k-1) \oplus 4y_1(k-1) \oplus y_2(k-1) \\
\beta_{10}(k) &= 8\beta_{10}(k-1) \oplus 4y_1(k-1) \oplus y_2(k-1) \\
\beta_{11}(k) &= 8\beta_{11}(k-1) \oplus y_1(k) \oplus 4y_2(k-1) \\
\beta_{12}(k) &= 8\beta_{12}(k-1) \oplus y_1(k) \oplus 4y_2(k-1) \\
\beta_{13}(k) &= 8\beta_{13}(k-1) \oplus y_1(k) \oplus 4y_2(k-1) \\
\beta_{14}(k) &= 8\beta_{14}(k-1) \oplus 4y_1(k-1) \oplus y_2(k-1) \\
\beta_{15}(k) &= 8\beta_{15}(k-1) \oplus y_1(k) \oplus 4y_2(k-1) \\
\beta_{16}(k) &= 8\beta_{16}(k-1) \oplus 4y_1(k-1) \oplus y_2(k) \\
\beta_{17}(k) &= 8\beta_{17}(k-1) \oplus y_1(k) \oplus 4y_2(k-1) \\
\beta_{18}(k) &= 8\beta_{18}(k-1) \oplus 4y_1(k-1) \oplus y_2(k)
\end{aligned}$$

Figure 4.19:  $Obs(WTEG)$ .

# Chapter 5

## Conclusion and Future Works

In this work, we described the algebraic concepts to model TEGs using dioids theory, because the dynamics of a TEG can be modeled by linear equations in the Max-plus algebra and in Appendix A we defined dioid  $\mathcal{M}_{in}^{ax}[[\gamma, \delta]]$ , to obtain transfer functions for TEGs. We also introduced Observer for TEG, in order to compute  $L_{opt+}$  and to build the Simulator. We proposed Input and Output Interface, that is required to connect WTEG to  $L_{opt+}$  and  $L_{opt+}$  to Simulator. The Interfaces are a specific Petri net, which allows the connections without modifying the system's features. An example to illustrate the Observer for WTEGs realization is presented.

In summary, this work contributes with the literature by (i) presenting an Algorithm to convert a consistent WTEG in an equivalent TEG using an adaptation of the algorithm introduced in [18], (ii) proposing Input and Output Interface and (iii) design an Observer for WTEGs.

### Future Works

An approach as a future work would be to design a feedback controller, where the estimated state would be used to compute the control action instead of the unavailable true state. The question to construct the observer-based control for WTEGs in a dioid structure is that WTEGs have an event-variant behavior and can not be described by  $\mathcal{M}_{in}^{ax}[[\gamma, \delta]]$ . Therefore, it is necessary an investigation into some dioids that have been proposed to deal with this performance.

# Bibliography

- [1] BRUNSCH, T., RAISCH, J., HARDOUIN, L., et al. “Chapter 21 : Discrete-Event Systems in a Dioid Framework: Modeling and Analysis”. v. 433, pp. 431–450, 01 2013.
- [2] BRUNSCH, T., HARDOUIN, L., RAISCH, J. “Modelling Manufacturing Systems in a Dioid Framework”. pp. 29–74, 02 2014.
- [3] HARDOUIN, L., BERTRAND, C., SHANG, Y., et al. “Control and State Estimation for max-plus Linear Systems”, *Foundations and Trends in Systems and Control*, v. 6, n. 1, pp. 1–116, 2018.
- [4] XAVIER, D.-H., HARDOUIN, L., RAISCH, J., et al. “Holding time maximization preserving output performance for timed event graphs”, *IEEE Transactions on Automatic Control*, v. 59, n. 7, pp. 1968–1973, 2014.
- [5] CASSANDRAS, C. G., LAFORTUNE, S. *Introduction to discrete event systems*. Springer Science & Business Media, 2009.
- [6] FARHI, N., GOURSAT, M., QUADRAT, J. P. “Derivation of the fundamental traffic diagram for two circular roads and a crossing using minplus algebra and Petri net modeling.” In: *Proceedings of the 44th IEEE Conference on Decision and Control*, pp. 2119–2124, Dec 2005.
- [7] HEIDERGOTT, B., OLSDER, G. J., VAN DER WOUDE, J. *Max Plus at work: modeling and analysis of synchronized systems: a course on Max-Plus algebra and its applications*, v. 48. Princeton University Press, 2014.
- [8] LE BOUDEC, J.-Y., THIRAN, P. *Network calculus: a theory of deterministic queuing systems for the internet*, v. 2050. Springer Science & Business Media, 2001.
- [9] COHEN, G., DUBOIS, D., QUADRAT, J., et al. “A linear-system-theoretic view of discrete-event processes and its use for performance evaluation in manufacturing”, *IEEE Transactions on Automatic Control*, v. 30, n. 3, pp. 210–220, March 1985.



- [10] BACCELLI, F., COHEN, G., OLSDER, G., et al. “Synchronization and Linearity - An Algebra for Discrete Event Systems”, *The Journal of the Operational Research Society*, v. 45, 01 1994.
- [11] CAVORY, G., DUPAS, R., GONCALVES, G. “A genetic approach to solving the problem of cyclic job shop scheduling with linear constraints”, *European Journal of Operational Research*, v. 161, pp. 73–85, 02 2005.
- [12] TROUILLET, B., BENASSER, A., GENTINA, J.-C. “Transformation of the cyclic scheduling problem of a large class of fms into the search of an optimized initial marking of a linearizable weighted t-system”. In: *Sixth International Workshop on Discrete Event Systems, 2002. Proceedings.*, pp. 83–90. IEEE, 2002.
- [13] GIUA, A., SEATZU, C. “Observability of place/transition nets”, *IEEE Transactions on Automatic Control*, v. 47, n. 9, pp. 1424–1437, Sep. 2002.
- [14] HARDOUIN, L., MAIA, C. A., COTTENCEAU, B., et al. “Observer Design for (max, +) Linear Systems”, *IEEE Transactions on Automatic Control*, v. 55, n. 2, pp. 538–543, Feb 2010.
- [15] GONÇALVES, V. M., MAIA, C. A., HARDOUIN, L. “On Max-plus linear dynamical system theory: The observation problem”, *Automatica*, v. 107, pp. 103 – 111, 2019.
- [16] HARDOUIN, L., SHANG, Y., MAIA, C. A., et al. “Observer-Based Controllers for Max-Plus Linear Systems”, *IEEE Transactions on Automatic Control*, v. 62, n. 5, pp. 2153–2165, May 2017.
- [17] LUENBERGER, D. “An introduction to observers”, *IEEE Transactions on Automatic Control*, v. 16, n. 6, pp. 596–602, December 1971.
- [18] SRIRAM, S., BHATTACHARYYA, S. S. *Embedded Multiprocessors: Scheduling and Synchronization*. 2nd ed. Boca Raton, FL, USA, CRC Press, Inc., 2009. ISBN: 9781420048018.
- [19] MURATA, T. “Petri nets: Properties, Analysis and Applications”, *Proceedings of the IEEE*, v. 77, n. 4, pp. 541–580, 1989.
- [20] APAYDIN-ÖZKAN, H., MAHULEA, C., JÚLVEZ, J., et al. “A control method for distributed continuous mono-T-semiflow Petri nets”, *International Journal of Control*, v. 87, 02 2014.
- [21] MARCHETTI, O., MUNIER-KORDON, A. “Cyclic Scheduling for the Synthesis of Embedded Systems”. pp. 129–157, 11 2009.

- [22] NAKAMURA, M., SILVA, M. “Cycle time computation in deterministically timed weighted marked graphs”. pp. 1037 – 1046 vol.2, 02 1999.
- [23] DE GROOTE, R. “On the analysis of synchronous dataflow graphs: a system-theoretic perspective”, 2016.
- [24] GREENE, S. S. *Security policies and procedures*. New Jersey: Pearson Education, 2006.
- [25] BLYTH, T., JANOWITZ, M. *Residuation theory*. Pergamon Press, 1972.
- [26] COTTENCEAU, B., LHOMMEAU, M., HARDOUIN, L., et al. “Data processing tool for calculation in dioid”. In: *WODES’2000, Workshop on Discrete Event Systems*, p. xx, 2000.
- [27] HARDOUIN, L., SHANG, Y., MAIA, C. A., et al. “Extended version with source code of the paper observer-based controllers for max-plus linear systems”. In: *Laris, Internal Report*, 2016.
- [28] HARDOUIN, L., MAIA, C., COTTENCEAU, B., et al. “Max-plus Linear Observer: Application to Manufacturing Systems”, *IFAC Proceedings Volumes*, v. 43, n. 12, pp. 161 – 166, 2010. 10th IFAC Workshop on Discrete Event Systems.

# Appendix A

## Dioid $\mathcal{M}_{in}^{ax}[\gamma, \delta]$

This section affords some algebraic preliminaries about dioid of formal series used in this work. For a more complete presentation of this subject please refer to [2, 3, 10].

### A.0.1 Dioid $\mathcal{M}_{in}^{ax}[\gamma, \delta]$

In order to obtain transfer functions for TEGs, a specific dioid on formal power series called  $\mathcal{M}_{in}^{ax}[\gamma, \delta]$  was introduced in [4]. In the following, some definitions and basic results for computations in  $\mathcal{M}_{in}^{ax}[\gamma, \delta]$  are given.

**Definition 28 (Formal power series)** *A formal power series in  $p$  (commutative<sup>1</sup>) variables with coefficients in a complete dioid  $\mathcal{D}$  is a mapping  $s$  from  $\mathbb{Z}^p$  into  $\mathcal{D} : \forall k = (k_1, \dots, k_p) \in \mathbb{Z}^p$ , the coefficients of  $z_1^{k_1} \dots z_p^{k_p}$  are represented by  $s(k)$ , or equivalently:*

$$s = \bigoplus_{k \in \mathbb{Z}^p} s(k_1, \dots, k_p) z_1^{k_1} \dots z_p^{k_p}.$$

The sum and product of formal power series are defined based on the corresponding operations on  $\mathcal{D}$ .

**Definition 29 (Dioid of series)** *The set of formal power series with coefficients in an dioid  $\mathcal{D}$  endowed with the following sum and Cauchy product:*

$$\begin{aligned} s \oplus s' : (s \oplus s')(k) &= s(k) \oplus s'(k) \\ s \otimes s' : (s \otimes s')(k) &= \bigoplus_{i+j=k} s(i) \otimes s'(j), \end{aligned}$$

*is a dioid denoted  $\mathcal{D}[[z_1, \dots, z_p]]$ . If  $\mathcal{D}$  is complete,  $\mathcal{D}[[z_1, \dots, z_p]]$  is complete. The greatest lower bound of two series is given by*

$$s \wedge s' : (s \wedge s')(k) = s(k) \wedge s'(k)$$

---

<sup>1</sup> $z_1 z_2$  and  $z_2 z_1$  are considered to be the same object.

A series having only a single term with coefficient different from  $\varepsilon$  is called a monomial. Any series can be seen as a sum of monomials. Now, consider the set of formal power series in two variables,  $\gamma$  and  $\delta$ , with Boolean coefficients.

**Definition 30 (Diod  $\mathbb{B}[[\gamma, \delta]]$ )** *The dioid of formal power series in two commutative variables  $\gamma$  and  $\delta$  with Boolean coefficients, i.e.,  $\mathbb{B} = \{\varepsilon, e\}$ , and exponents in  $\mathbb{Z}$  is denoted  $\mathbb{B}[[\gamma, \delta]]$ . A series  $s \in \mathbb{B}[[\gamma, \delta]]$  is represented by*

$$s(\gamma, \delta) = \bigoplus_{k,t \in \mathbb{Z}} \bar{s}(k,t) \gamma^k \delta^t,$$

with  $\bar{s}(k,t) \in \mathbb{B}$ .  $\mathbb{B}[[\gamma, \delta]]$  is a complete and commutative dioid. The zero and unit element are  $\varepsilon(\gamma, \delta) = \bigoplus_{k,t \in \mathbb{Z}} \varepsilon \gamma^k \delta^t$  and  $e(\gamma, \delta) = \gamma^0 \delta^0$ , respectively.

Every such series can be represented graphically on the  $\mathbb{Z}^2$ -plane, with the exponents of  $\gamma$  on the horizontal axis and those of  $\delta$  on the vertical axis, by drawing a dot for each element of the series with coefficient different from  $\varepsilon$ . An example is shown in Figure A.1 for  $s = \gamma^1 \delta^1 \oplus \gamma^3 \delta^4 \oplus \gamma^4 \delta^3$ .

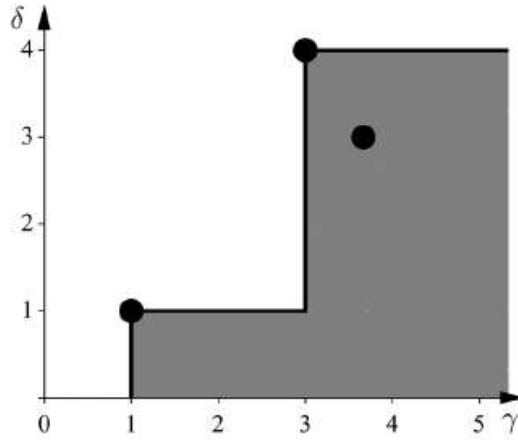


Figure A.1:  $s$  and its south-east cone (gray) [4].

The gray area represents the union of all “south-east cones” of all dots. It is clear that different series may generate the same such area; for instance, the series  $s' = \gamma^1 \delta^1 \oplus \gamma^3 \delta^4$  generates the exact same gray area as  $s$  (see Figure A.1).

We may then consider all series whose union of south-east cones covers the same area on the  $\mathbb{Z}^2$ -plane as “equivalent”. From this perspective, for any set of south-east cones, the series formed exactly by the terms given by the apexes of the cones is the “minimal representative” of all its equivalent series, in the sense that it is the series

with the smallest number of terms whose cones cover the corresponding area in the graph. These minimal representatives constitute the (complete) dioid  $\mathcal{M}_{in}^{ax}[\gamma, \delta]$ .

More formally, defining an order relation for monomials by:

$$\gamma^n \delta^t \preceq \gamma^{n'} \delta^{t'} \Leftrightarrow n \geq n' \text{ and } t \leq t',$$

and denoting  $\gamma^n \delta^t \leq \gamma^{n'} \delta^{t'}$  when  $\gamma^n \delta^t \preceq \gamma^{n'} \delta^{t'}$  and  $\gamma^n \delta^t \neq \gamma^{n'} \delta^{t'}$ .  $\mathcal{M}_{in}^{ax}[\gamma, \delta]$  is the set of series in  $\gamma$  and  $\delta$  with coefficients in  $\mathbb{B}$  defined as:

$$\{s = \bigoplus_{(n,t) \in \mathbb{Z}^2} s(n,t) \gamma^n \delta^t \mid \forall (n,t), (n',t') \in \mathbb{Z}^2, s(n,t) = s(n',t') = e \Rightarrow \gamma^n \delta^t \not\leq \gamma^{n'} \delta^{t'}\}.$$

**Definition 31 (Congruence)** *In a dioid  $(\mathcal{D}, \oplus, \otimes)$ , a congruence relation is an equivalence relation denoted  $\equiv$ , which satisfies  $\forall a; b, c \in \mathcal{D}$ :*

$$a \equiv b \Rightarrow \begin{cases} a \oplus c \equiv b \oplus c \\ a \otimes c \equiv b \otimes c. \end{cases}$$

**Definition 32 (Equivalence class)** *Given a dioid  $(\mathcal{D}, \oplus, \otimes)$  equipped with an equivalence relation  $\equiv$ . The equivalence class represented by an element  $a \in \mathcal{D}$  is denoted  $[a]_{\equiv}$  and is defined as*

$$[a]_{\equiv} = \mathcal{X} \in \mathcal{D} \mid \mathcal{X} \equiv a$$

Thus, an equivalence class  $[a]_{\equiv}$  is the set of all elements which are equivalent to  $a$  with respect to the equivalence relation  $\equiv$ .

**Lemma 4 (Quotient dioid)** *The quotient of a dioid  $(\mathcal{D}, \oplus, \otimes)$  with respect to a congruence relation  $\equiv$  is itself a dioid. It is called quotient dioid and is denoted  $\mathcal{D}_{/\equiv}$ . For addition and multiplication the following properties hold [10]*

$$[a]_{\equiv} \oplus [b]_{\equiv} = [a \oplus b]_{\equiv}$$

$$[a]_{\equiv} \otimes [b]_{\equiv} = [a \otimes b]_{\equiv}$$

**Definition 33 (Dioid  $\mathcal{M}_{in}^{ax}[\gamma, \delta]$ )** *The quotient dioid of  $\mathbb{B}[\gamma, \delta]$  with respect to the congruence relation in  $\mathbb{B}[\gamma, \delta]$ :*

$$a \equiv b \Leftrightarrow \gamma^*(\delta^{-1})^* a = \gamma^*(\delta^{-1})^* b,$$

is denoted  $\mathcal{M}_{in}^{ax}[\gamma, \delta]$ , i.e.,  $\mathcal{M}_{in}^{ax}[\gamma, \delta] = \mathbb{B}[\gamma, \delta]_{/\gamma^*(\delta^{-1})^*}$ , where  $*$  refers to the Kleene star.  $\mathcal{M}_{in}^{ax}[\gamma, \delta]$  constitutes a complete dioid and the zero and unit elements are  $\varepsilon(\gamma, \delta) = \bigoplus_{k,t \in \mathbb{Z}} \varepsilon \gamma^k \delta^t$  and  $e(\gamma, \delta) = \gamma^0 \delta^0$ , respectively.

## A.0.2 Causal Series in $\mathcal{M}_{in}^{ax}[\gamma, \delta]$

In this section, some definitions about causal series are presented.

**Definition 34 (Causality)** *A series  $s \in \mathcal{M}_{in}^{ax}[\gamma, \delta]$  is causal if  $s = \varepsilon$  or if all exponents of  $\gamma$  and  $\delta$  are in  $\mathbb{N}_0$ .*

The set of causal elements of  $\mathcal{M}_{in}^{ax}[\gamma, \delta]$  has a complete dioid structure and is denoted  $\mathcal{M}_{in}^{ax+}[\gamma, \delta]$ .

**Remark 9** *A matrix  $A$  with entries in  $\mathcal{M}_{in}^{ax}[\gamma, \delta]$  is causal, if all its entries are causal.*

**Theorem 3** *(see [3]) The canonical injection  $\text{Id}_{\mathcal{M}_{in}^{ax+}[\gamma, \delta]} : \mathcal{M}_{in}^{ax+}[\gamma, \delta] \rightarrow \mathcal{M}_{in}^{ax}[\gamma, \delta]$ ,  $s \mapsto s$ , is residuated and its residual is denoted  $\text{Pr}_+ : \mathcal{M}_{in}^{ax}[\gamma, \delta] \rightarrow \mathcal{M}_{in}^{ax+}[\gamma, \delta]$ .*

Formally, the series  $\text{Pr}_+(s)$  is the greatest causal series less than or equal to series  $s \in \mathcal{M}_{in}^{ax}[\gamma, \delta]$ . It can be computed by:

$$\text{Pr}_+(s) = \text{Pr}_+ \left( \bigoplus_{(n,t) \in \mathbb{Z}} s(n,t) \gamma^n \delta^t \right) = \bigoplus_{(n,t) \in \mathbb{Z}} s_+(n,t) \gamma^n \delta^t \quad (\text{A.1})$$

where,

$$s_+(n,t) = \begin{cases} s(n,t) & \text{if } n \geq 0, t \geq 0 \text{ and } s(n,t) = e, \\ \varepsilon & \text{otherwise.} \end{cases}$$

**Remark 10** *Theorem 3 can also be applied to matrices.*